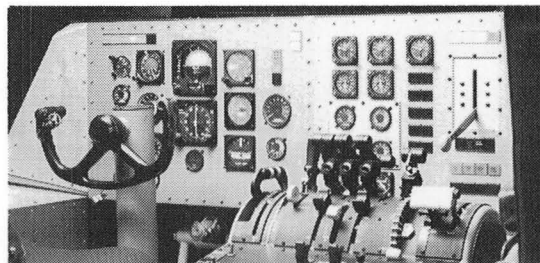
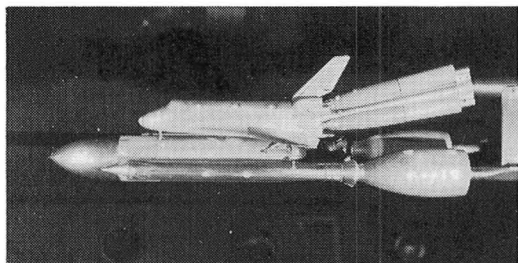
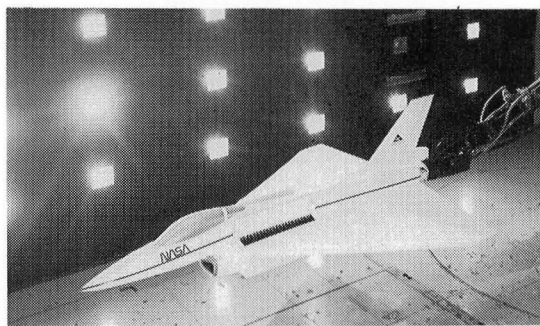
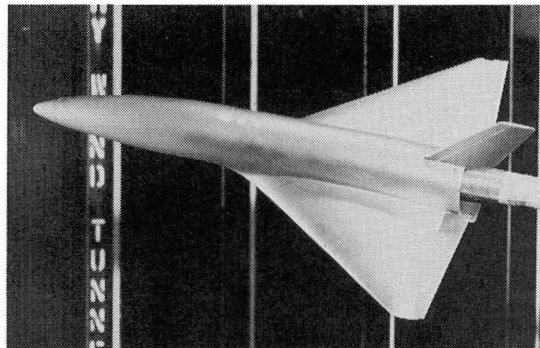
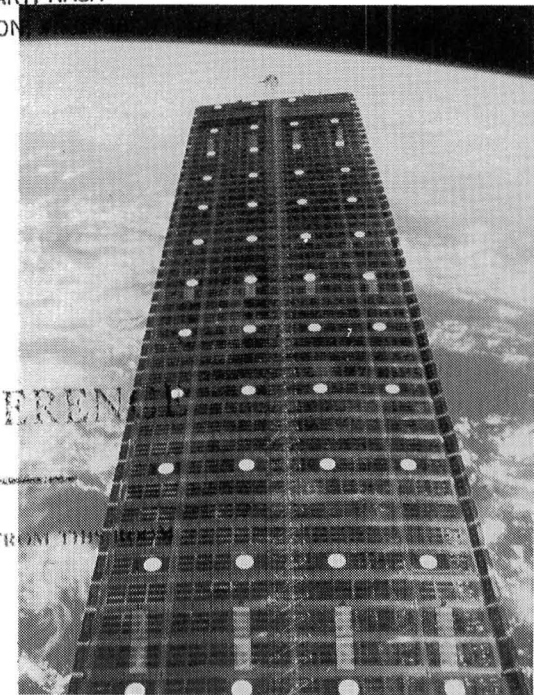


LIBRARY COPY

DEC 11 1985

LANGLEY RESEARCH CENTER
LIBRARY, NASA
HAMPTON



National Aeronautics and
Space Administration



Langley Aeronautics and Space Test Highlights 1984



National Aeronautics and
Space Administration

Langley Research Center
Hampton, Virginia 23665-5225

1985

N85-35151#

Foreword

The role of the Langley Research Center is to perform basic and applied research necessary for the advancement of aeronautics and space flight, to generate new and advanced concepts for the accomplishment of related national goals, and to provide research advice, technological support, and assistance to other NASA installations, other government agencies, and industry. This report highlights some of the significant tests which were performed during calendar year 1984 in Langley test facilities, a number of which are unique in the world. The report illustrates both the broad range of the research and technology activities at the Langley Research Center and the contributions of this work toward maintaining United States leadership in aeronautics and space research. Other highlights of Langley research and technology for 1984 are described in "Research and Technology—1984 Annual Report of the Langley Research Center." Further information about both reports is available from the Office of the Chief Scientist, Mail Stop 103, Langley Research Center, Hampton, Virginia 23665 (804-865-3316).

A handwritten signature in black ink, appearing to read "Richard H. Petersen". The signature is fluid and cursive, with a large, stylized 'R' at the beginning.

Richard H. Petersen
Director

Availability Information

For additional information on any highlight, contact the individual identified with the highlight. This individual is generally either a member or a leader of the research group. Commercial telephone users may dial the listed extension preceded by (804) 865. Telephone users with access to the Federal Telecommunications System (FTS) may dial the extension preceded by 928.

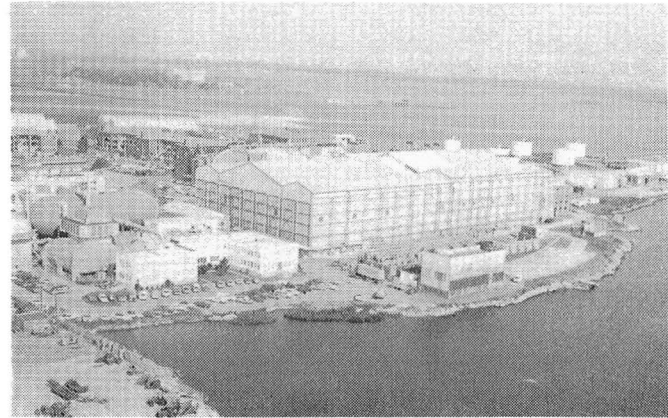
Contents

Foreword	iii
Availability Information	iv
30- by 60-Foot Tunnel (Building 643)	1
Stall/Spin-Resistant Natural Laminar Flow Wing	1
Multi-Axis-Vectoring Two-Dimensional Nozzle Free-Flight Tests	2
General Aviation Semispan Wing Tests	2
Vortex Flap Investigation on Full-Scale F-106 Semispan Model	3
Low-Turbulence Pressure Tunnel (Building 582A)	4
Laser Velocimeter Measurements of Juncture Flow Fields and Taylor-Görtler Vortices	4
Görtler Experiment	5
High-Speed Natural Laminar Flow Airfoil	6
Laminar Suction Surface Investigations	7
20-Foot Vertical Spin Tunnel (Building 645)	8
Spin Tunnel Investigation of Australian Basic Pilot Training Airplane	8
Testing Modifications and Updates of Military Aircraft	9
7- by 10-Foot High-Speed Tunnel (Building 1212B)	10
NTF Pathfinder-I Lockheed-Georgia Wing Correlation Studies	10
Wing-Tip-Mounted Pusher Turboprop	10
F-106 Vortex Flap Study	11
Subsonic Tests of Circular-Body Earth-to-Orbit Transport	11
4- by 7-Meter Tunnel (Building 1212C)	13
Advanced Powered-Lift STOVL Fighter Configuration	13
Propulsive Wing/Canard Fighter for STOL Operations	14
Two-Dimensional Tests of Heavy Rain Effects on Airfoil Performance	14
Critical Fastener Preloading for Army Helicopter Model	15
Advanced Rotor Design for AH-64 Helicopter	15
Advanced Helicopter Scale Model Wind Tunnel Tests	16
Grumman 698 V/STOL Transport Configuration	16
Rain on Radome During Simulated Flight	17
8-Foot Transonic Pressure Tunnel (Building 640)	18
Laminar Flow Control Tests	18
Transonic Dynamics Tunnel (Building 648)	20
Effects of New Multipurpose Pylons on F-16 Flutter Characteristics	20
Spanwise Curvature Raises Flutter Dynamic Pressure	21
Flutter of Four-Engine Transport Wing With Winglet Predictable by Analysis	22
TDT Test Provides Essential Data Base for JVX Preliminary Design Development	22
16-Foot Transonic Tunnel (Building 1146)	24
Improved Aft-Mounted Nacelles	24
Thrust Vectoring and Reversing for Control at High Angles of Attack	24

Voice-Controlled Model Pressure Leak Checking System	25
Installation Effects of Advanced Turboprops on Swept Supercritical Wing.....	25
Two-Dimensional Convergent-Divergent Afterbody Boattail Study	26
Effect of Jet Exhaust Plume on Shuttle Ascent Configuration Aerodynamics	27
National Transonic Facility (Building 1236)	28
Model Deformation Measurements in the NTF	28
0.3-Meter Transonic Cryogenic Tunnel (Building 1242)	30
Boundary Layer Transition Detection at Cryogenic Conditions With Hot Films	30
Flutter Testing Techniques Developed For Use in Cryogenic Wind Tunnels	31
Advanced Technology Airfoil Test (ATAT) Program	31
Reynolds Number Effects on Unsteady Pressure Studies	32
Unitary Plan Wind Tunnel (Building 1251)	34
Nonlinear Analysis/Design Techniques for Advanced Supersonic Wing Design	34
Vertical Launch Antisubmarine Rocket	35
Cavity Flow Field Studies at Supersonic Speeds	35
Hybrid Flap Study	36
Fighter Wing Study	36
Nonintrusive Simultaneous Measurement of Three Flow Parameters in a Supersonic Flow	37
Fighter Wing Design Study	37
Advanced Space Transportation Vehicle Investigation	38
Hypersonic Facilities Complex (Buildings 1247B, 1247D, 1251A, 1275)	39
Aerodynamics for an Entry Research Vehicle	39
Flow Field and Surface Measurements on a 2:1 Elliptical Cone.....	40
Experimental Aerodynamic Coefficients on Shuttle-Like Vehicle	41
Aerodynamic Coefficients for General-Purpose Heat Source Module	41
Experimental Investigation of Maneuvering Reentry Research Vehicle at Mach 6 and 20.3	42
Real-Gas Simulation on the Space Shuttle Orbiter.....	42
Forward-Located Jet Interaction Nozzles Study	43
Aerothermal Loads Complex (Building 1265)	44
Aerothermal Tests of Advanced Carbon-Carbon TPS	45
Aerothermal Test of Shuttle Split-Elevon Model	45
Aerothermal Tests of Spherical Dome Protuberance Models	46
Development of Alternate Mach Number Capability for 8-ft HTT	46
Aircraft Noise Reduction Laboratory (Building 1208)	48
Acoustic Loading From Dual Supersonic Jets.....	48
Verification of Propeller Aircraft Interior Noise Model	49
Acoustic Properties of Nonaxisymmetric Supersonic Nozzle	49
Noise Transmission of Aircraft Sidewall and Noise Control Materials	50
Comparison of Hot-Film Probe and Pressure Probe Responses	50
Laboratory Study of Sidewall Acoustic Treatment.....	51

Tip Vortex Broadband Noise.....	52
Avionics Integration Research Laboratory—AIRLAB (Building 1220)	53
Fault-Tolerant Software Experiment	54
Fault-Free Performance Validation of Fault-Tolerant Computers	54
Validation Methodology for Fault-Tolerant Clock Synchronization	55
DC-9 Full-Workload Simulator (Building 1220)	56
CDTI Cockpit Procedures Study	57
Effects of Digital Altimetry on Pilot Workload.....	57
Transport Systems Research Vehicle (TSRV) and TSRV Simulator (Building 1268)	59
Advanced Airborne Energy Management	60
Crew Station Systems Research Laboratory (CSSRL) (Building 1298)	61
Advanced Media Interface for Control of Modern Transport	
Aircraft Navigational Systems.....	61
Multifunction Control Throttle and Stick As Autopilot Interface	62
General Aviation Simulator (Building 1268A)	64
Light Twin Automatic Engine-Out System	64
Mission Oriented Terminal Area Simulation (MOTAS) (Building 1268A)	65
Differential Maneuvering Simulator (Building 1268A)	66
Control of Highly Maneuverable Unstable Aircraft	66
Visual/Motion Simulator (Building 1268A)	67
Allowable Time Delays in Large Aircraft Response.....	67
Structural Dynamics Research Laboratory (Building 1293B)	69
Photogrammetric Measurement Tests for Solar Array Experiment	69
Generic Space Station Model Dynamic Tests.....	70
Vehicle Antenna Test Facility (Building 1299)	71
Compact Range Technology	72
Impact Dynamics Research Facility (Building 1297)	73
Full-Scale Impact Testing of F-111 Crew Escape Capsule	73
Full-Scale Crash Test Evaluation of Two General Aviation Airframe Subfloor	
Load-Limiting Concepts	74
Boeing 707 Fuselage Section Drop Test	74
Aircraft Landing Dynamics Facility (Building 1257)	76
Vortex Research Facility (Building 720B)	77
Density Stratification Effects on Vortex Flows	77
Flight Research Facility (Building 1244)	79
Storm Hazards Program—1984 Results	81

30- by 60-Foot Tunnel



The Langley 30- by 60-Foot Tunnel is a continuous-flow open-throat double-return tunnel powered by two 4000-horsepower electric motors, each driving a four-blade 35.5-ft-diameter fan. The tunnel test section is 30 ft high and 60 ft wide and is capable of speeds up to 100 mph. The tunnel was first put into operation in 1931 and has been used continuously since then to study the low-speed aerodynamics of commercial and military aircraft. The large open-throat test section lends itself readily to tests of large-scale models and to unique test methods with small-scale models.

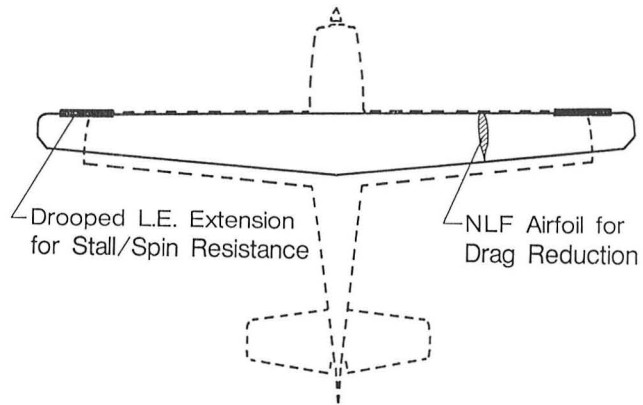
Large-scale and full-scale aircraft tests are conducted with the strut mounting system. This test method can handle airplanes up to the size of present-day light twin-engine airplanes. Such tests provide static aerodynamic performance and stability and control data, including the measurement of power effects, wing pressure distributions, and flow visualization.

Small-scale models can be tested to determine both static and dynamic aerodynamics. For all captive tests, the models are sting mounted with internal strain gage balances. The captive test methods include conventional static tests for performance and stability and control, forced-oscillation tests for aerodynamic damping, and rotary tests for spin aerodynamics. Dynamically scaled subscale models, properly instrumented, are also freely flown in the large test section with a simple tether to study their dynamic stability characteristics at low speed and at high angles of attack. A small computer is used in this free-flight test technique to represent the important characteristics of the airplane flight control system.

Stall/Spin-Resistant Natural Laminar Flow Wing

As part of the research effort at NASA Langley to develop the technology to improve the stall/spin resistance of general aviation aircraft, an outboard leading-edge droop modification has been developed for application to an advanced natural laminar flow wing. The leading-edge droop design was developed during tests in the 30- by 60-Foot Tunnel with a scale model of a high-performance single-engine airplane as a test vehicle. A new airfoil, designed at NASA Langley for 70-percent natural laminar flow on both the upper and lower surfaces, was used for the droop application.

Since previous outboard droop designs have not been concerned with natural laminar flow, the design approach used an existing NLF airfoil to define the droop airfoil geometry. This approach was intended to provide natural laminar flow on the drooped as



Natural laminar flow wing with drooped leading-edge modification.

well as undrooped portions of the wing. The design procedure was further validated by the use of an airfoil analysis code to examine the pressure distribution for conditions conducive to natural laminar flow. Results of static and dynamic force tests showed the NLF wing with modified leading edge to have improved stall departure resistance characteristics without adverse affects on the natural laminar flow to 70-percent wing chord.

(Frank L. Jordan, Jr., 2184)

Multi-Axis-Vectoring Two-Dimensional Nozzle Free-Flight Tests

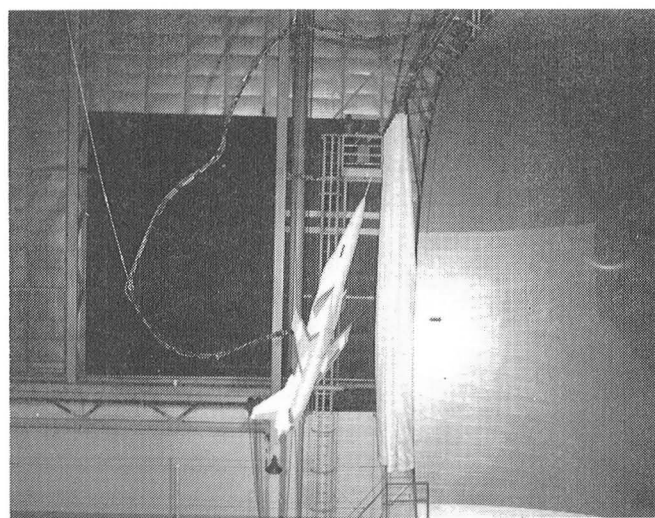
As part of a broad program to investigate advanced propulsive controls, free-flight tests of a 0.16-scale model of the X-29A demonstrator aircraft, which incorporates a two-dimensional nozzle with pitch and yaw vectoring capability, were conducted in the 30- by 60-Foot Tunnel. A primary objective of the test was to assess the viability of a novel type of thrust vectoring simultaneously in pitch and yaw which used no mechanical interference with the vectoring flaps. The second objective was to assess the impact of thrust vectoring on the high-angle-of-attack stability and control characteristics of the configuration.

During the tests, the model was flown unconstrained in the test section of the tunnel and was

remotely controlled by pilots located at appropriate positions around the test section. Inputs from the pilots and motion sensor signals from the model were fed into a digital computer, which generated commands to drive the control surfaces on the model. With this system, the effects of various controls and control laws could be assessed easily.

The test results indicated that the pitch and yaw vectoring flaps could effectively provide simultaneous pitch and yaw vectoring control forces. Also, with the thrust vectoring controls activated, the model was more controllable and could be flown to higher angles of attack than with aerodynamic controls only.

(Daniel G. Murri, 2184)



Free-flight test of X-29 model with thrust vectoring.

General Aviation Semispan Wing Tests

Inadvertent stalls and departures from controlled flight at low altitudes are a leading cause of fatal accidents involving light general aviation airplanes. Past flight experiments have shown that a discontinuous wing leading-edge design can significantly improve the spin resistance of this class of airplane by increasing the stall angle of attack on the outer portion of the wing. Tests were conducted recently in the 30- by 60-Foot Tunnel to better understand the significance of high-angle-of-attack aerodynamic changes produced by wing leading-edge modifications on a representative general aviation semitapered wing design. The model was a full-scale



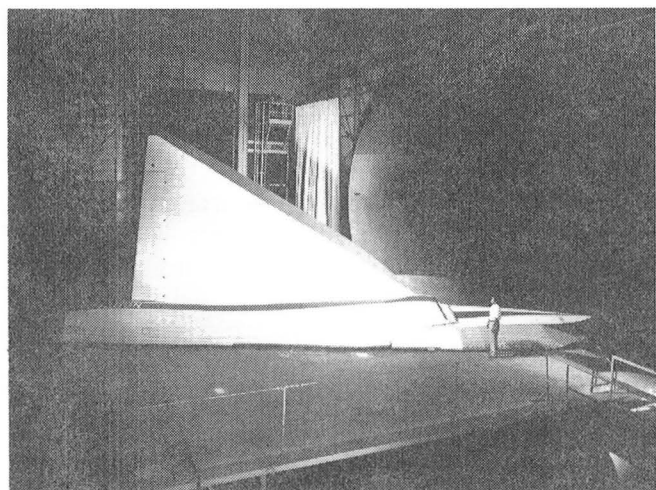
Full-scale semispan model mounted in 30- by 60-Foot Tunnel.

semispan copy of the modified Piper PA-28R stall/spin research airplane without empennage. Various spanwise lengths of wing leading-edge droop were added to the basic airfoil to duplicate flight test configurations. Forces, moments, and surface pressures were measured for angles of attack between -10° and $+84^\circ$ at a Reynolds number of 2.7×10^6 .

Results showed that the addition of an outboard droop extending from the wing tip inboard to between 50 to 60 percent semispan provided the largest increase in stall angle of attack. Compared with that of the unmodified wing, the stall angle of attack was doubled to about 35° , which therefore reduced the likelihood of inadvertent spin entry. Such improvements in the stall/spin characteristics correlate well with flight test results. For this spin resistant configuration, the drag penalty caused by the wing modification was found to reduce cruise speed by only about 2 mph.

(Daniel J. DiCarlo, 2064)

flap concepts on the F-106 airplane. These tests with realistic components have indicated improved L/D characteristics at maneuver lift conditions which are similar to results obtained from previous flat-plate vortex flap studies. Flow visualization with surface tufts and smoke indicated an instability in the vortex flow formation at the flap apex near the wing root juncture. Extension of the flap apex from a point to a finite chord provided a stable vortex flow formation. (Long P. Yip, 2184)



Vortex Flap Investigation on Full-Scale F-106 Semispan Model

Research efforts conducted largely at NASA Langley Research Center have indicated that the vortex flap concept could provide substantial improvement in the lift-to-drag (L/D) characteristic to enhance the maneuver capability of aircraft with slender wing design. As part of the concept validation, a flight demonstration of the F-106B airplane is planned. In support of the vortex flap flight research program, tests were conducted in the 30- by 60-Foot Tunnel on a full-scale semispan airplane to determine the low-speed aerodynamic characteristics. The model was instrumented with over 300 pressure orifices distributed on the wing and flap surfaces as well as with hinge moment gages on the flap. The model was mounted on the external scale balance system of the tunnel so that overall aerodynamic forces and moments of the model could be measured. Test conditions included an angle-of-attack range from -10° to 28° and a Reynolds number of about 12.5×10^6 based on the mean aerodynamic chord.

Tests of the full-scale F-106 semispan model have provided a large aerodynamic data base of longitudinal aerodynamic characteristics, pressure distribution, hinge moment measurements, and flow visualization for the analysis and design of vortex

F-106 semispan airplane mounted in 30- by 60-Foot Tunnel.

Low-Turbulence Pressure Tunnel



The Langley Low-Turbulence Pressure Tunnel (LTPT) is a single-return closed-circuit tunnel which can be operated at pressures from near vacuum to 10 atm. The test section is rectangular in shape (3 ft wide and 7.5 ft in height and length) and the contraction ratio is 17.6:1. The LTPT is capable of testing at Mach numbers from 0.05 to 0.50 and unit Reynolds numbers from 0.1×10^6 to 15×10^6 per foot. The tunnel has provisions for removal of the sidewall boundary layer by means of a closed-loop suction system mounted inside the pressure chamber. This system utilizes slotted vertical sidewalls just ahead of the model test section, and the removed air is re-injected through an annular slot downstream of the test section. A flow control system allows the flow and pressure requirements to be varied as dictated by tunnel operation. This system can be used to provide boundary layer control (BLC) for low-drag airfoil research.

A BLC system for high-lift airfoil testing is also available. This system utilizes compressed dry air and involves tangential blowing from slots located on the sidewall mounting endplates. Flowmeters can be used to monitor the amount of air blown into the tunnel. An automatically controlled vent valve is utilized to remove the air injected into the tunnel by this system. A high-lift model support and force balance system is provided to handle both single-element and multiple-element airfoils.

The measured turbulence level of the LTPT is very low due to the large contraction ratio and the many fine-mesh antiturbulence screens. The excellent flow quality of this facility makes it particularly suitable for testing low-drag airfoils. Recent flow quality measurements in the LTPT indicate that the velocity fluctuations in the test section range from 0.025 percent at Mach 0.05 to 0.30 percent at Mach 0.20 at the highest unit Reynolds number.

The drive system is a 2000-horsepower direct-current motor with power supplied from a motor-generator set. The tunnel stagnation temperature is controlled by a heat exchanger, which provides both heating and cooling via steam injectors and modulated valves that control the flow volume of water through a set of coils.

Laser Velocimeter Measurements of Juncture Flow Fields and Taylor-Görtler Vortices

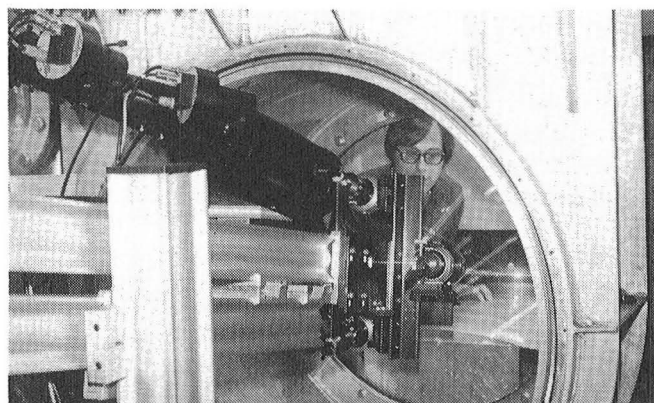
A specialized single-axis five-beam three-component laser velocimeter (LV) was constructed and used to study juncture flow fields and Taylor-Görtler vortices in the Langley Low-Turbulence Pressure Tunnel. The juncture was defined by a blunt-leading-edge vertical splitter plate and a sharp-leading-edge horizontal plate. The Taylor-Görtler vortices were generated in the flow field above a supercritical airfoil model.

The juncture flow field measurements were performed at 50-, 75-, and 95-percent chord positions covering a 3- by 3-cm area normal to the directed tunnel flow. The study consisted of measurements above a flat horizontal plate and a curved horizontal plate with a sharp juncture and a juncture with a 1-in. radius of curvature. The closest point of approach was 3.5 mm to the vertical surface and 1.0 mm to the horizontal surface. The LV sample volume was 80 μm in diameter and 120 μm in length. The goal of the investigation was to determine basic information about the flow field within the juncture for use in

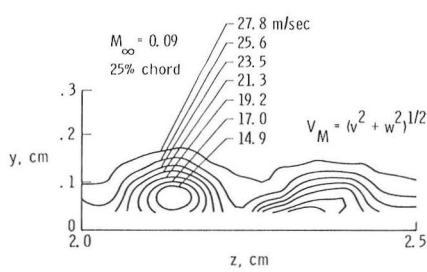
developing a theory to describe this basic three-dimensional flow field. Classical instrumentation such as hot-wire anemometry cannot be used because of the very thin boundary layers and heat transfer problems when the hot wire is placed close to a wall.

The measurements of Taylor-Görtler vortices made over a chord range of 15 to 32.75 percent every 0.25 percent chord and from 0.3 to 3.0 mm above the model surface were the first experimental verification of the theory describing their spacing above the surface as a function of free-stream parameters. (See the following highlight.) The experimental results will provide information to expand the theory to account for vortex growth as a function of chord position and will help derive a nonlinear theory to better predict the phenomenon. The photograph shows the model installed in the facility along with the multicomponent laser velocimeter beams above the model. Typical results are shown in the contour map of the resultant two-component (v and w) velocity magnitude contours at the 25-percent-chord position for the Mach 0.09 run condition.

(James F. Meyers, 2791)



Laser Doppler velocimeter installation in LTPT.



Contour map of mean velocity magnitude, V_M (m/sec).

Görtler Experiment

Görtler vortices arise in boundary layers along concave surfaces due to centrifugal effects. These streamwise vortices are one of the three known principal sources of instability that lead to transition from laminar to turbulent flow. There are a number of flow situations in which the fluid encounters concave curvature (e.g., the lower surface of an LFC supercritical wing). This experiment, which was supported by the Langley Director's Discretionary Fund, was the first of its kind to study the development of Görtler vortices on an airfoil with a significant pressure gradient.

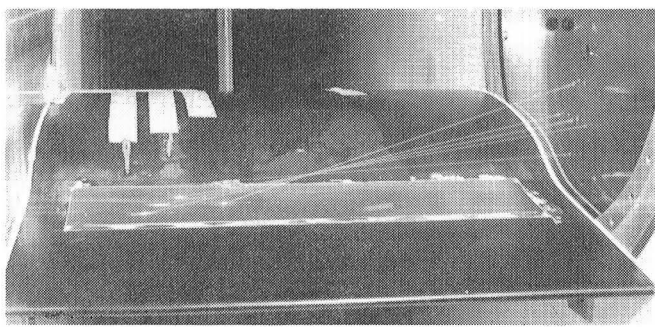
A 6-ft-chord experimental model was tested in the Langley Low-Turbulence Pressure Tunnel. Görtler vortices were visualized with sublimating chemicals. The streamwise vortices were observed as alternating light and dark streaks on the surface because of the differential shear stress pattern of the vortex layer. Each pair of light and dark streaks indicates one wavelength of the counterrotating streamwise vortex layer. A five-beam laser velocimeter was used to measure the three velocity components in the boundary layer and a dedicated computer system was used to record and process the data.

Theoretical studies of the Görtler instability have shown that the vortex amplification varies with free-stream velocity (i.e., with Reynolds number and Görtler number). An experimental investigation would be expected to show a vortex spacing corresponding to the theoretically predicted maximum amplified wavelength. However, previous experiments conducted in curved channels with zero pressure gradient did not find this correlation. Indeed, the wavelength was found to be almost independent of free-stream velocity, which probably indicated that some portion of the test apparatus, such as the turbulence damping screens, had "selected" the wavelength. In the present experiment, the Görtler number was varied via changes in the free-stream velocity. The experimentally determined wavelength fell near the theoretically predicted maximum amplified wavelength and clearly varied with Görtler number as predicted. These results probably were obtained because of the excellent low-turbulent environment and the absence of the opposite channel wall in this experiment.

There are still considerable discrepancies between the various theoretical models of the Görtler vortex phenomena. These discrepancies are most significant in the region of the neutral curve, where disturbance amplification begins. However, these theoretical

models all agree as to the predicted correlation between spacing and Görtler number. The results of the present experiment confirm this important correlation, and thus lend increased credibility to the theoretical predictions.

(J. Ray Dagenhart, 4515)



Görtler model in LTPT with five-beam laser velocimeter.

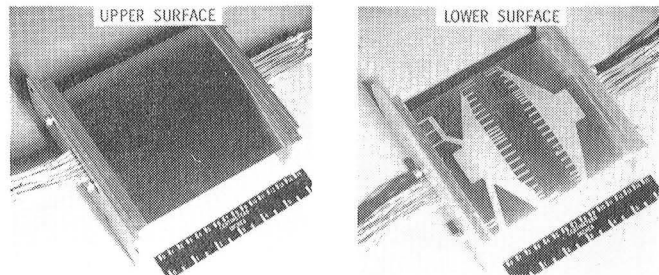
High-Speed Natural Laminar Flow Airfoil

Recent airfoil tests have been conducted at NASA Langley Research Center to aid in the design of high-performance business jets. The airfoil, designated the HSNLF(1)-0213, was tested in the Langley 6- by 28-Inch Transonic Tunnel for cruise performance and in the Low-Turbulence Pressure Tunnel for low-speed maximum lift. The airfoil was an out-growth of a low-speed general aviation airfoil originally generated by Jeff Viken of ESCON, Inc. Together with Viken, Langley researchers applied both two- and three-dimensional transonic codes to modify the low-speed airfoil to operate at a Mach number of 0.7 and a lift coefficient of approximately 0.25. The resulting airfoil pressure distribution provided laminar boundary layers on approximately 50 percent of the upper surface and 70 percent of the lower surface at the design Mach number.

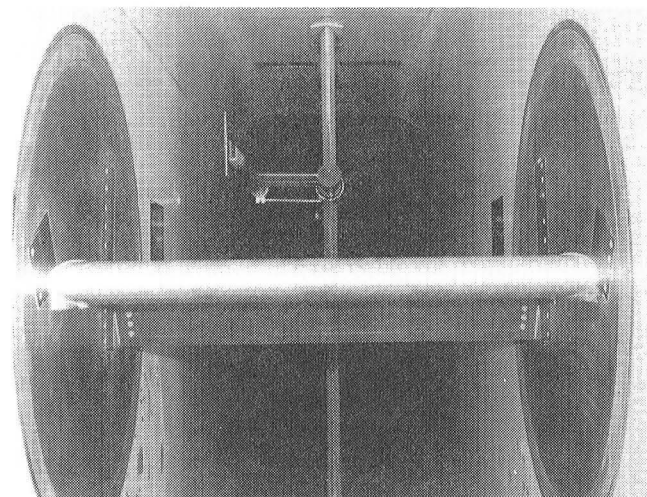
The airfoil was first tested in the 6- by 28-in. tunnel to determine its performance at cruise and climb conditions. The model had a 6-in. chord and was instrumented for static pressure measurements with 51 orifices distributed on both upper and lower surfaces of the model. The tubes to the orifices were routed entirely on the lower surface and the passage-

ways were covered with metal filler. This allowed the smooth upper surface necessary to achieve the maximum laminar boundary layer lengths possible with the existing turbulence level in the tunnel. Pressures measured on the model were integrated to give normal force and pitching moment, and drag was determined by total pressure surveys of the vertically traversing wake probe. The model was tested with smooth surfaces and with forced transition located 0.05 chord downstream of the nose (both sides). Although the smooth model surfaces did result in drag reductions relative to the forced-transition test, the high turbulence level in this tunnel (a blowdown facility) reduced the extent of the laminar boundary layers below their expected free-air values.

After the high-speed investigation, the airfoil was tested at low speeds in the Low-Turbulence Pressure Tunnel with the 2-ft chord length model shown here. These tests determined the maximum lift of the



Pressure model of HSNLF(1)-0213 airfoil tested in 6- by 28-in. tunnel.



Force balance model of HSNLF(1)-0213 airfoil with split flap mounted in LTPT.

airfoil and were conducted with and without the split flap, which acted as a simple high-lift device. In contrast to the model used in the high-speed test, this model had no pressure instrumentation and was mounted into a unique external balance system especially designed for high-lift models. The balance system provided normal force and pitching moment, and a wake survey probe behind the model furnished the drag data. The preliminary data from this test indicated that the basic airfoil produced maximum lift values that were very close to earlier theoretical estimates.

(William G. Sewall, 4514)

Laminar Suction Surface Investigations

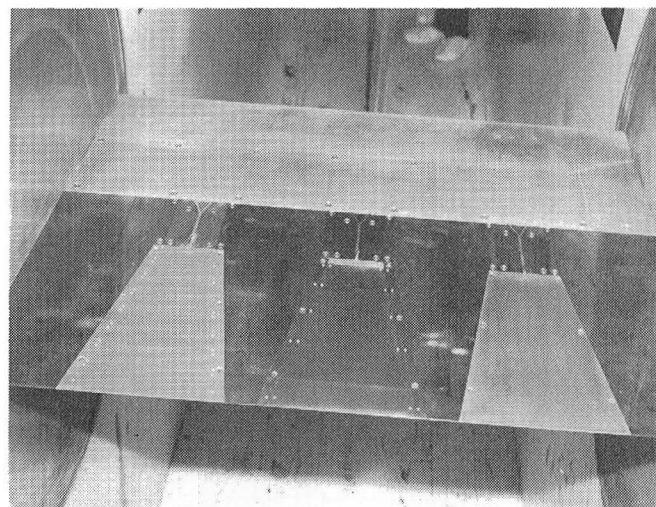
Present-day underwater weapons operate at Reynolds numbers per foot up to 6×10^6 and are expected to approach 10×10^6 . If a laminar boundary layer could be maintained on these weapons, their effectiveness and efficiency would benefit greatly. The application of surface suction is one of the most effective means of controlling the boundary layer; however, there was considerable doubt whether surface and suction detail could be sufficiently refined to prevent premature transition of the very thin laminar boundary layer near the start of suction. The purpose of this experiment was to parametrically investigate suction stabilization of the laminar boundary layer up to unit Reynolds numbers of 10×10^6 per foot. The model, which was basically a flat plate with a wedge-shaped lower surface, spanned the 3-ft test section width. The plate had a leading-edge radius of 0.03 in. and was mounted at a fixed angle of attack of -0.5° to avoid an adverse pressure gradient at the leading edge. This arrangement produced a slight flow acceleration over the chord of the plate.

The primary instrumentation was a twin total-head probe, which was used to detect thickening of the boundary layer at transition. This instrumentation was supplemented by flush hot-film burst detectors. Chordwise and spanwise pressure distributions and differential pressures across the skin and associated suction flow rates were measured, recorded, and analyzed as part of the experiment. A major model design feature was the provision for three spanwise inserts in the plate, as illustrated. The three-panel model was employed primarily to minimize the adverse effects of stream particulates. Although the

Low-Turbulence Pressure Tunnel stream is as particle free as that of any known facility, at the highest pressures required to generate the high Reynolds numbers, premature transition is sometimes triggered by particle impingement. With the model used in this experiment, if one surface became contaminated at the higher Reynolds numbers (as it did approximately 5 percent of the time for nonsuction and 14 percent of the time for suction surfaces), the test could be continued and useful data obtained on the remaining two surfaces without the loss of time required to depressurize the tunnel and clean the model.

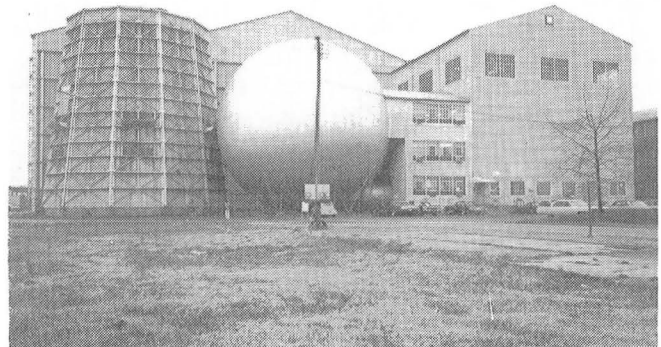
A matrix of 12 types of suction surfaces was investigated over a range of Reynolds numbers up to 10×10^6 . All porous inserts were 1 ft long, so that the length Reynolds numbers corresponded directly to unit Reynolds numbers. The results showed that several of the candidate suction surfaces could be successfully employed to maintain laminar flow over the full Reynolds number range.

(Robert J. McGhee, 4514)



Three-panel laminar suction model mounted in LPTP.

20-Foot Vertical Spin Tunnel



The Langley 20-Foot Vertical Spin Tunnel is the only operational spin tunnel in the United States and one of only two in the free world. The tunnel, which is used to investigate spin characteristics of dynamically scaled aircraft models, is vertical with a closed-circuit annular return passage. The vertical test section has 12 sides and is 20 ft wide and 25 ft high. The test medium is air. Tunnel speed can be varied from 0 to 90 ft/sec with accelerations to 15 ft/sec². This facility is powered by a 1300-horsepower main drive.

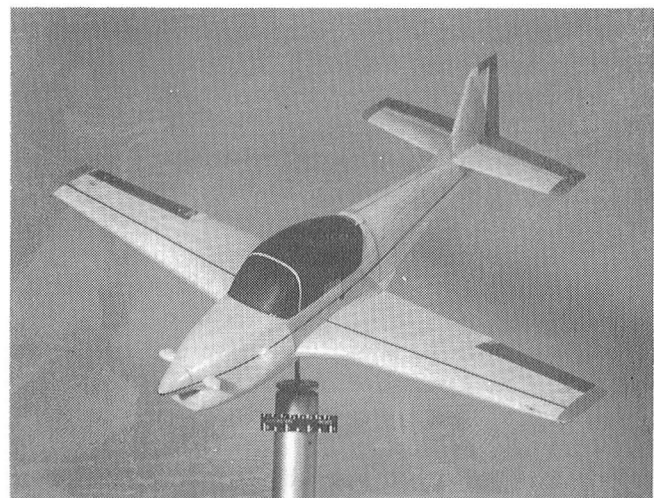
Spin recovery characteristics are studied via remote actuation of the aerodynamic controls of models to predetermined positions. Force and moment testing is performed with a gooseneck rotary-arm model support, which permits angles of attack from 0° to $\pm 90^\circ$ and sideslip angles from 0° to $\pm 20^\circ$. Motion picture and video records are used to record the spinning and recovery characteristics in the spin tunnel tests. Force and moment data from the rotary balance tests are recorded in coefficient form and stored on magnetic tapes.

The free-spinning tests showed a moderately flat, smooth spin near 60° angle of attack at 2 to 3 seconds per turn. Acceptable recovery from this mode required full aft stick while the rudder and aileron were reversed. With elevators deflected, neutral, or trailing edge down, the rudder was rendered ineffective for recovery. Rotary balance tests studied the geometric variables involved in the horizontal- and vertical-tail interference and a number of promising modifications were developed, including changes in horizontal-tail location, changes in rudder design, changes in elevator planform, and aft fuselage strakes. Free-spinning tests confirmed the effectiveness of these modifications.

The success of this initial effort has produced a cooperative follow-on research program in which the pressure fields on the BPTA empennage at spinning attitudes will be studied in the spin tunnel.
(Raymond D. Whipple, 2244)

Spin Tunnel Investigation of Australian Basic Pilot Training Airplane

At the request of the Department of Defense, an investigation was conducted in the 20-Foot Vertical Spin Tunnel to evaluate the spin and recovery characteristics of the proposed Australian Basic Pilot Training Airplane (BPTA) and to provide the designers with configuration development information pertinent to the spinning characteristics. The investigation consisted of free-spinning tests with a $1/15$ dynamically scaled model and rotary balance tests with a $1/7$ -scale model.



Australian BPTA $1/15$ dynamically scaled wind tunnel model.

Testing Modifications and Updates of Military Aircraft

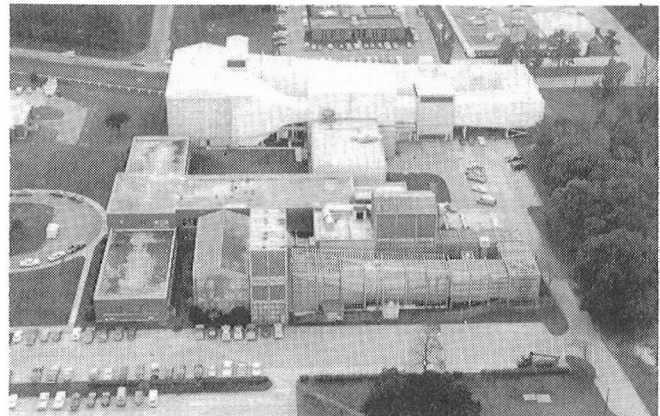
Many changes occur in a configuration during the design, development, and subsequent service life of a military airplane. Some of these changes may affect the spinning characteristics, and follow-on model tests are then often requested by the Department of Defense.

The original spin tunnel investigations of the YF-16 and F-16A configurations were performed in 1975 and 1978, respectively. The U.S. Air Force then requested new tests of the F-16C/D to assess the effects of inertial changes and the adequacy of the existing emergency spin recovery parachute for flight tests of large lateral asymmetry external store loadings. Model tests showed that the existing spin recovery parachute would provide acceptable emergency recovery for spins with up to 35,000 ft-lb of lateral asymmetry providing the automatic spin prevention control system was functioning properly.

The T-46A Air Force Trainer design was originally tested in the spin tunnel in 1983. The model tested had an aspect ratio of 8.5, but during subsequent configuration development the aspect ratio was changed to 9.0 and model tests were requested to assess any effects on the spinning characteristics due to this change. Scaled wing tip extensions were fabricated and experiments were performed for both erect and inverted spins. Model results showed only minor effects on the spin and spin recovery characteristics of the T-46A due to the increased aspect ratio.

(Raymond D. Whipple, 2244)

7- by 10-Foot High-Speed Tunnel



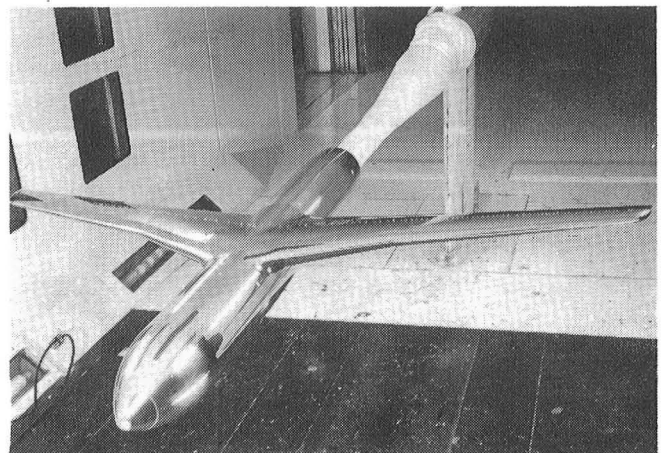
The Langley 7- by 10-Foot High-Speed Tunnel is a closed-circuit single-return continuous-flow atmospheric tunnel with a test section 6.6 ft high, 9.6 ft wide, and 10 ft long. A 14,000-horsepower electric motor drives a series of fan blades to provide subsonic operating speeds from Mach 0.2 to Mach 0.9 and to produce a maximum Reynolds number of 4×10^6 per foot. In addition to static testing of complete and semispan models, the facility is equipped for both steady-state roll and oscillatory stability testing.

Currently the facility is playing an important role in a wide range of basic and applied aerodynamics research, including advanced vortex lift concepts, fuel-conservative aircraft design technology, highly maneuverable aircraft concepts, and the development of improved aerodynamic theories such as the difficult separated-flow and jet interaction effects needed for computer-aided design and analysis.

numbers from 1.2 to 4.0×10^6 with wing transition both fixed and free and with vortex generators mounted on the wing.

Preliminary comparisons between results for the baseline wing and the current wing show better aerodynamic characteristics for the current wing. The current wing has a flatter pressure distribution with a slightly weaker shock, which is located further aft. It also appears to have better drag rise characteristics at the higher lift coefficient.

(E.B. Plentovich, 2601)



NTF Pathfinder-I Lockheed-Georgia Wing Correlation Studies

A cooperative test with Lockheed-Georgia was conducted in the 7- by 10-Foot High-Speed Tunnel. A Lockheed-Georgia supercritical wing was tested on the National Transonic Facility (NTF) Pathfinder-I fuselage to develop a data base for comparison with results from a future NTF investigation. The results of this investigation will also aid Lockheed-Georgia in validating their current theoretical wing design procedure. (The present wing was designed with Lockheed-Georgia's current design procedure in an effort to increase the aerodynamic efficiency of a previous baseline wing.) The model was tested at Mach numbers from 0.20 to 0.85 and Reynolds

NTF Pathfinder-I with Lockheed-Georgia wing mounted in 7- by 10-Foot High-Speed Tunnel.

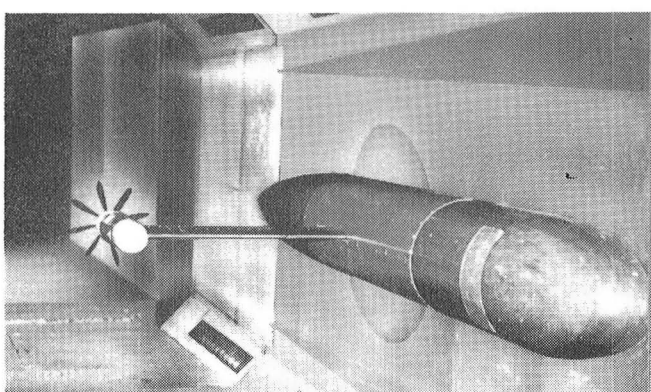
Wing-Tip-Mounted Pusher Turboprop

It has been proposed that a wing-tip-mounted pusher turboprop will enhance installed propeller performance. Tests have been conducted recently in

the 7- by 10-Foot High-Speed Tunnel to determine this performance increase. Force data were obtained for a semispan model with an SR-2 high-speed propeller mounted on the tip of the unswept, untapered wing at a Mach number of 0.7 and angles of attack from -2.0° to 5.0° .

Preliminary analyses of these data indicated that the propeller performance was increased through the positive-angle-of-attack range as a result of the propeller's location just aft of the wing trailing edge at the wing tip, where it is immersed in the lift-induced vortex flow. This improvement in performance, or vortex energy recovery, is manifested as a reduction in power required from the propulsion system of an aircraft to maintain the required thrust level for each mode of operation. In addition, a large reduction in induced drag on the wing was also obtained as a result of the high-speed turboprop wake causing the now-weakened wing tip vortex to dissipate.

(J.C. Patterson, Jr., 2673)



Semispan model with wing-tip-mounted high-speed propeller.

F-106 Vortex Flap Study

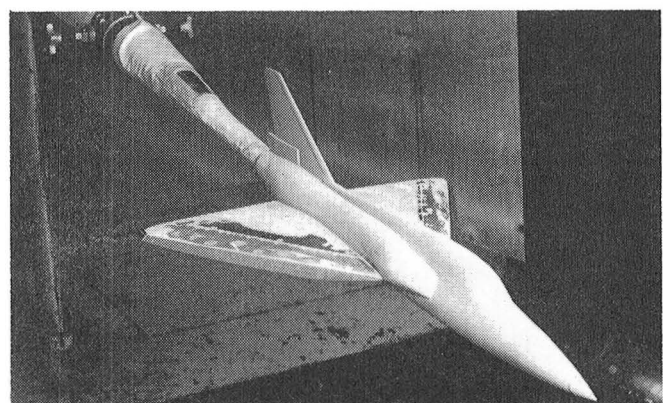
In support of a proposed flight demonstration of the vortex flap concept, four vortex flap configurations were designed for the F-106B aircraft with the use of analytical tools developed at Langley. These configurations were subsequently tested in the Langley 7- by 10-Foot High-Speed Tunnel with a 1/20-scale model. Static longitudinal force and moment data and dynamic wing root bending moment data were obtained for a range of vortex flap and elevon deflection angles at Mach numbers up to 0.8 and angles of attack up to 24° . Lateral-directional

data and dynamic wing root bending moment data were obtained for a limited number of configurations.

Test results indicated that several of these vortex flap configurations developed the desired design point flow field, which called for a leading-edge vortex with primary reattachment at the flap hinge line. The effective leading-edge suction and vehicle performance levels were close to those predicted. The performance of these flaps also exhibited a markedly low sensitivity to flap deflection angle and to some geometric changes made during the investigation. Other flap configurations, however, did not achieve the design flow field and the performance was lower than predicted. Test results indicate that the low performance is associated with a weaker leading-edge vortex system than was predicted theoretically and also with significant surface flow separation at the wing-flap juncture. Further experimental research has shown that these effects are due in part to the small hinge line radius and low test Reynolds number used.

Dynamic wing root bending moment measurements obtained for several flap configurations indicated significant improvements in buffet onset lift coefficient relative to the conically cambered baseline wing.

(James B. Hallissy, 2601)



F-106B 1/20-scale vortex flap model.

Subsonic Tests of Circular-Body Earth-to-Orbit Transport

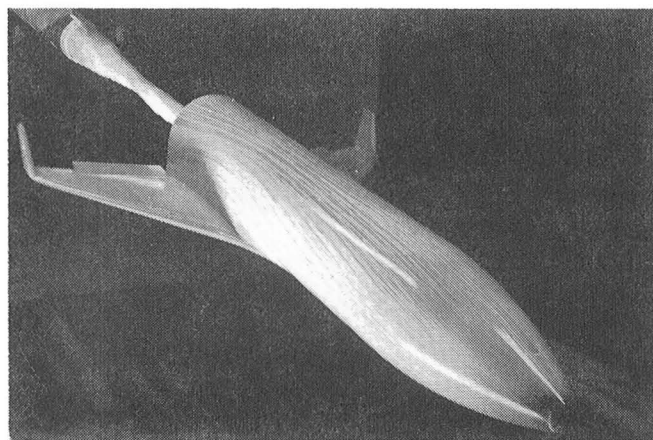
Structural mass of Earth-to-orbit transports is a critical factor in determining their developmental cost and operational efficiency. In this regard, an

advanced transport has been configured with a circular body cross section to determine if such a shape will be suitable from the standpoint of heating and aerodynamics for the Earth-to-orbit and return mission. Force and moment tests at Mach 20 and heating tests at Mach 10 suggest that the round fuselage configuration is suitable.

Wind tunnel tests were conducted in the 7- by 10-Foot High-Speed Tunnel at a Mach number of 0.3 to determine the longitudinal stability and trim characteristics of the circular-body/delta-wing combination. As an adjunct to the basic tests, three different aerocontrol devices for directional control were assessed: a center tail, two tip fins, and a forward-mounted dorsal. Results showed that the tip-fin vehicle is longitudinally stable and trims near the maximum lift-to-drag ratio to give a landing speed of about 200 knots. The results are only slightly different for the tail and dorsal configurations.

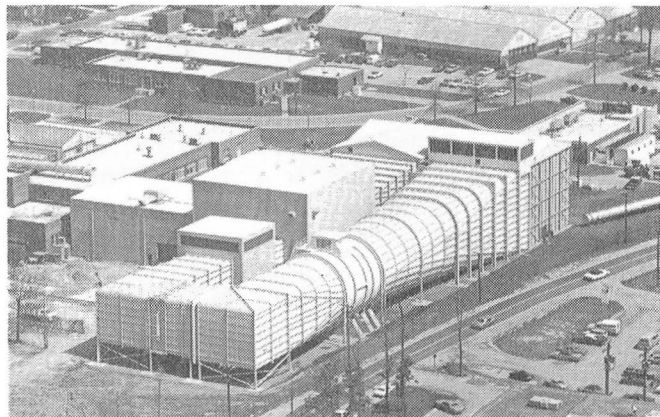
Tests of the yaw control devices show that the dorsal (a forward-located top-mounted vertical fin) is the most effective for yaw control based on profile area and the amount of control obtained per degree of control surface deflection. However, the device requires active controls. Tip fins were found to be intermediate relative to the vertical tail and the dorsal in surface area (and weight) and levels of lateral stability. Analysis of the data is in progress and oil flow photographs taken during the tests are being used to assist in the analysis of the force and moment data. No pilot canopy is utilized in the design; the vehicle is landed either with the use of an autopilot system or with the aid of a nose-gear-deployable television camera.

(Ian O. MacConochie, 4953)



Circular-body Earth-to-orbit transport model during oil flow tests in 7- by 10-Foot High-Speed Tunnel.

4- by 7-Meter Tunnel



The Langley 4- by 7-Meter Tunnel (formerly V/STOL Tunnel, or Vertical/Short Takeoff and Landing Tunnel) is used for low-speed testing of powered and unpowered models of various fixed- and rotary-wing civil and military aircraft. The tunnel is powered by an 8000-horsepower electrical drive system, which can provide precise tunnel speed control from 0 to 200 knots with the Reynolds number per meter ranging from 0 to 0.64×10^7 . The test section is 4.4 m high, 6.6 m wide, and approximately 15.2 m long. The tunnel can be operated as a closed tunnel with slotted walls or as one or more open configurations when the side walls and ceiling are removed to allow extra testing capabilities, such as flow visualization and acoustic tests. The tunnel is equipped with a two-component laser velocimeter system. Furthermore, boundary layer suction on the floor at the entrance to the test section and a moving-belt ground board for operation at test section flow velocities up to 70 knots can be installed for ground effect tests.

augmentor operating and a flow-through inlet) from hover through transition to cruise flight. The model was tested from static free-stream conditions (Mach = 0) to a free-stream Mach number of 0.20. The augmentor was operated up to a maximum nozzle pressure ratio of 3.5. The angle of attack was varied from 0° to 25° and sideslip angles were varied from -15° to 15°. In addition, elevon deflections were tested together and differentially from -20° to 20° to evaluate control effectiveness (pitch and roll) with and without the augmentor operating.

Preliminary results indicate that the augmentor performance would be sufficient for hover and transition at landing weight when used in combination with a vectoring main nozzle. The overall configuration aerodynamics and control effectiveness, with and without the augmentor operating, indicate acceptable characteristics for this type of configuration throughout the transition flight regime.

(D.W. Banks, 3611)

Advanced Powered-Lift STOVL Fighter Configuration

A 30-percent scale model of the General Dynamics E-7 advanced short takeoff and vertical landing (STOVL) configuration was tested in the Langley 4- by 7-Meter Tunnel. The E-7 configuration employs an in-wing-mounted augmentor in conjunction with a vectoring main nozzle to generate the necessary powered lift for STOVL. In cruise flight, the augmentor doors are designed to fold into the wing to provide a clean profile. The purpose of this investigation was to determine the static augmentor performance and the overall configuration aerodynamics (with the



Advanced powered-lift fighter configuration tested in 4- by 7-Meter Tunnel.

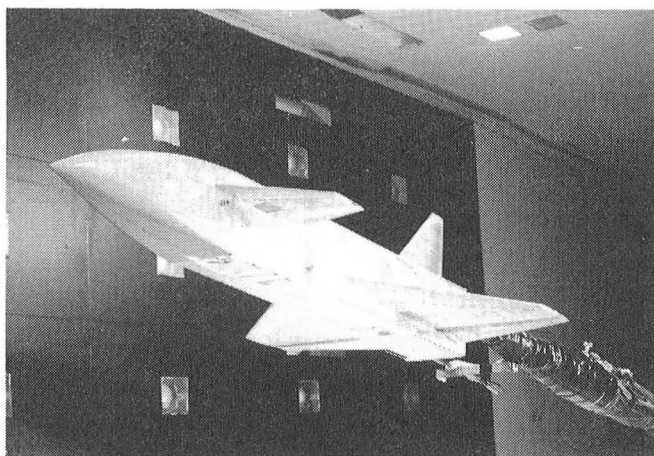
Propulsive Wing/Canard Fighter for STOL Operations

As part of the aerodynamic research directed at short takeoff and landing (STOL) performance for advanced fighter aircraft, an internally blown flap system was tested on a close-coupled wing/canard configuration. The main objectives of the investigation were to determine the effect of the relative locations of the wing and canard on the aircraft longitudinal aerodynamics and define the relationship between the percentage of the flap (on both the wing and canard) subjected to blowing and increases in induced lift. Measurements of surface pressure distributions and of the downwash behind the wing were also made.

As a result of this test and other tests on this configuration, the high-canard/low-wing combination was determined to be best for overall performance. Blowing over the entire span of the flaps resulted in the most induced lift. The large nose-down pitching moments produced by the wing flaps can be offset by the significant nose-up pitching moments generated by the blown canard. The configuration can be trimmed by adjustments to the flow to each surface.

This program, supported by NASA Langley, the U.S. Air Force Wright Aeronautical Laboratories, Rockwell-Columbus, and the U.S. Navy, will continue with extensive testing of the preferred configuration (high canard, low wing) and a modified fuselage.

(G.T. Kemmerly, 3611)



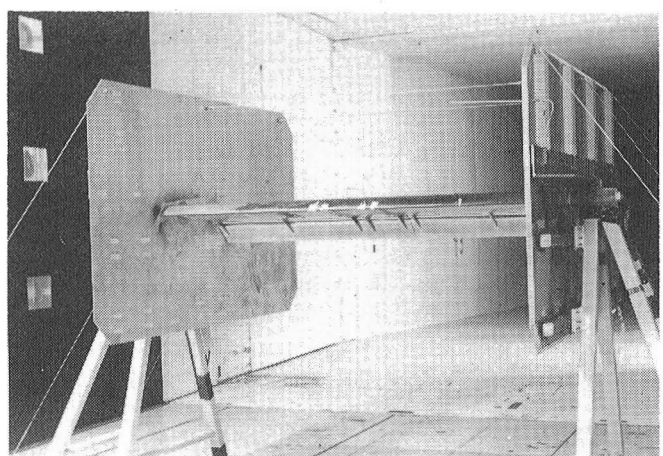
Propulsive wing/canard fighter model in 4- by 7-Meter Tunnel.

Two-Dimensional Tests of Heavy Rain Effects on Airfoil Performance

Tests were conducted recently in the 4- by 7-Meter Tunnel to investigate the effects of heavy rain on airplane performance. The wing model used was an NACA 64-210 airfoil with a leading-edge slat and double-slotted flap. The model had an 8-ft span and a 2½-ft chord and was mounted between two end-plates. The center 1-ft span of the wing was isolated from the outboard panels through a six-component balance. The center section was also instrumented with a few static pressure ports and 12 electrical resistivity sensors to determine water film thickness on the airfoil surface. Additionally, a photographic technique incorporating a fluorescent dye in the water was used to characterize the water film on the wing surface.

The spray manifold was located 25 ft upstream from the model so as to produce a nearly uniform spray over the center section of the wing. The spray concentration could be varied to produce equivalent rainfall rates from 14 to 59 in/hr. The tunnel dynamic pressure was varied from 15 to 70 psf. Results indicated that for the flapped configuration, the maximum lift capability was significantly reduced. Additionally, the wing was found to stall at a lower angle of attack when water was sprayed on it. The water spray increased the airfoil drag prior to stall. The extrapolation of these two-dimensional model test results to full scale and to complete aircraft configurations is being assessed.

(R. Earl Dunham, Jr., 3274)



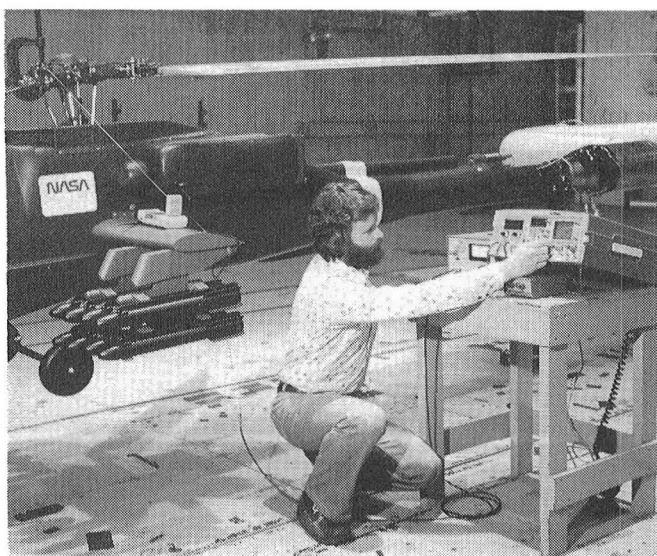
Heavy rain effects wing model installed in 4- by 7-Meter Tunnel.

Critical Fastener Preloading for Army Helicopter Model

An emerging problem in aerospace structures is the integrity of critical fasteners. This problem manifests itself in the determination of proper bolt preload in practical systems. The current practice of torquing bolts can lead to serious errors in preload brought on by statistical variations of friction. Because it is difficult to achieve accuracies better than 20 percent under optimum conditions, unacceptable errors in torquing systems can occur. Langley has developed a family of instruments for achieving critical preload. The system utilizes ultrasonic natural velocity characterization to determine changes in stress.

The latest concept is a pulsed phase-locked loop (P2L2) device capable of resolving 1 psi in steel. The system is neither continuous wave (CW) nor pulse echo (PE); it is a narrowband device that eliminates propagation complexities in broadband pulsed systems while bypassing standing-wave CW problems. The capability of the technique was recently demonstrated when critical fasteners were tested on a model helicopter rotor assembly in the 4- by 7-Meter Tunnel.

(Joseph S. Heyman, 3036)



Critical fastener preloading tested on model helicopter rotor assembly in 4- by 7-Meter Tunnel.

Advanced Rotor Design for AH-64 Helicopter

A 27-percent scale model of the U.S. Army AH-64 main rotor and fuselage was tested in the 4- by 7-Meter Tunnel. Two different rotors were evaluated during the test program. The first rotor was an aerodynamically scaled model of the current AH-64 rotor configuration and the second was an advanced configuration designed by Army researchers to have improved hover and forward-flight performance. The aerodynamic design of the advanced blades is based on a methodology of integrating rotor and airfoil technology which was developed and successfully demonstrated during an earlier UH-1 configuration study. The advanced blades utilize three airfoils developed at Langley especially for helicopter application. Thin tapered tips were used to reduce drag, and the blade twist was increased from 9° to 12°. The advanced blade is rectangular to 0.8 radius and then tapered to the tip with a taper ratio of 5. The nonrectangular planform is made practical by the use of composite materials.

The test data indicated performance improvements in hover and forward flight with an increase in figure of merit (hover efficiency) of 6 percent at design gross weight, sea level standard. This result indicates a power saving of 6 percent in hover, or a 4-percent (580-lb) increase in lift capability. These values are judged to be conservative because of model scale effects. Improvements in forward-flight performance have also been measured and will result in fuel savings and increased range. The results of this research can now be coupled with other recent technology developments in advanced rotor design to enhance not only hover performance but high-speed flight and maneuverability as well.

(Henry Kelley, 3611)



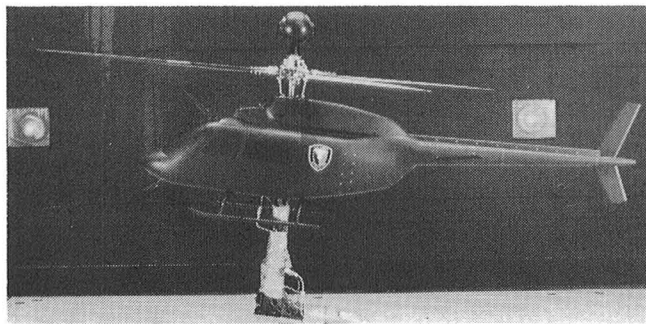
AH-64 scale model in 4- by 7-Meter Tunnel.

Advanced Helicopter Scale Model Wind Tunnel Tests

The Army Helicopter Improvement Program (AHIP) for development of an OH-58D helicopter is the latest in a series of Army efforts to develop and acquire an advanced scout helicopter. One of the more unusual features to be incorporated into the OH-58D is a MAST-Mounted Sight (MMS) located above the rotor hub. Because the effect of the MMS wake on the aircraft characteristics and the empennage performance is difficult to predict with confidence, a wind tunnel test was conducted with a powered scale model in the Langley 4- by 7-Meter Tunnel.

The primary purpose of the test was to evaluate major flow field characteristics rather than to define rotor performances parameters or evaluate dynamic properties of the rotor. Therefore, an existing general research model rotor was used in conjunction with a newly fabricated 21-percent scale model of the OH-58D airframe. Six components of force and moment data were obtained for the airframe and rotor separately at each test condition. Wind speeds ranged from 0 to 100 knots and rotor speed was maintained at full-scale tip speed. Thrust, angle of attack, and angle of yaw were varied to represent full-scale flight conditions. The data obtained from the tests showed that with the rotor off, the MMS caused an increase in D/q (equivalent flat-plate drag) of about 3.2 ft² and resulted in a nose-up trim moment, as expected. However, with the rotor on at low wind speeds (approximately 40 knots) the D/q increased to 15 ft². At higher wind speeds, D/q decreased to the rotor-off value. An extensive analysis of the data has been conducted and information regarding the tests has been given to the AHIP contractor.

(Arthur Phelps, 3611)



OH-58D advanced helicopter scale model in 4- by 7-Meter Tunnel.

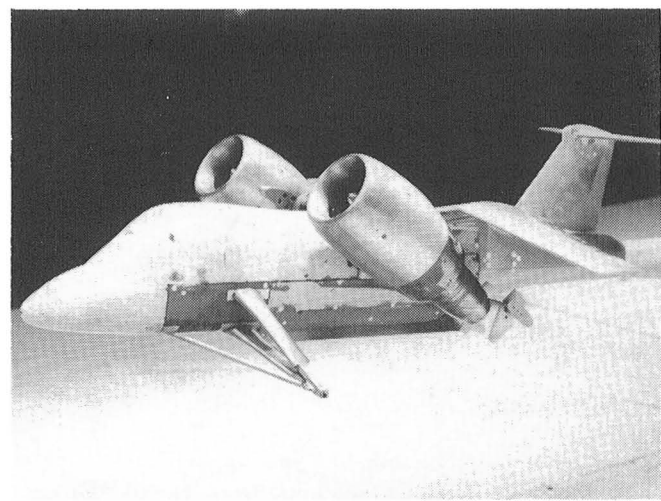
Grumman 698 V/STOL Transport Configuration

In support of vertical short takeoff and landing (V/STOL) transport research being conducted at the NASA Ames Research Center, a test was conducted in the Langley 4- by 7-Meter Tunnel to measure the transition aerodynamics of the Grumman 698 V/STOL concept. The 698 configuration was developed by Grumman Aerospace Corp. for possible use by the U.S. Navy. The configuration uses tilt nacelles to provide powered lift and has lateral and longitudinal deflector vanes in the engine exhaust for control during hover and transition flight. It has a high wing with a slight degree of forward sweep and is designed for deployment at sea.

The wind tunnel model was equipped with two six-component balances (one for nacelle forces, the other for total model forces), surface pressure ports on the wing and nacelles, and pressure rakes in the engine intakes and exhaust. The engines were simulated by tip-driven turbines.

The measured test results provided the required database on the configuration lateral and longitudinal characteristics to conduct flight simulations of hover and transition for pilot evaluation. The measured wing and external nacelle pressures are used to define engine/airframe interactions in various flight regions, and the pressures measured inside the engine simulations are used to indicate nacelle performance and flow distortion.

(P. Frank Quinto, 3611)

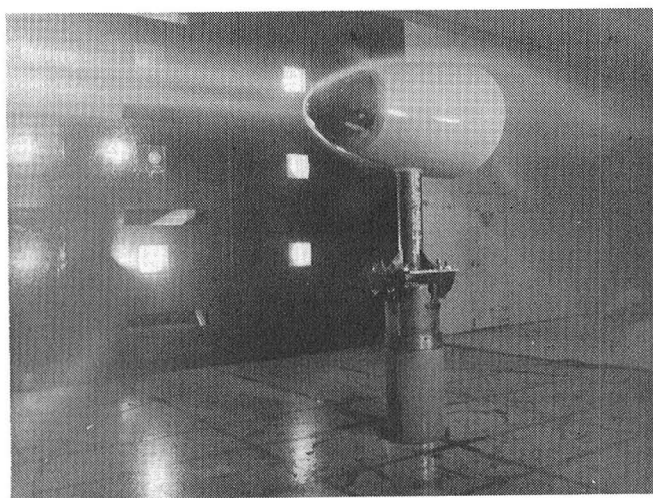


V/STOL transport configuration in 4- by 7-Meter Tunnel.

Rain on Radome During Simulated Flight

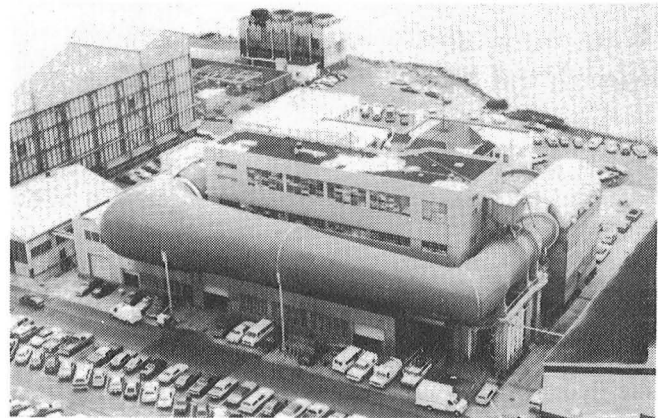
A joint research effort was conducted by NASA and the FAA to examine whether aircraft weather radomes could support a significant surface water layer when subjected to conditions simulating flight in heavy precipitation. An experiment was conducted in the 4- by 7-Meter Tunnel, which was equipped with a water spray system. A T-39 radome was instrumented with two microwave reflectometer sensor units, one at the stagnation point and the other approximately 30° off the stagnation point. The amplitude and phase of the reflected microwave signals were recorded during several tests in which the water spray concentration and wind speed were varied to simulate flight in heavy rain. The surface water layer thickness was inferred from these reflectometer measurements through analytical models. The results indicated that no significant liquid water layer formed on the radome under the tunnel test conditions. However, a concentrated water "sheath" was observed standing away from the radome, and its effects on weather radar performance should be investigated further. Additional wind tunnel experiments as well as flight tests will likely be required in order to more conclusively determine weather radar performance degradation due to flight in heavy rain.

(M.C. Bailey, 3631)



T-39 radome mounted in 4- by 7-Meter Tunnel.

8-Foot Transonic Pressure Tunnel



The Langley 8-Foot Transonic Pressure Tunnel is a closed-circuit single-return variable-density continuous-flow wind tunnel. The test section walls are slotted (5 percent porosity) top and bottom, with solid sidewalls fitted with windows for schlieren flow visualization. In 1982 the facility was modified for flow quality improvements and reconfigured for low-drag testing of a large-chord swept laminar flow control airfoil at transonic speeds. A honeycomb and screens were permanently installed in the settling chamber to suppress the turbulence level in the test section. A contoured liner was installed on all four walls of the test section to simulate interference-free flow about an infinite yawed wing. This contoured liner produces a contraction ratio of 25:1 and covers existing floor and ceiling slots. An adjustable sonic throat is also located at the end of the test section to block upstream propagation of diffuser noise.

The combination of honeycomb, screens, and choke provides a very low disturbance level in the test region at transonic speeds. Except for the honeycomb and screens, the changes are reversible. In the current configuration, the stagnation pressure can be varied from about 0.25 to 1.25 atm up to a Mach number of less than 0.85 with the transonic slots closed by the liner. The stagnation temperature is controlled by water-cooled fins upstream of the settling chamber. Tunnel air can be dried by a dryer that uses silica gel desiccant to prevent fogging due to expansion in the high-speed nozzle.

Laminar Flow Control Tests

The reduction of drag and hence an increase in vehicle performance has always been one of the primary research goals of aerodynamicists. Large

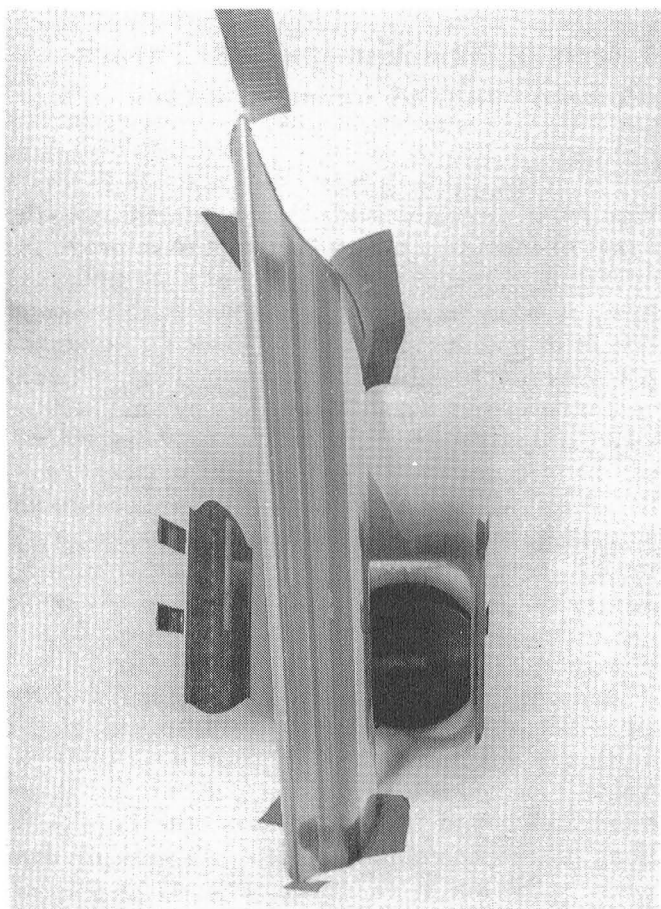
decreases in friction drag can be realized if a laminar boundary layer can be maintained either by passive natural laminar flow (NLF) controlled through geometric shaping or by active laminar flow control (LFC), which usually depends both on shaping and on mass transfer through local surface suction. Langley researchers have defined an experiment with the overall objective of investigating the physical phenomena associated with laminar flow and low-profile drag on advanced swept supercritical airfoils. Furthermore, tests will allow the evaluation and documentation of the combination of suction control laminarization and supercritical airfoil technology at conditions typical of high-performance transports.

Performance testing with the Laminar Flow Control (LFC) Experiment installed in the 8-Foot Transonic Pressure Tunnel has been ongoing since September 1982. This research has involved the advanced swept supercritical airfoil, the suction system, and the tunnel liner. Two suction surface concepts will be evaluated for maintaining laminar flow over the same airfoil geometry for separate tunnel tests. One concept involves the slow-moving air near the surface being removed through discretely spaced fine slots along the airfoil span and the other accomplishes this by suction through porous spanwise strips.

Results to date on the swept airfoil with discrete slots indicate that full-chord suction laminarization can be achieved with very low drag up to high speeds and high Reynolds numbers. Suction laminarization over an extensive supercritical zone was also obtained for high chord Reynolds numbers before transition moved forward. The measured suction drag represents about two-thirds and the wake drag about one-third of the total drag, and this drag is considerably below that for an equivalent turbulent airfoil. Hybrid LFC concepts were investigated on the present airfoil configuration by a progressive turning off of suction

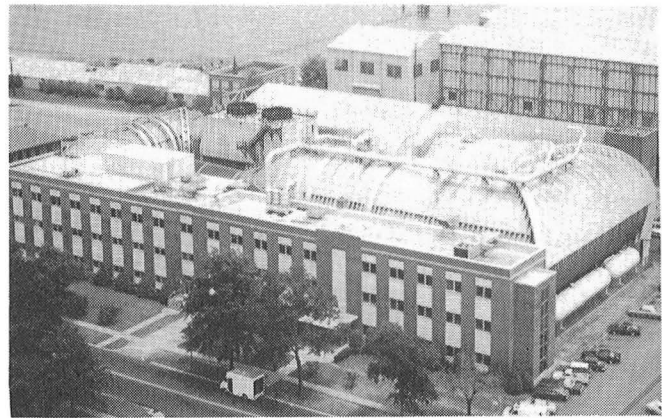
from the trailing-edge to leading-edge regions. The hybrid results indicated that extensive LFC could be maintained beyond chordwise termination of suction for subcritical speeds and significantly beyond for supercritical speeds. The extent of these hybrid LFC results decreased with increasing Reynolds number. The overall slotted surface results demonstrated that LFC and supercritical airfoil technology is compatible with low drag, depending upon the extent of the suction laminarization zone applied.

(W.D. Harvey, 2631)



LFC equipment installed in 8-ft TPT.

Transonic Dynamics Tunnel



Conversion of the original Langley 19-Foot Pressure Tunnel into the Transonic Dynamics Tunnel (TDT) was begun in the late 1950's to satisfy the need for a large transonic wind tunnel dedicated specifically to work on the dynamics and aeroelastic problems associated with the development of high-speed aircraft. Since the facility became operational in 1960, it has been used almost exclusively to clear new designs for safety from flutter and buffet, to evaluate solutions to aeroelastic problems, and to research aeroelastic phenomena at transonic speeds.

The tunnel is a slotted-throat single-return closed-circuit wind tunnel with a 16-ft² test section. The stagnation pressure can be varied from slightly above atmospheric to near vacuum, and the Mach number can be varied from 0 to 1.2. Both test section Mach number and density are continuously controllable. The facility can use either air or Freon 12 as the test medium. Freon is usually used because it has several advantages over air as a test medium for dynamically scaled aeroelastic model testing. The tunnel has a Freon reclamation system so that the gas can be purified and reused.

The facility is equipped with many features uniquely suited to dynamic and aeroelasticity testing. These include a computerized data acquisition system especially designed to rapidly process large quantities of dynamic data, a means of rapidly reducing test section Mach number and dynamic pressure to protect models from damage when aeroelastic instabilities occur, a system of oscillating vanes to generate sinusoidal variations in tunnel flow angle for use in gust response studies, and special mount systems which enable simulation of airplane free-flight dynamic motions.

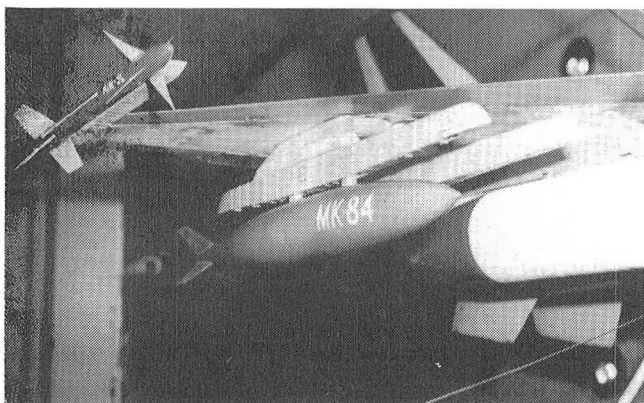
Effects of New Multipurpose Pylons on F-16 Flutter Characteristics

Modern fighter airplanes such as the F-16 are required to carry stores on pylons mounted under the wings of the aircraft. In an attempt to improve the operating efficiency of the F-16, a new multipurpose pylon is being developed which will enable several bombs or missiles to be quickly loaded onto an airplane in order to reduce the turnaround time between combat missions. The multipurpose pylons (MPPs), which are larger and heavier than previous pylons, can carry stores on two side-by-side launcher rails.

A test was conducted in the TDT with a $\frac{1}{4}$ -scale aeroelastic model of the F-16 airplane to determine the effects of MPPs on F-16 flutter characteristics. The model, which was mounted on the two-cable mount system, had a wing span of about 7.5 ft. The photograph shows a view looking downstream and up underneath the right wing of the model. An air-to-air missile can be seen on the wing tip and the aft portion of a fuel tank near the wing root. An MPP, which is located at the wing midspan, has an MK-84 bomb attached to its outer rail. For other configurations, different combinations of stores were installed on the MPPs and at the other store locations on each wing. A total of 21 configurations were tested.

The experimental results showed that the airplane flight envelope will be restricted by flutter if MPPs like the ones tested are used on the F-16. This result was consistent with those obtained by analysis. In an attempt to reduce the flight restrictions, the location and stiffness of attachment points between the stores and the MPPs were varied. The changes,

however, had little effect on the flutter characteristics. General Dynamics, the MPP designer, is currently using the wind tunnel test data and analytical results to develop modifications to the MPP design that will provide satisfactory flutter characteristics. (Moses G. Farmer, 2661)



Multipurpose pylons tested on F-16 model.

Spanwise Curvature Raises Flutter Dynamic Pressure

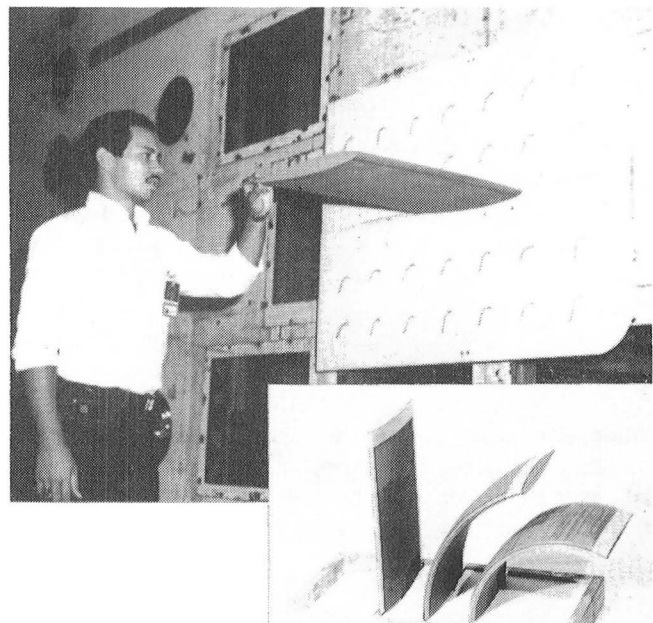
The U.S. Navy is designing curved fins for use on a new missile. These fins, which are curved in the spanwise direction, fold around the missile body so it can fit into existing submarine missile storage tubes. Because there is no information in the literature on the effects of spanwise curvature on flutter, the Navy sought NASA Langley's help to provide the needed data.

An experimental and analytical study of a generic wing planform was conducted to determine the effect of spanwise curvature on flutter. A series of rectangular planform wings of aspect ratio 1.5 were flutter tested in the Transonic Dynamics Tunnel. The only difference between models in the series was in their curvature, which ranged from zero (flat) to 1.05. (Curvature as used here is the reciprocal of the radius of curvature.) Each model had an NACA 65-A010 airfoil section. Flutter analyses were conducted with structural finite element methods and planar subsonic lifting surface theory to establish correlation with the experimental results.

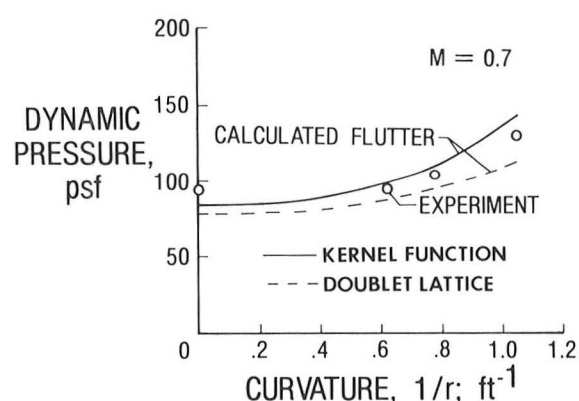
Measured and calculated results obtained are shown in the figure as the variation of dynamic pressure at flutter with wing curvature. All results are for

a Mach number of 0.7. These results showed that curvature increased the flutter speed for wings with an airfoil cross section. Although the reason for this increase was not specifically determined during this study, the increase is believed to be caused by a change in character of the vibration mode shapes as curvature is increased. The kernel function analysis gave conservative results for the uncurved wing and became slightly unconservative as curvature increased, whereas the doublet lattice results were conservative throughout; however, both analytical approaches are in good agreement with the experimental results.

(Jose A. Rivera, 2661)



Wing model mounted in TDT.



Measured and calculated results.

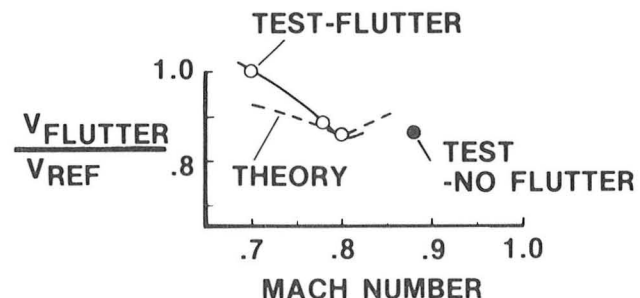
Flutter of Four-Engine Transport Wing With Winglet Predictable by Analysis

Transonic flutter tests were conducted jointly with the Douglas Aircraft Co. in the TDT with a Douglas built, 0.08-size semispan flutter model of an advanced four-engine transport type wing to determine experimentally the effects of winglets on the transonic flutter characteristics and to obtain steady pressure data and aeroelastic load and deformation data for comparison with results calculated from current fluid dynamics computer codes. This study is part of ongoing winglet flutter research that has included cooperative efforts with the Grumman Corp. on an executive jet transport wing (no wing-mounted engines) and with the Boeing Co. on a twin-engine transport type wing.

The model was cantilever mounted through a soft roll spring to a NASA five-component aerodynamic force balance on the tunnel sidewall. Flutter configurations investigated included the nominal wing and engines with a basic winglet, a lightweight winglet, and a wing tip with the winglet replaced by a boom having the same mass as the lightweight winglet. The basic winglet was also flutter tested on the wing with the inboard pylon softened in pitch. Aerodynamic load and pressure measurements were made primarily on a clean wing (no engines) with wing tip boom configuration. The flutter mode was in all cases an outer wing bending-torsion mode which was strongly influenced by the winglet presence.

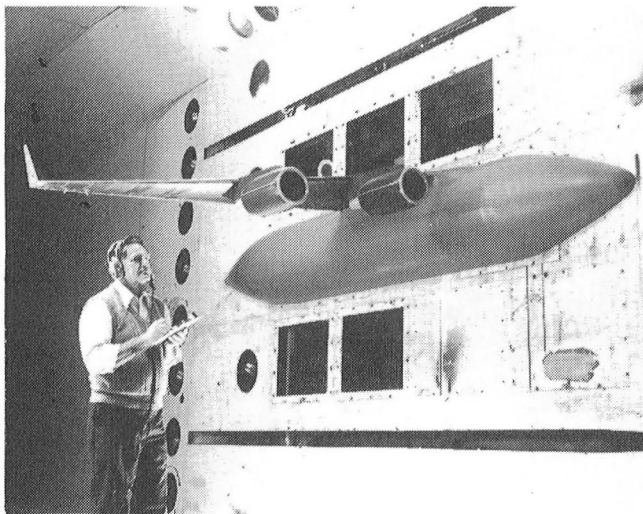
A typical flutter test-analysis correlation is shown in the plot of normalized flutter speed against Mach number for the nominal wing and engines with the basic winglet. It can be seen that the theory agreed well with test results at the critical Mach number (0.8), but was somewhat low at the lower Mach numbers. The "no-flutter" point indicates the maximum velocity tested at the highest Mach number. The analysis employed doublet lattice aerodynamics corrected by a scalar (based on experimental data) at each Mach number.

(Charles L. Ruhlin, 2661)



Measured and predicted results for nominal wing and engines with basic winglet.

TDT Test Provides Essential Data Base for JVX Preliminary Design Development



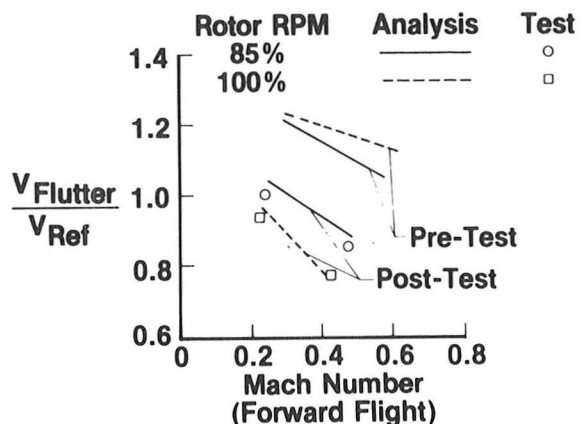
Semispan flutter model with winglet mounted in TDT.

The Department of Defense has awarded a preliminary design contract to Bell Helicopter Textron and the Boeing Vertol Co. for a Joint Advanced Vertical Lift (JVX) aircraft. The JVX will have wing tip mounted tilting engines driving prop-rotors that will allow operation in both a low-speed helicopter mode and a high-speed airplane mode. To provide the experimental data base needed for the JVX design development, a 0.2-size aeroelastically scaled semi-span model of a preliminary JVX design was tested in the TDT.

Specific test objectives were to determine wing/rotor stability in the airplane mode, measure rotor and control system loads and vibration data primarily in the helicopter-to-airplane conversion mode, and correlate these results with analysis. The model shown in the figures consisted of a scaled, cantilevered wing and pylon/rotor system that could be operated with the rotor either powered or windmilling. During

the test, the pylon and rotor could be remotely tilted from the helicopter mode to the airplane mode. Sub-critical damping data were obtained by excitation of the model in the wing beam, chord, and torsion modes. The system damping was then extracted from the model response to this excitation. The measured damping results were compared with pretest predictions made by Bell and Boeing Vertol with two analyses, DYN4 (developed in-house by Bell) and CAMRAD (developed at NASA Ames by W. Johnson and used by Boeing Vertol). Because the experimental aeroelastic instabilities occurred at scaled speeds considerably below those predicted by either analysis, the major impact of this test was to cause a detailed re-examination of, and changes to, the inputs and degrees of freedom used in both DYN4 and CAMRAD.

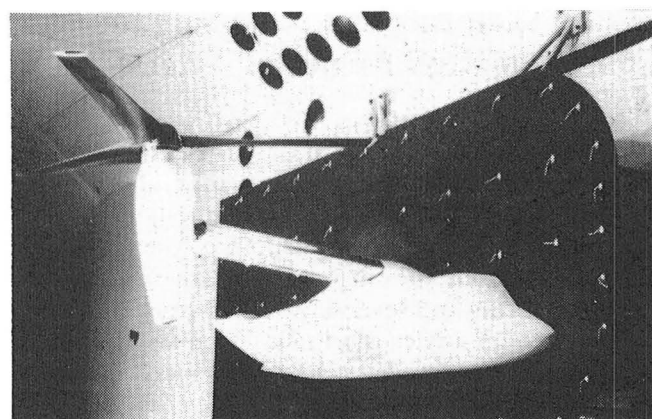
(William T. Yeager, Jr. 2661)



Airplane mode instabilities.

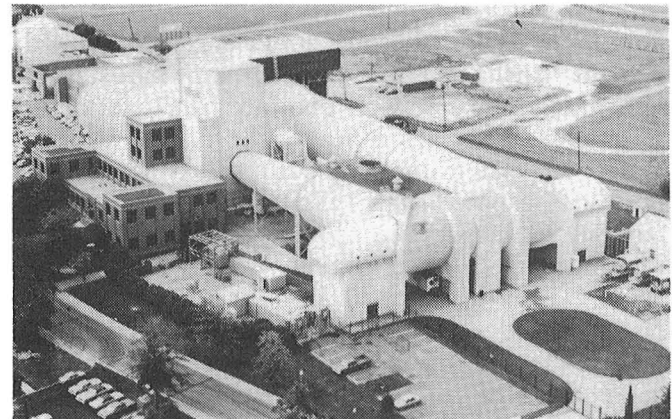


Airplane — high speeds.



Helicopter — low speeds.

16-Foot Transonic Tunnel

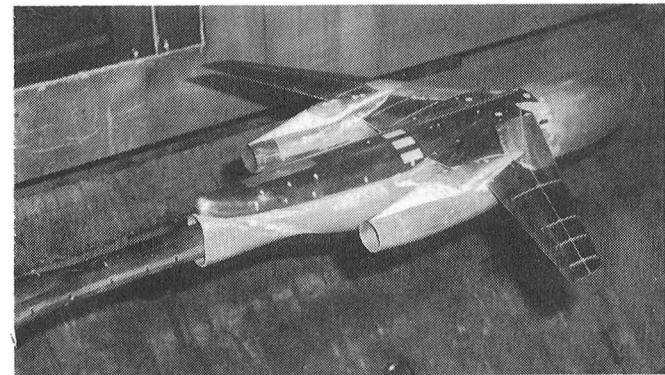


The Langley 16-Foot Transonic Tunnel is a closed-circuit single-return continuous-flow atmospheric tunnel. Speeds up to Mach 1.05 are obtained with the tunnel main-drive fans, and speeds from Mach 1.05 up to Mach 1.30 are obtained with a combination of main-drive and test section plenum suction. The slotted octagonal test section measures 15.5 ft across the flats. The tunnel is equipped with an air exchanger with adjustable intake and exit vanes to provide some temperature control. This facility has a main drive of 60,000 horsepower and a 36,000-horsepower compressor provides test section plenum suction.

This tunnel is used for force, moment, pressure, flow visualization, and propulsion-airframe integration studies. Model mounting consists of sting, sting-strut, and fixed-strut arrangements. Propulsion simulation studies are made with dry, cold, high-pressure air.

wing affected by the nacelle pressure field. This favorable lift interference resulted in a nacelle installation drag increment which was less than the skin friction drag of the nacelle.

(J.C. Patterson, Jr., 2673)



Transonic transport with aft-mounted nacelles.

Improved Aft-Mounted Nacelles

A second series of tests have been conducted in the 16-Foot Transonic Tunnel on a high-wing transport configuration with flow-through D-nacelles mounted beneath the wing in an extreme aft position. Antishock bodies were installed above each nacelle to provide the structural volume necessary for this aft-mounted nacelle installation. Force and pressure data were obtained at Mach numbers of 0.70 to 0.85 for angles of attack from -2.5° to 4.0° .

Preliminary analysis of these data indicated that the increase in lift associated with the installation of nacelles during the initial tests was further increased when the nacelles were moved to a more inboard spanwise position, which increased the angle of the

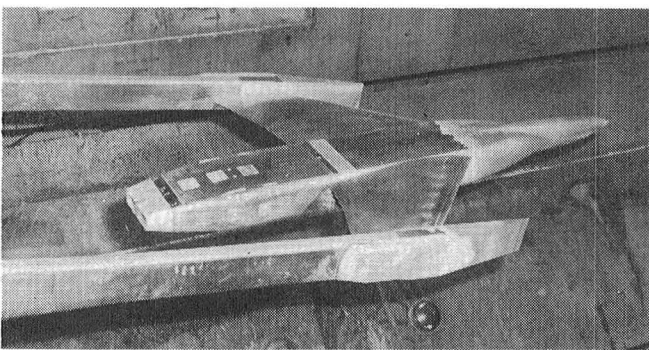
Thrust Vectoring and Reversing for Control at High Angles of Attack

Tests were conducted in the 16-Foot Transonic Tunnel to study the installation of multifunction (nonaxisymmetric) nozzles on a twin-engine fighter type aircraft. The primary purpose of the investigation was to extend the current data base on the use of thrust vectoring and reversing as the primary aircraft control to high angles of attack. Pitch and yaw vectoring control effectiveness and pitch vectoring combined with thrust reversing were studied. The effect of nozzle sidewall cutback on pitch vectoring effectiveness was also determined. The test was conducted at

Mach numbers from 0.15 to 1.20 and angles of attack from -3° to 35° . The nozzle pressure ratio varied from 1 (jet off) to 10.

The results of this investigation indicated that nozzle control effectiveness was maintained up to angles of attack of 35° . At these angles of attack, aerodynamic controls normally lose effectiveness. Nozzle sidewall cutback showed a slight reduction in control effectiveness at low nozzle pressure ratios, but at the higher pressure ratios, control effectiveness was maintained.

(Francis Capone, 2673)



Thrust vectoring model.

Voice-Controlled Model Pressure Leak Checking System

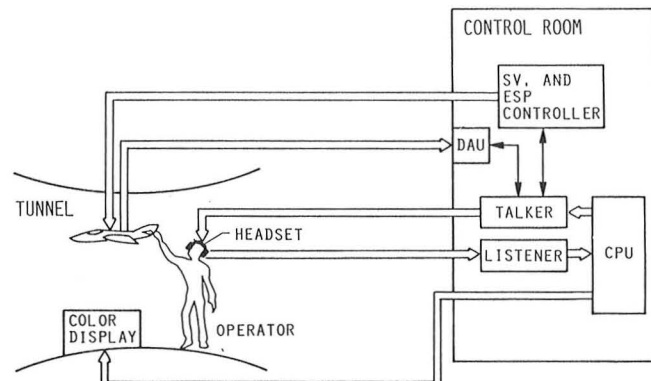
Model pressure leak checking is an important but time-consuming process that requires many man-hours to complete. The standard method of performing this task requires three people. A technician in the control room monitors the pressure on an orifice, which is displayed on a CRT, and uses a control panel to select which orifice will be monitored. Two technicians in the tunnel share the responsibilities of applying pressure to the orifices and keeping records. Communications between the tunnel and the control room are handled via an intercom system.

In an effort to increase accuracy and reduce the number of manhours required to perform this task, a more automated system has been developed and tested in the 16-Foot Transonic Tunnel. The technician wears a headset with microphone and earpiece which is connected to a voice recognition unit and a voice response unit. The technician can then speak commands to the computer and hear the computer's

response. The computer can select an orifice and then monitor the pressure on that orifice when the technician tells it to start. Rather than commanding the computer to position to a particular orifice, the user can just place a pressure on the desired orifice and have the computer search for an orifice with pressure on it. After an orifice is selected, the computer checks to see if the leak rate is within an allowable range and reports its findings to the user. If desired, a plot of the data gathered and the best linear fit of the data can be sent to the CRT screen in the tunnel. The pressure on an orifice is also continuously displayed, along with the current orifice positional information. The results of the leak check are recorded in a database and can be listed, by voice command, on the line printer or the CRT.

A test of this system in the 16-ft tunnel showed that a technician was able to perform the leak check procedure without the assistance of others, so that two technicians were freed to do other work. The test also showed the speed of the new system to be at least equal to that of the old system, and it is believed that as the technicians become more familiar with the new system their speed will increase.

(William E. Larson, 3446)



Automated pressure leak checking system.

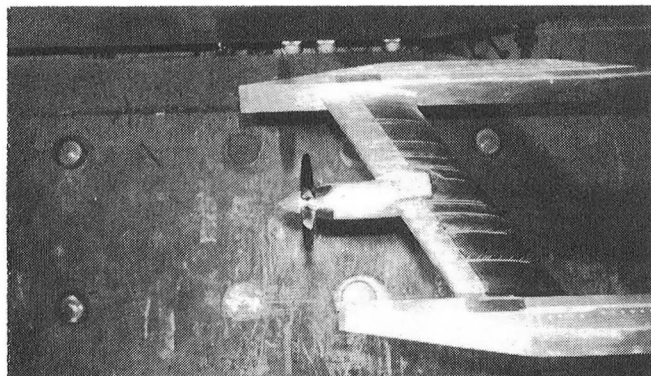
Installation Effects of Advanced Turboprops on Swept Supercritical Wing

A test was conducted in the 16-Foot Transonic Tunnel as part of a broad study to determine the effects of the slipstream from an advanced-design

propeller and nacelle on the flow over a thick supercritical wing. A 20° swept, untapered 14-percent-thick supercritical wing section was mounted on a bifurcated strut support system. The turboprop nacelle employed SR-2 design blades, which were studied in both underwing and overwing locations. The propeller was rotated in both clockwise and counterclockwise directions. Extensive static pressure data were obtained on the wing and nacelles at Mach numbers from 0.50 to 0.80 and angles of attack from 0° to 3°. Other variables included in the study were geometric pitch angle and rpm of the propeller configuration. The primary purpose of this study was to acquire the very detailed data necessary to verify new computational methods and develop an understanding of the complex flow interactions associated with turboprop-wing integration.

The results of the study showed that the propeller slipstream can cause an extremely detrimental flow situation. If the wing is considered in the standard sense, as an aft-swept wing, the propeller upwash occurring on the inboard wing panel causes excessive flow velocities and separation on that portion of the wing. This effect was not observed for propeller upwash occurring on the outboard panel. The data also showed that a large portion of the swirl was recovered by the wing.

(J.R. Carlson, 2673)



Turboprop swept-wing model.

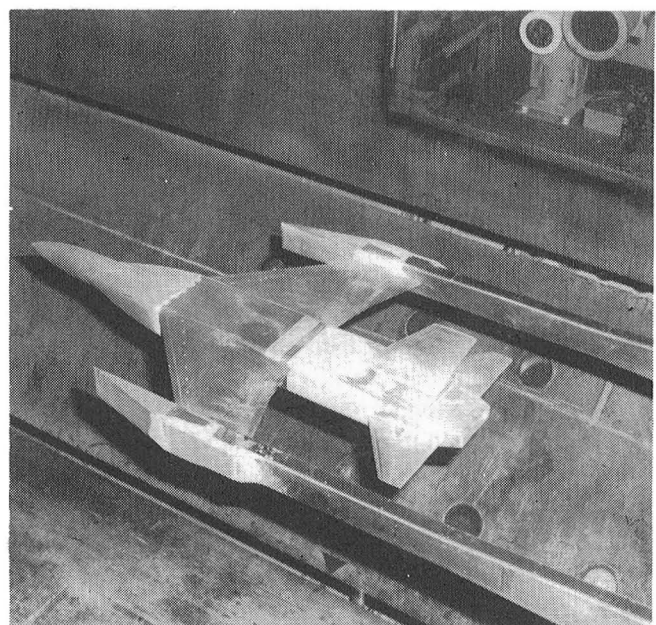
Two-Dimensional Convergent-Divergent Afterbody Boattail Study

An investigation has been conducted in the 16-Foot Transonic Tunnel to determine the effects of

varying afterbody/nozzle boattail angles on installed performance of a twin-engine afterbody model. One axisymmetric (baseline) nozzle and three nonaxisymmetric nozzle configurations were tested. In previous studies the majority of the fuselage-to-nozzle-exit closure was achieved by variation of the upper and lower nozzle flap boattail angles, with relatively small boattail angles on the nozzle sidewalls. In this investigation the three nonaxisymmetric afterbody/nozzle configurations were: (1) a nozzle in which the upper/lower nozzle flap boattail angle was approximately twice that of the nozzle sidewall boattail angle, (2) a nozzle in which the sidewall boattail angle was approximately twice that of the upper/lower nozzle boattail angle, and (3) a nozzle with equal boattail angles on the upper/lower nozzle flaps and sidewalls. Nozzle vector angle varied from 0° to 20°.

Three empennage arrangements were tested: a four-surface (similar to the F-18), a three-surface (similar to the F-16), and a two-surface (similar to the F-18 without the horizontal tails). The test was conducted at Mach numbers from 0.60 to 1.2 and angles of attack from -3.0° to 9.0°. Nozzle pressure ratio varied from 1.0 (jet off) to 12. Steady-state force and pressure data were taken. Preliminary results indicated that best installed performance resulted for the nonaxisymmetric configuration in which the upper/lower nozzle flap and nozzle sidewall boattail angles were equal.

(Linda Bangert, 2673)



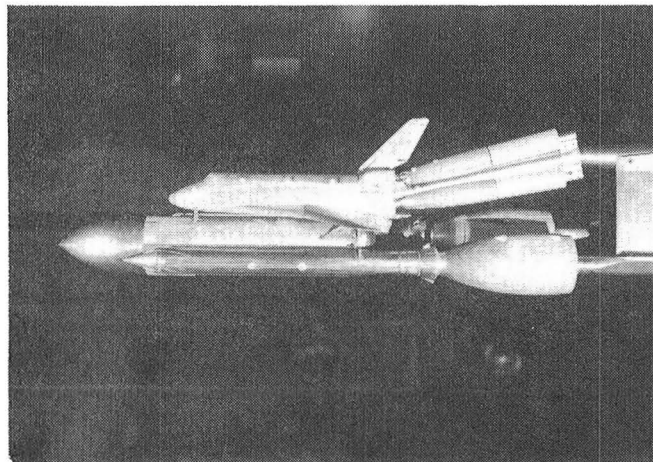
Afterbody boattail model.

Effect of Jet Exhaust Plume on Shuttle Ascent Configuration Aerodynamics

A test was conducted in the 16-Foot Transonic Tunnel to determine the effects of the jet exhaust plumes from the main engines and solid rocket boosters on the aerodynamic characteristics of a 1-percent scale model of the Shuttle ascent configuration. Measurements of wing shear, bending moment, and torsion were made. Elevon hinge moments and wing pressure distributions were also measured. The tests were made at Mach numbers from 0.80 to 1.25 at angles of attack from -6° to 2° . The Reynolds number of the test was about 4×10^6 per foot. Solid-plume simulators were developed experimentally. A series of plume shapes were tested, and the set that provided the best agreement between experimental and flight values of the orbiter, external tank, and solid rocket booster base pressures was selected to be used in the study of the effects of jet exhaust plumes on the orbiter aerodynamic characteristics.

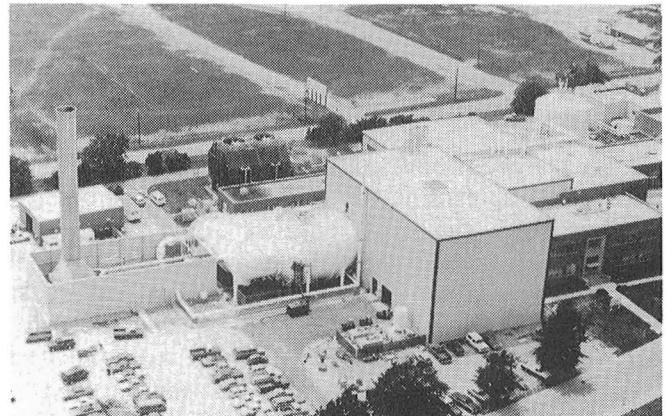
The results of the investigation showed that the jet exhaust plumes had a significant effect on the hinge moments of the configuration. Comparison of the wing pressure distributions measured in the wind tunnel with similar measurements obtained in flight showed that there is probably a large Reynolds number effect on the wing lower surface pressures.

(L.E. Putnam, 2673)



One-percent Shuttle ascent model with jet exhaust plumes.

National Transonic Facility



The most difficult aerodynamic regime for aircraft designers to understand is the transonic region, where speeds near Mach 1 (760 mph at sea level) are attained. At these speeds, the flow around an aircraft is distorted by shock waves, and the resulting turbulence decreases lift and increases drag in such complex patterns that designers cannot accurately predict the results. To develop a test facility that would allow full-scale testing of aircraft at such speeds would be very costly and would require an enormous power supply.

NASA Langley's approach to this problem was to use nitrogen gas at high pressures and ultralow, cryogenic temperatures to simulate the transonic flow about full-sized aircraft. The principle that allows this simulation is that even if the sizes, speeds, and altitudes of two aircraft are very different, the aerodynamic properties of the flow about them will be identical if the Reynolds number (a parameter describing the flow which is a function of aircraft size and speed as well as of the density and viscosity of the flow) and the Mach number are the same for the two aircraft. The use of ultralow temperatures in a new tunnel enables the viscosity of the nitrogen gas to be greatly reduced, and Reynolds numbers can be achieved with small models which are identical to those characteristic of the airflow about full-sized aircraft in the real, more viscous atmosphere.

The new tunnel, the National Transonic Facility (NTF), is a cryogenic fan-driven transonic wind tunnel designed to provide full-scale Reynolds number simulation in the critical flight regions of most current and planned aircraft. It can operate at Mach numbers from 0.2 to 1.2, stagnation pressures from 1 to 9 bars, and stagnation temperatures from 340 to 80 K. The maximum Reynolds number capability is 120×10^6 at a Mach number of 1.0, based on a reference length of 0.25 m.

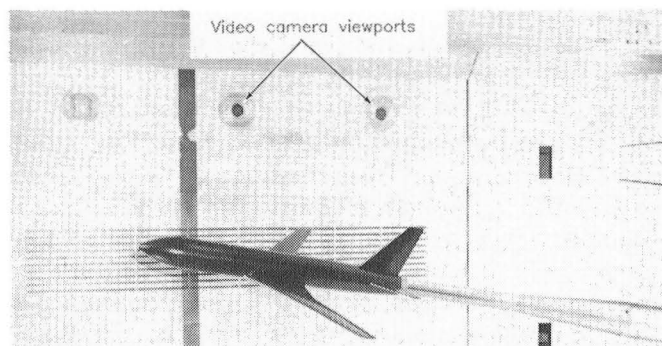
Construction of the National Transonic Facility was completed in September 1982, and checkout operations started the following month, with the maximum Reynolds number obtained in May 1983. Efforts were then directed toward installation of the model access housings and adjustment or alteration of various tunnel hardware systems. In May 1984, preliminary aerodynamic calibration of the tunnel was initiated in parallel with checkout of the tunnel operating systems, and in August 1984 the tunnel was declared operational and turned over to the user organization for a complete aerodynamic calibration and research and development testing. In December 1984 the first aerodynamic vehicle, Pathfinder-I, was installed for checkout of instrumentation systems. Results of a preliminary steady-state calibration, which included centerline Mach number and total pressure and temperature distributions, indicated excellent flow characteristics. Further calibrations to determine the dynamic characteristics of the flow will be made in 1985.

Model Deformation Measurements in the NTF

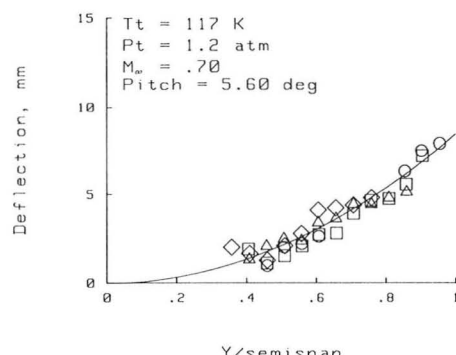
A photogrammetric closed-circuit television system has been used to measure model deformation in the National Transonic Facility. The photogrammetric approach was chosen because of its inherent rapid data recording of the entire object field. Video cameras are used instead of film cameras to acquire data because the cameras must be housed within the cryogenic high-pressure plenum of the NTF and are therefore inaccessible.

Preliminary model deformation measurements under both conventional and cryogenic conditions were obtained for the Pathfinder model with solid wing. Experimental scatter was within 0.5 mm over the 68-cm semispan. A calibration scheme to reselect camera positions which used known roll positions under no-flow conditions proved effective. Both electroconductive defrosters and heated air purge rings maintained frost-free windows and permitted high-quality video imagery under cryogenic conditions. A video disk system effectively captured data within the tightly scheduled cryogenic operating sequence. Vibration-induced electronic distortion associated with the camera tube construction may severely degrade video data for some conditions anticipated in future NTF runs. Solid-state cameras may alleviate this problem. Surface smoothness constraints were relaxed somewhat to allow for high-contrast painted targets to exercise the video photogrammetric system. Effective, nonperturbing, passive photogrammetric targets have yet to be devised for the current approach.

(Alpheus W. Burner, Jr., 3234)

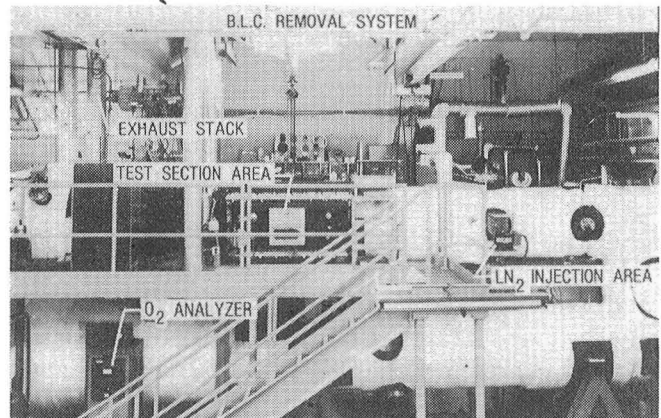


Video camera setup in NTF.



Measured wing deflection.

0.3-Meter Transonic Cryogenic Tunnel



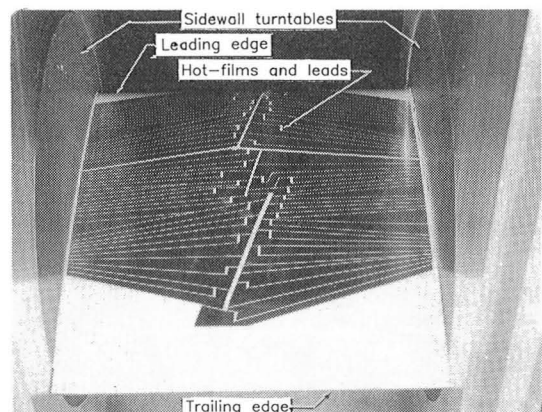
The Langley 0.3-Meter Transonic Cryogenic Tunnel (TCT) is a continuous-flow fan-driven transonic tunnel that uses nitrogen gas as the test medium. It is capable of operating at Mach numbers up to about 0.85, stagnation pressures up to 6 atm and stagnation temperatures from 340 to about 80 K. At the maximum test condition, a Reynolds number (based on a model chord of 15.24 cm) of 50×10^6 can be achieved. In its present configuration, a two-dimensional slotted-wall test section is installed. The test section is 20 cm wide and 60 cm high and the slotted top and bottom walls have a 5-percent open-area ratio. It is equipped with motorized model support turntables and a traversing wake survey probe, both of which are computer controlled.

This facility was first placed in operation in 1973 as a pilot three-dimensional tunnel to demonstrate the cryogenic wind tunnel concept at transonic speeds. The successful demonstration of this concept in the 0.3-m TCT played a major role in the decision to build the National Transonic Facility. In its present mode of operation, the 0.3-m TCT is used for routine airfoil testing at high Reynolds numbers, as a test bed for components and instrumentation for the NTF, and for advanced cryogenic wind tunnel testing techniques.

method to apply the extremely thin hot films to the surface of the model as part of a NASA/DAC cooperative program to develop a specialized system for detecting boundary layer transition in cryogenic wind tunnels. The tests, conducted in the Langley 0.3-Meter Transonic Cryogenic Tunnel, were done at both adiabatic and nonadiabatic wall conditions with liquid nitrogen circulating through the model to cool the surface below the adiabatic recovery temperature. The surface cooling was done to determine the effect of wall temperature on the location of boundary layer transition.

The test results indicated that with the proper electronic data acquisition equipment, an "on-line" location of boundary layer transition could be obtained at both ambient and cryogenic conditions. The "on-line" signal from the hot films clearly indicated either a laminar, a transitional, or a turbulent boundary layer. Preliminary results indicated that model cooling actually decreased the transition Reynolds number because of the apparent dominance of surface roughness on transition at this condition.

(Charles B. Johnson, 4380)



Airfoil upper surface instrumented with hot films.

Boundary Layer Transition Detection at Cryogenic Conditions With Hot Films

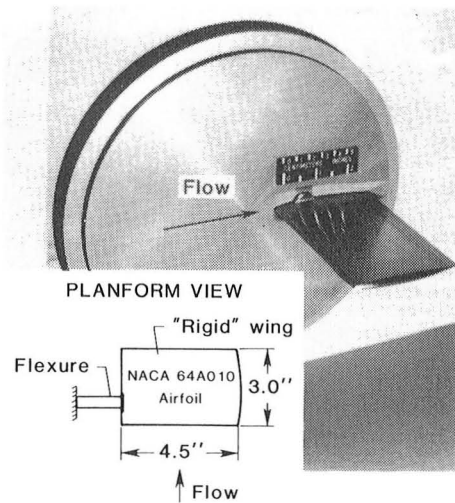
An investigation to determine the location of boundary layer transition was carried out on a 9-in. 12-percent-chord supercritical two-dimensional airfoil instrumented with 48 hot films. The Douglas Aircraft Company (DAC) used a newly developed

Flutter Testing Techniques Developed For Use in Cryogenic Wind Tunnels

A test was conducted in the 0.3-m TCT to examine the feasibility of conducting flutter tests in cryogenic wind tunnels. The model consisted of a relatively rigid wing mounted on an integral rectangular beam flexure. The model had a 1.5-aspect-ratio rectangular wing with an NACA 64-A010 airfoil shape. During the wind tunnel test, experimental flutter predictions were made for several Mach numbers and Reynolds numbers.

It was found that although useful flutter testing is possible in a cryogenic tunnel, many factors must be considered which are not usual concerns for flutter tests in conventional wind tunnels. The primary concern is the large changes in material properties which occur with changing temperature. The operating procedure that was found to be most desirable for this test was to increase pressure in the tunnel while Mach number and temperature were held constant. This procedure required that the Reynolds number be varied as the flutter condition was approached. Analytical trends obtained through flutter analysis were used to adjust the experimental results for the extraneous effects of mass ratio and temperature variations so that changes in the flutter boundary could be attributed to Reynolds number effects. The effects of Reynolds number on flutter were found to be small for this model. A slight decrease in the flutter dynamic pressure was found to occur with increasing Reynolds number over the range from 5 to 20×10^6 .

(Stanley R. Cole, 2661)



Model mounted in 0.3-m TCT.

Advanced Technology Airfoil Test (ATAT) Program

The 0.3-Meter Transonic Cryogenic Tunnel with the two-dimensional test section installed provides one of the foremost airfoil test capabilities available. The combined transonic Mach number, cryogenic temperature, and increased pressure test capabilities of this unique facility enable the simulation of flight-equivalent airfoil conditions. For the past 4 to 5 years the 0.3-m TCT has been used for a very extensive airfoil research program with the U.S. transport industry and the DFVLR of West Germany. This ambitious program, referred to as the Advanced Technology Airfoil Test (ATAT) program, was initiated by Langley. The primary objective of this airfoil study is to strengthen the position of U.S. commercial transport industries in the increasingly competitive world marketplace.

The scope of the 0.3-m TCT airfoil program includes a series of well-known correlation airfoils as well as advanced NASA, U.S. transport industry, and European airfoils. Several of the airfoils were tested with and without tunnel sidewall boundary layer control. One of the airfoil designs, the CAST 10, was examined with two different chord lengths to provide an indication of the extent of the tunnel wall effects.

The experimental portion of this cooperative program has been completed and the final results are now being analyzed. They clearly demonstrated the need to obtain high Reynolds number airfoil results. This observation was very apparent during the studies of the supercritical types of transonic cruise airfoils. For example, traditional transition "fixing" techniques for low Reynolds number testing were shown to be only partially successful in simulating "full-scale" Reynolds number results. In other cases where strong shock systems existed on the airfoils, the test results indicated that considerable error could occur in the extrapolation of low Reynolds number air results to flight-equivalent conditions. Large Reynolds number effects were noted throughout the studies, especially for the aerodynamic characteristics affected by the drag characteristics. The premature drag rise or "drag creep" which sometimes occurs with supercritical airfoils at Mach numbers below the abrupt Mach divergence drag rise was shown to be highly dependent on boundary layer conditions and the associated fluid shape of the airfoil. This complex phenomenon and other elusive local flow effects cannot be simulated or modeled accurately with current analytical techniques. Several of the state-of-the-art

airfoils displayed as much as a 45-percent increase in the aerodynamic range parameter when the Reynolds number was increased from low values to flight-equivalent conditions.

Several convincing demonstrations were provided during the airfoil program which illustrated the importance of contour accuracy for the highly aft-loaded airfoil models. One airfoil study showed that relatively small contour inaccuracies could severely degrade the expected performance of a transonic cruise airfoil.

This program has again shown that under certain conditions, wall interference effects can be severe and, if not accounted for, can completely overshadow the accurate determination of the actual airfoil characteristics. Moreover, the wall effects themselves can be affected by changes in Reynolds number, and can thus appear as "true" Reynolds number effects. It has been shown that wall interference effects can be determined in order to enable the separation of the effects of the tunnel walls from the actual aerodynamic characteristics of the airfoil. Combined examinations of wall effects and current airfoil analytical techniques have provided additional evidence that the apparent agreement between "uncorrected" experimental results and theoretical pressure distributions developed with nonconservative algorithms may be misleading. Selected comparisons of corrected experimental pressure distributions with theoretical results developed with the conservative GRUMFOIL theory have indicated reasonable and good agreement.

An advanced test section is now being installed in the 0.3-m TCT which features adaptive floor and ceiling walls and provisions for the active "treatment" of the sidewall boundary layer. These updates should provide the ability to obtain interference-free results at even higher Reynolds number test conditions.

(Edward J. Ray, 4395)

Correlation

NACA 0012
NACA 65-213
NASA SC(2)0510
NASA SC(2)0714

Advanced NASA

NASA SC(3)0712A
NASA SC(3)0712B

Industry Program

BCAC 1
BCAC 2
DAC
LAC 1
LAC 2
LAC 3

DFVLR Program

CAST 10
CAST 10, c/2
R-4

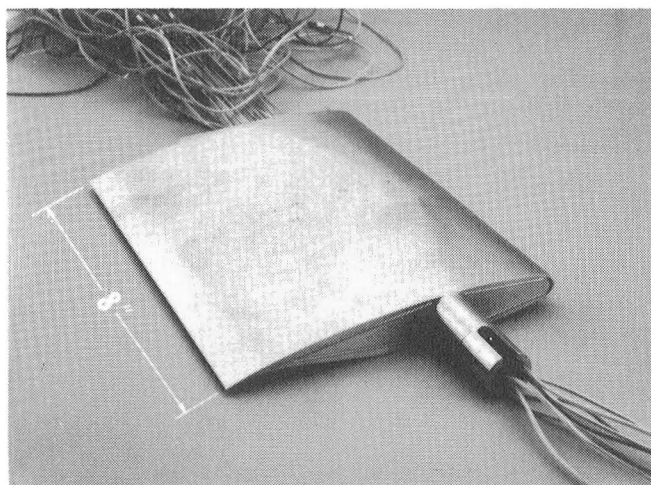
Airfoils tested in ATAT program.

Reynolds Number Effects on Unsteady Pressure Studies

The purpose of this study was to develop and test experimental techniques to measure unsteady pressures in a cryogenic environment and also to measure the effects of Reynolds number on the unsteady pressure distribution of an oscillating two-dimensional supercritical airfoil with free transition. The airfoil tested is a well-documented 14-percent-thick supercritical airfoil.

A series of preliminary investigations were conducted to develop and test the instrumentation system. The oscillating drive system was designed to accommodate thermal expansion and contraction experienced by the tunnel test section during operation. (Stagnation temperatures ranged from 120 to 340 K and pressures ranged from 1 to 6 atm. Measurements were made over a range of Reynolds numbers, based on a chord length of 6 in., from 6×10^6 to 35×10^6 . Mach number was varied at Reynolds numbers (R_e) of 15×10^6 and 30×10^6 . For each data set, static pressure measurements were made from -2.5° to 2.5° in 0.5° increments. Unsteady pressure measurements were taken at mean angles of attack (α) from -2° to $+2^\circ$ in 1° increments. For those tunnel conditions where both frequency and amplitude were varied, frequency was varied from 5 Hz to a maximum of 60 Hz and amplitude was varied from 0.25° to a maximum of 1° .

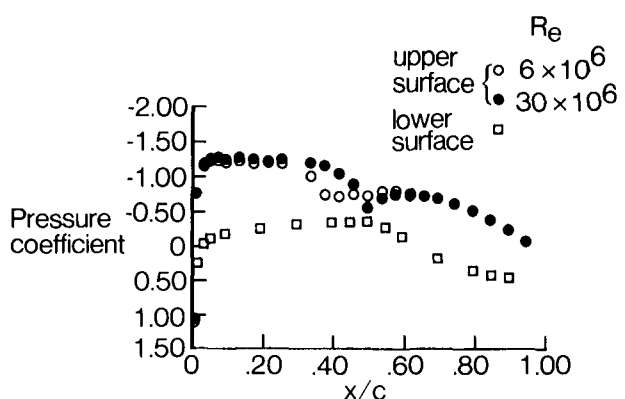
The uncorrected static pressure distributions shown in the figure indicate laminar flow and a weak shock at a Reynolds number of 6×10^6 and a stronger shock in a turbulent boundary layer at a Reynolds



Fourteen-percent supercritical airfoil.

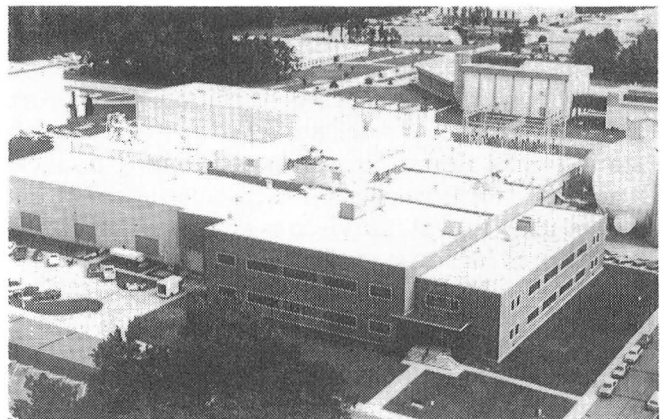
number of 30×10^6 . Unsteady pressure measurements were made at static angles of attack to obtain data that will be used to locate transition. Steady and unsteady pressures were surveyed in the wake and static tunnel floor and wall pressure measurements were made for flow correction calculations. The data will be used to evaluate viscous and inviscid coupling procedures for unsteady boundary layer codes.

(Robert W. Hess, 4236)



Static pressure distributions. $M = 0.72$, $\alpha = 1.5^\circ$.

Unitary Plan Wind Tunnel



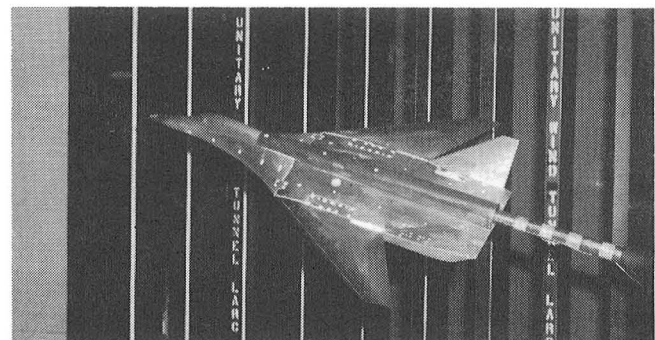
Immediately following World War II, the need for wind tunnel equipment to develop advanced airplanes and missiles was recognized. The military and the National Advisory Committee for Aeronautics (NACA) developed a plan for a series of facilities which was approved by the U.S. Congress in the Unitary Wind Tunnel Plan Act of 1949. This plan included five wind tunnel facilities, three at NACA laboratories and two at the Arnold Engineering Development Center. The Langley Unitary Plan Wind Tunnel was among the three built by NACA. The Unitary Plan Wind Tunnel is a closed-circuit continuous-flow variable-density tunnel with two 4-by 4- by 7-ft test sections. The low-range test section has a design Mach number range of 1.5 to 2.9 and the high-range section Mach number varies from 2.3 to 4.6. The tunnel has sliding-block type nozzles which allow continuous variation in Mach number while on-line. The maximum Reynolds number per foot varies from 6×10^6 to 11×10^6 depending on Mach number. The tunnel is used for force and moment, pressure distribution, jet effects, dynamic stability, and heat transfer studies. Flow visualization data, which are available in both test sections, include schlieren, oil flow, and vapor screen.

solution of the supersonic potential-flow equations. The cooperative program included both the aerodynamic design and testing of several outboard wing panels for an advanced supersonic fighter concept. The purpose of the experimental investigation was to determine the effect on supersonic aerodynamic characteristics of increasing wing sweep and provide a data base for code validation.

The wind tunnel model is a preliminary design version of a Rockwell fighter concept. Five outboard wing panel geometries were tested: a 48° leading-edge sweep baseline, a 55° leading-edge sweep wing with a camber distribution biased toward a maneuver lift coefficient for Mach 1.6, an uncambered 55° reference wing, and two redesigned 48° leading-edge sweep wing panels (multi-operating point wings—subsonic, transonic, supersonic). The redesigned 48° wings represented a low-twist cruise wing ($M = 1.5$) and a high-twist maneuver concept ($M = 1.6$). Testing was performed at Mach numbers of 1.5 to 2.5 in the Unitary Plan Wind Tunnel. Both longitudinal and lateral aerodynamic force characteristics were measured. Surface pressure data were obtained at Mach numbers of 1.5 to 1.8 for the 55° cambered wing and the 48° low- and high-twist wings.

Nonlinear Analysis/Design Techniques for Advanced Supersonic Wing Design

NASA Langley and the Rockwell International Corp. are engaged in a cooperative effort to demonstrate the applicability of new nonlinear analysis/design techniques for advanced supersonic wing design. The effort was aimed at demonstrating the ability of a nonlinear analysis technique based on



Advanced supersonic fighter installed in UPWT.

Results indicated that as expected, the 55° wing panel was more efficient at the design Mach number of 1.6 since the 48° wings have a supersonic leading edge. The predicted results of the potential-flow solver also indicated good correlation with the experimental force data and early comparisons with surface pressure data appear good. This experimental investigation and companion theoretical studies should provide a strong data base for advanced supersonic fighter designs.

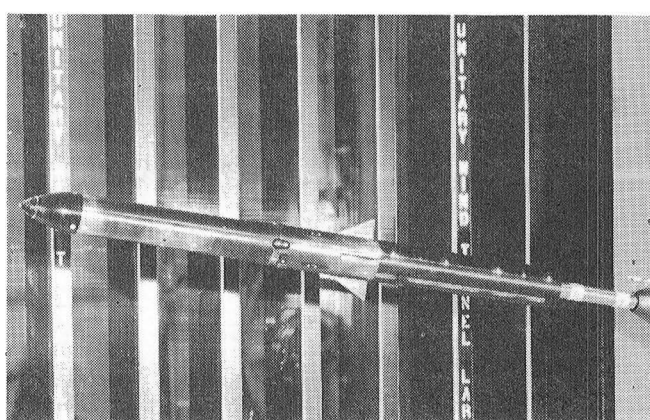
(Noel A. Talcott, 3294)

Vertical Launch Antisubmarine Rocket

A 20-percent scale model of a two-stage cruciform rocket was tested in the Unitary Plan Wind Tunnel for the purpose of investigating the longitudinal aerodynamic characteristics of four low-drag nose shapes and two sets of tail fins. Testing was performed in the low-speed leg of the wind tunnel at Mach numbers of 1.6 to 2.4. The Reynolds number was maintained at 2×10^6 at a stagnation temperature of 125° F.

Results showed that the 1.25 von Karman 15-percent blunt-nose shape had the lowest drag of the four nose shapes tested. This nose shape was selected to be used on future vertical-launch antisubmarine rocket tests. Several pressure runs were then made to measure the local static pressures at the surface of the nose. The tail fin assembly with the larger root chord provided the necessary aerodynamic static stability characteristics over the test Mach number range.

(Jeffrey Hill, 3181)



Vertical launch antisubmarine rocket.

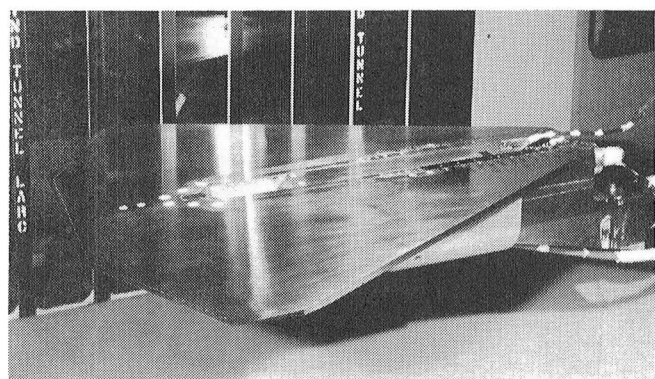
Cavity Flow Field Studies at Supersonic Speeds

An experimental program has been initiated to define cavity flow field properties at supersonic speeds. The first phase of the program has been completed and consisted of detailed surface pressure distribution measurements for box cavities through a wide range of cavity depth, length, and width with a Mach number range from 1.5 to 2.86. These pressure distributions are needed to define the local surface loadings on the cavity and to determine the type of cavity flow field ("open" or "closed"). For the "closed" cavity flow field, the flow expands around the cavity leading edge, impinges on the cavity floor, and exits ahead of the rear face, whereas for the "open" cavity flow field the flow simply bridges the cavity. The type of cavity flow field has a major impact on local flow angles, surface pressure gradients, cavity resonance, and cavity drag levels.

In order to accurately establish the geometric variable at which the cavity flow field switches from "open" to "closed" or vice versa, the cavity model was designed such that the face of the cavity could be remotely positioned to vary the cavity length.

Results from the tests provided a detailed definition of the variation of critical length-to-depth ratios with Mach number for a wide range of cavity depths and widths. The pressure measurements have been integrated over the front and rear faces of the cavities to define cavity drag levels associated with "open," "transitional," or "closed" cavity flow fields. The results show that the cavity drag levels for closed cavity flows are much greater than for open cavity flows. The detailed pressure distributions will also be invaluable as a guide for modeling the cavity flow field by computational methods.

(Robert L. Stallings, Jr., 4004)



Cavity model installed in UPWT.

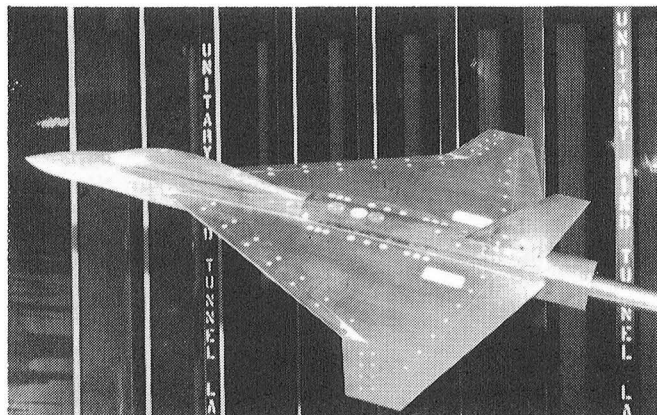
Hybrid Flap Study

Since future military aircraft will be required to cruise and maneuver efficiently at subsonic, transonic, and supersonic speeds, a wing design concept that employs hybrid flaps is under investigation. The hybrid flap concept couples a fixed-camber surface with leading- and trailing-edge flaps to provide acceptable aerodynamic performance across the speed range. Both attached-flow and separated-flow principles would be considered in the selection of the camber surface and the flap geometries. This wind tunnel test was conducted to obtain supersonic data on a series of six uncambered wings with different planforms. Each wing in the series had several geometrically different leading-edge flaps which were designed with the most recent subsonic flap design concepts. This supersonic data will be used for method validation and the development of a hybrid flap design logic.

The wind tunnel models were a series of six uncambered wings with leading- and trailing-edge flaps mounted on a generic body. The series of six wings consisted of three delta wings with aspect ratios of 1.25, 1.75, and 2.95 and a corresponding set of three wings with cranked leading edges. Force tests were conducted on all six wings with streamwise leading-edge flap deflections of 0° , 5° , 10° , and 15° and trailing-edge flap deflections of $+10^\circ$, 0° , -10° , and -20° at Mach numbers from 2.6 to 2.86.

Preliminary results indicated that flap performance is a strong function of both the supersonic leading-edge sweep parameter and flap planform. The data also showed that performance improvements can be obtained at both cruise and maneuver levels of lift with leading-edge flap deflections.

(Richard M. Wood, 4008)



Advanced aerodynamic wing concept.

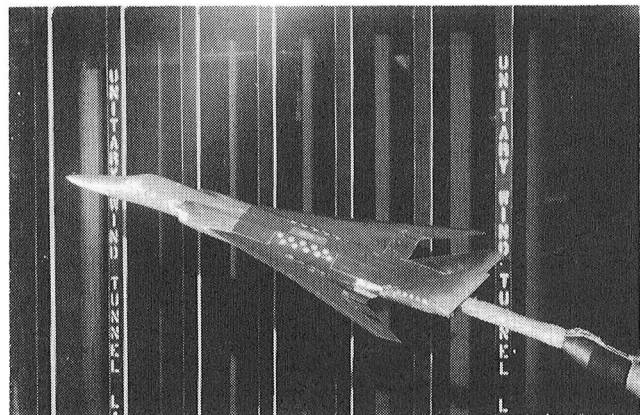
Fighter Wing Study

Existing supersonic wing camber design procedures have been proven adequate for wing-alone and supersonic-transport type configurations in which the near-field interference effects of the various components are minimal compared to wing aerodynamics. In contrast, a fighter type fuselage could have a significant impact on wing aerodynamics, and the application of wing-alone design methods to fighter aircraft can result in extensive modifications to minimize fuselage effects. For this reason, a new wing design approach has been explored for fighter aircraft. The new wing camber design employs the PAN AIR code for computing fuselage aerodynamics and fuselage-induced interference effects, which are then incorporated into the existing wing-alone design procedure as an aerodynamic wing loading.

A wind tunnel test was conducted to obtain supersonic force and moment data on two cambered, highly swept cranked arrow wings which were designed with the new wing camber design procedure. The supersonic data will be used for validation of the design approach and will be compared to the uncambered wing data. The wind tunnel models consisted of a representative fighter fuselage, twin vertical tails, and two interchangeable cambered wings. The two planforms tested were cambered wings of $70^\circ/66^\circ$ and $70^\circ/30^\circ$ leading-edge sweep angles. Force tests were conducted on both wings at Mach numbers of 1.6, 1.8, 2.0, and 2.16.

Preliminary results indicated that both of the cambered wing designs met the design lift and pitching moment requirements and provided a 5- to 10-percent improvement in trimmed lift-to-drag ratio compared to that of the uncambered wings.

(Richard M. Wood, 4008)



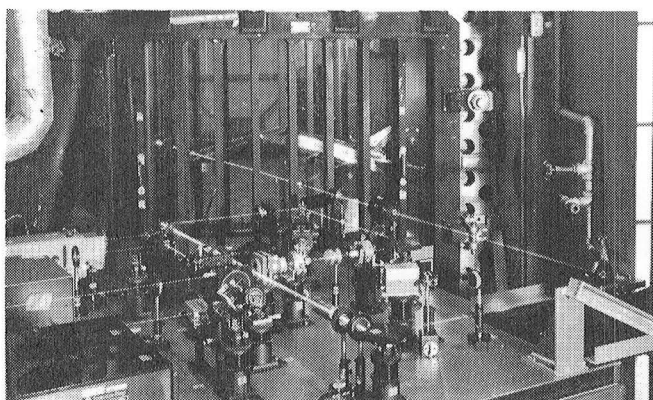
Generic fighter model.

Nonintrusive Simultaneous Measurement of Three Flow Parameters in a Supersonic Flow

Coherent Raman spectroscopy has been used for the first time to remotely and simultaneously measure the (particle-free) flow velocity in nitrogen, the static pressure, and the translational temperature in the Unitary Plan Wind Tunnel. Nonintrusive laser techniques were used to measure these three quantities simultaneously at a single point. The system employs two lasers, one CW (continuous-wave) probe and one pulsed pump, arrayed on a single optical table along with an optical retrometer located opposite the flow. The retrometer yields a vibration-free optical system which has the additional advantage of simultaneously capturing both the forward and backward (counterpropagating laser beams) Raman scattering. Spectral line shape analysis of the forward- and backward-scattered nitrogen spectra allows the temperature and pressure to be determined, and the Doppler shift between the two yields the velocity of the nitrogen molecules.

The system was deployed in an inverse Raman mode with a laser resolution of 190 MHz. This resolution represents an order-of-magnitude improvement in spectral resolution since the first UPWT measurements and has enabled pressure to be added to the system capability. The UPWT demonstration of the concept included measurement of velocity and temperature—and hence Mach number—over the Mach number range from 2.50 to 4.63, static pressure measurements (at Mach 2.50) corresponding to a Reynolds number per foot range of 1 to 5×10^6 , and measurements behind the shock wave of a flat-plate model.

(Reginald J. Exton, 2791)



Inverse Raman spectroscopy in UPWT.

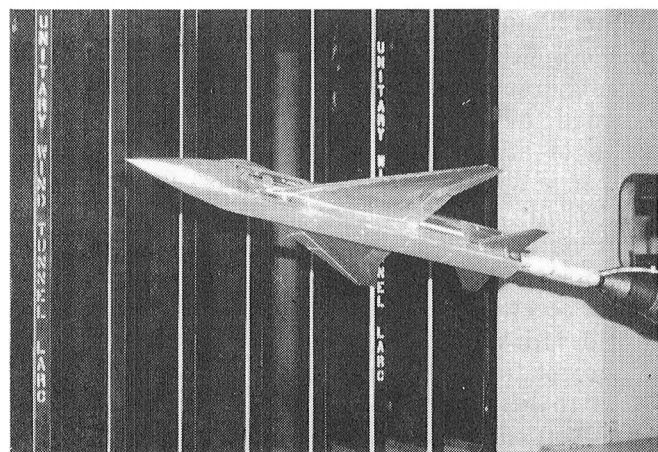
Fighter Wing Design Study

A series of tests were made in the Unitary Plan Wind Tunnel as part of ongoing research into supersonic cruise fighter concepts designed for efficient supersonic cruise and high maneuverability at transonic speeds. For these tests, a generic type fuselage without inlets were used. This fuselage can accommodate canards, wings, and tail surfaces in various combinations and locations.

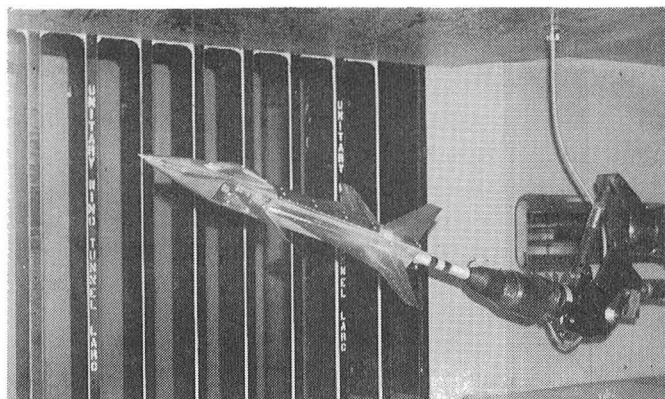
Two different wings were tested with both leading- and trailing-edge flap deflections at Mach numbers ranging from 1.5 to 2.16. One of these wings is twisted and cambered for cruise at Mach 1.8, at which point the 60° sweep leading edge is subsonic. For good transonic maneuverability, the wing has an aspect ratio near 2.2 and uses full-span leading- and trailing-edge flaps. Preliminary results indicated that small deflections of these flaps at supersonic speeds can improve supersonic maneuver performance.

The second wing tested has a 70°/20° leading-edge planform, sharp leading and trailing edges, and variable camber through the use of leading- and trailing-edge flaps. The 70° wing segment is efficient at supersonic speeds and can employ vortex flap technology at subsonic-transonic speeds, and the 20° segment provides increased span and maintains attached flow to provide high levels of wing performance. This wing was tested with and without a canard. Preliminary results indicated that the use of flaps in conjunction with the canard could increase performance, and linear analysis methods adequately predicted the lift and drag of the flapped wing-canard configuration.

(Gregory D. Riebe, 3294)

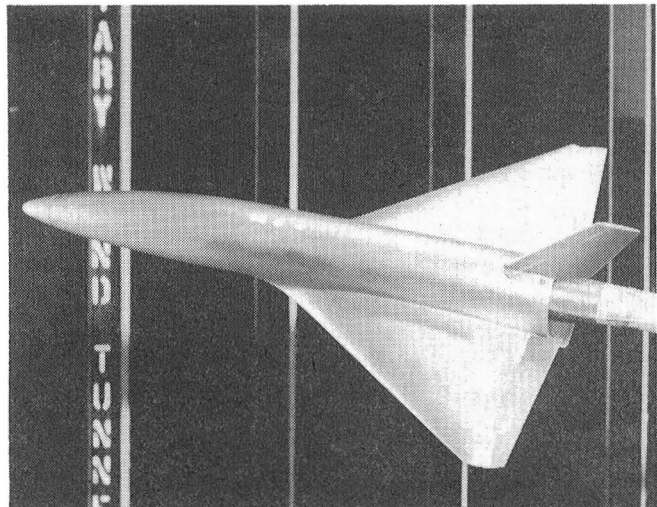


Supersonic cruise fighter with 60° leading-edge wing.



Supersonic cruise fighter with 70°/20° cranked-leading-edge wing.

vehicle, including the Space Shuttle.) Subsequent experimental studies will extend the aerodynamic data base for the Boeing vehicle to hypersonic speeds. (W. Pelham Phillips, 3911)



Model of Boeing advanced space transportation vehicle.

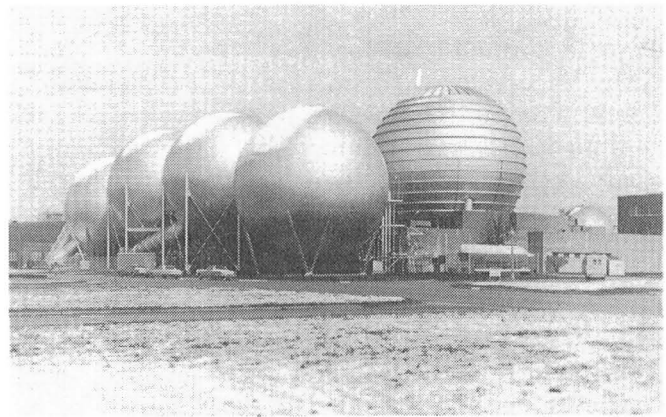
Advanced Space Transportation Vehicle Investigation

Future space transportation endeavors could utilize designs similar to the Boeing Aerospace Co. advanced space transportation vehicle concept shown. The Boeing vehicle is a manned, fully reusable, single-stage-to-orbit design that takes off horizontally from a runway-based ground accelerator. The vehicle has the capability of delivering light-weight to moderate-weight payloads to low Earth orbit and returning to conventional airfields. The design is characterized by a low planform wing loading and a far-aft center-of-gravity location during entry and landing.

A $1/120$ scale model was tested in the Langley Unitary Plan Wind Tunnel to determine the supersonic longitudinal and lateral-directional aerodynamic characteristics. The aerodynamic investigation was made at Mach numbers from 1.50 to 4.63 and angles of attack from -4° to 29° . The Reynolds number of the investigation was 2.0×10^6 per foot.

Results indicated that maximum lift-to-drag ratios varied from 3.2 at $M = 1.5$ to 2.2 at $M = 4.63$. The longitudinal trim capability and stability levels appear acceptable to allow nominal supersonic flight attitudes for vehicle centers of gravity as far aft as the 75-percent fuselage length station. The vehicle was found to be directionally unstable with either the center vertical tail or the tip fins that were tested as an alternate means of directional control. (This directional instability is characteristic of this type of space

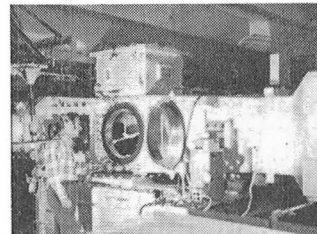
Hypersonic Facilities Complex



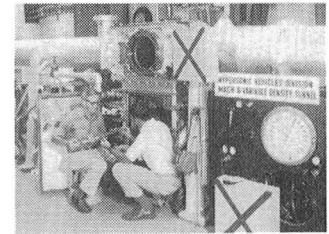
The Hypersonic Facilities Complex consists of several hypersonic wind tunnels located at four Langley sites. They are considered as a complex because these facilities represent a major unique national resource for wind tunnel testing. The complex currently includes the Hypersonic CF₄ (tetrafluoromethane) Tunnel ($M = 6$), the Mach 6 High Reynolds Number Tunnel, the 20-Inch Mach 6 Tunnel, the Mach 8 Variable-Density Tunnel, the 31-Inch Mach 10 Tunnel, the Hypersonic Nitrogen Tunnel ($M = 17$), and the Hypersonic Helium Tunnel and its open jet leg ($M = 20$). These facilities are used to study the aerodynamic and aerothermodynamic phenomena associated with the development of space transportation systems, including the current Space Shuttle and future advanced orbital-transfer and launch vehicles; to support the development of advanced military spacecraft capability; to support the development of future planetary entry probes; to support the development of hypersonic missiles and transports; and to perform basic fluid mechanics studies and develop measurement and testing techniques.

This complex of facilities provides an unparalleled capability at a single installation to study the effects of Mach number, Reynolds number, test gas, and viscous interactions on the hypersonic characteristics of aerospace vehicles.

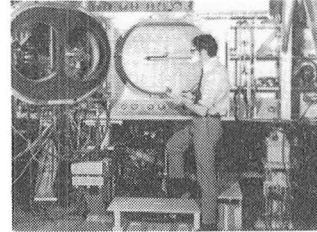
20-INCH M-6 TUNNEL
 $M_\infty = 6$ AIR $R_\infty = 0.7 - 9.0 \times 10^6$



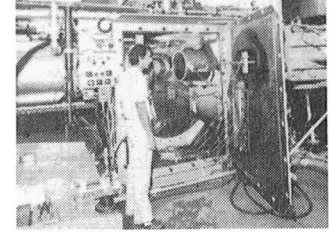
M-8 VAR.-DENS. TUNNEL
 $M_\infty = 8$ AIR $R_\infty = 0.1 - 10.7 \times 10^6$



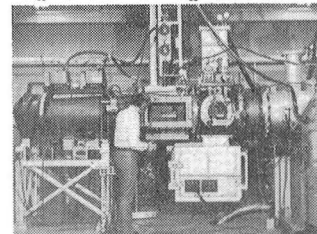
31-INCH M-10 TUNNEL
 $M_\infty = 10$ AIR $R_\infty = 0.4 - 2.4 \times 10^6$



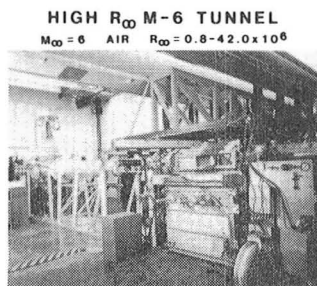
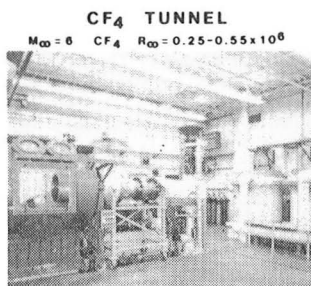
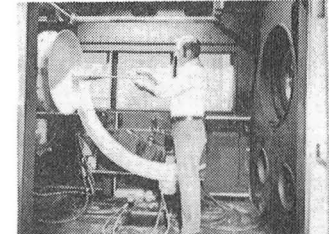
NITROGEN TUNNEL
 $M_\infty = 17$ N₂ $R_\infty = 0.35 \times 10^6$



HELIUM TUNNEL
 $M_\infty = 19 - 21.6$ He $R_\infty = 3.5 - 12.5 \times 10^6$



OPEN JET LEG-HE TUNNEL
 $M_\infty = 20$ He $R_\infty = 6.0 \times 10^6$



Aerodynamics for an Entry Research Vehicle

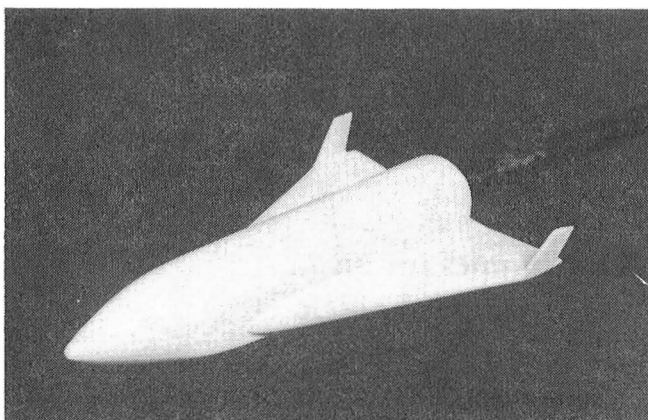
Currently, there is growing interest in the development of vehicles capable of flying at near-orbital velocity within the atmosphere. Because of the lack of

adequate ground test facilities to simulate low-density hypervelocity flight, there is also increasing interest in developing an entry research vehicle flight experiment. It is envisioned that such an entry research vehicle would be launched from the Shuttle and have the capability to fly several trajectories on entry. This would afford an opportunity to explore the environment over a large range of entry conditions. As part of the effort to develop the technical advocacy for an Entry Research Vehicle Experiment Flight Test Program, a candidate vehicle concept has been developed and evaluated for the proposed flight test requirements.

The candidate entry research vehicle (ERV) is 25 ft long with a wing span of 14 ft and is designed to occupy half the Shuttle cargo bay. The configuration has a distinct wing body design with conventional elevons for pitch and roll control and tip fin controllers for yaw control and stability augmentation. The fuselage was sized to accommodate the desired instrumentation and propellant to provide 7000 ft/sec delta velocity for a 20° synergetic plane change.

The aerodynamics of the ERV were predicted with a program called Aerodynamic Preliminary Analysis System (APAS), and tests of a two-percent model were conducted in the Hypersonic Helium Tunnel to verify the predictions of the APAS program. The results showed the vehicle to be longitudinally stable with a center of gravity of 67-percent body length. The estimated values of pitch and drag agreed quite well with the experimental data when the correct Newtonian coefficient was used in APAS. The estimating pitching moment from APAS did predict generally the same trim angle of attack as the wind tunnel data, but there were some differences in the shape of the curves.

(Mark J. Cunningham, 3911)



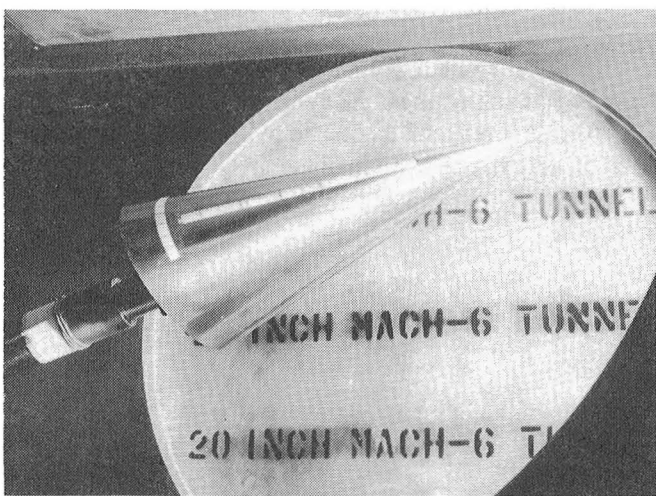
ERV 0.02-scale model in Hypersonic Helium Tunnel.

Flow Field and Surface Measurements on a 2:1 Elliptical Cone

Computer codes for both inviscid and viscous flow fields about aerodynamic configurations are currently being developed throughout the scientific community. Very little data for evaluating the codes are available. Since an elliptical cone is a basic shape that can be readily represented analytically and also appears to have application in the design of several classes of flight vehicles, a test program is under way to provide a data base for such a configuration. Total pressure, flow angle, and static temperature and pressure measurements in the flow field between the body and shock, as well as pressures and heat transfer rates on the surface of a 2:1 elliptical cone, are being measured at hypersonic speeds.

Initial measurements of heat transfer rates in the Langley 20-Inch Mach 6 Tunnel have been completed for the sharp-nosed cone at angles of attack of 0°, 5°, 10°, 15°, and 20° and free-stream Reynolds numbers per foot of 1.5×10^6 , 4.0×10^6 , 5.0×10^6 , and 7.0×10^6 . Preliminary results showed that boundary layer transition begins along the windward lower surface centerline at the three highest Reynolds numbers for angles of attack above about 5°. Circumferential distributions at the 91-percent axial station showed a decreased heating rate in the region close to the zero peripheral-velocity line (approximately 50° to 85° from the windward lower surface centerline) at positive angles of attack.

(George C. Ashby, Jr., 2483)



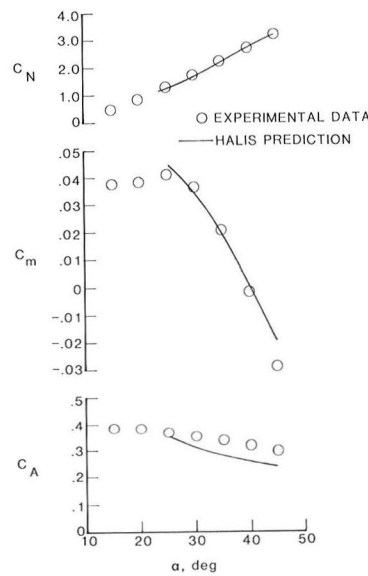
Heat transfer and surface pressures model of 2:1 elliptical cone in Langley 20-Inch Mach 6 Tunnel.

Experimental Aerodynamic Coefficients on Shuttle-Like Vehicle

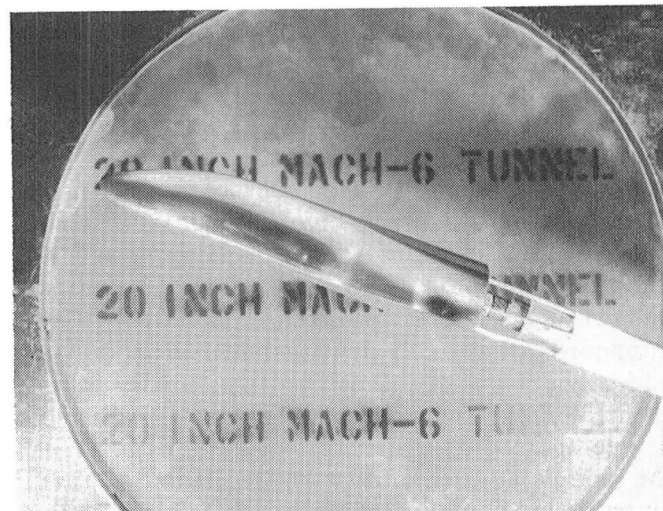
A study was recently initiated at Langley to verify an inviscid flow field code developed at this Center which is capable of predicting aerodynamic coefficients for a shuttle-like vehicle. This vehicle is an accurate representation of the orbiter windward side for 93 percent of the length, but the leeward side is defined by elliptical cross sections. A model (0.0075 scale) of this "modified orbiter" was tested in the 20-Inch Mach 6 Tunnel and the 31-Inch Mach 10 Tunnel to determine the effects of Mach number, Reynolds number, and angle of attack on aerodynamic coefficients, and most importantly to provide a data base with which predictions could be compared.

For the test Reynolds number of 0.5, 1.0, and 2.0×10^6 per foot, a negligible effect of Reynolds number on aerodynamic coefficients was observed. When calculated results obtained with the High Alpha Inviscid Solution (HALIS) code developed at Langley were compared to the measured data, excellent agreement was noted for normal-force (C_N) and pitching-moment (C_m) coefficients. However, for axial-force coefficient (C_A) HALIS tended to under-predict the experimental data at the lowest Reynolds number due to increased viscous effects.

(John R. Micol, 3031)



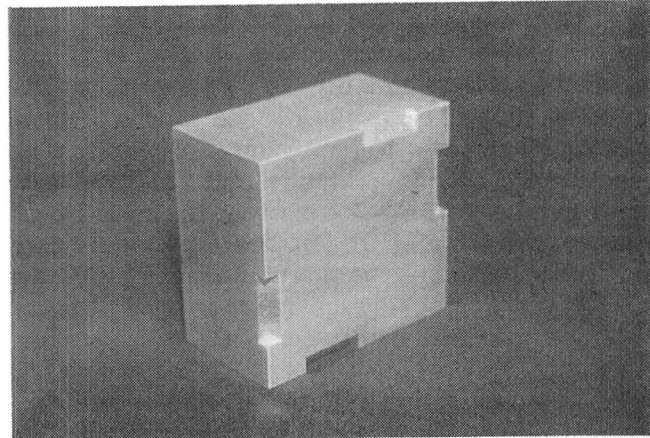
*Predicted and measured results for modified orbiter.
Reynolds number = 0.5×10^6 per foot, Mach number = 10.*



Shuttle-like force model in 20-Inch Mach 6 Tunnel.

Aerodynamic Coefficients for General-Purpose Heat Source Module

A General Purpose Heat Source (GPHS) module is the part of a Radioisotope Thermoelectric Generator (RTG) which contains the radioisotope heat source and protects the source in the event of an accident. RTGs will be the power sources for the *Galileo* and *Ulysses* spacecraft, which will be launched from the Shuttle Orbiter by a Centaur upper stage. If the Centaur should malfunction, the GPHS module will act as an aeroshell to protect the radioisotope heat source during reentry.



GPHS test module.

The aerodynamic coefficients for the GPHS module were measured during tests in the 31-Inch Mach 10 Tunnel as part of the safety review process. The configuration is a right-angle parallelepiped with a broadface of 3.83 by 3.67 in. and a thickness of 2.09 in. Two chamfers are cut on each of two opposing corners on one broadface. Five full-scale models with different sting locations were tested in order to cover a test envelope of 0° to 180° in both angle of attack and roll angle. The test results showed that the rolling moment is so strongly dependent on the roll angle and angle of attack that the sign of the rolling moment can change. The results will be used in six-degree-of-freedom trajectory calculations to define the module attitude during the hypersonic phase of an entry and combined with subsonic data to define the attitude at ground impact.

(Kenneth Sutton, 3031)

Experimental Investigation of Maneuvering Reentry Research Vehicle at Mach 6 and 20.3

A maneuvering reentry research vehicle (MRRV) has been proposed by the U.S. Air Force as a test bed for experiments in the hypersonic flight regime. The MRRV was conceived as a vehicle that flies in the hypersonic regime along trajectories that the Space Shuttle cannot fly because of aerodynamic and heating limitations. The MRRV would serve as a convenient means of testing thermal protection systems, structural concepts, guidance and control systems, and other future technologies, as well as alternative flight paths for advanced reentry spacecraft.

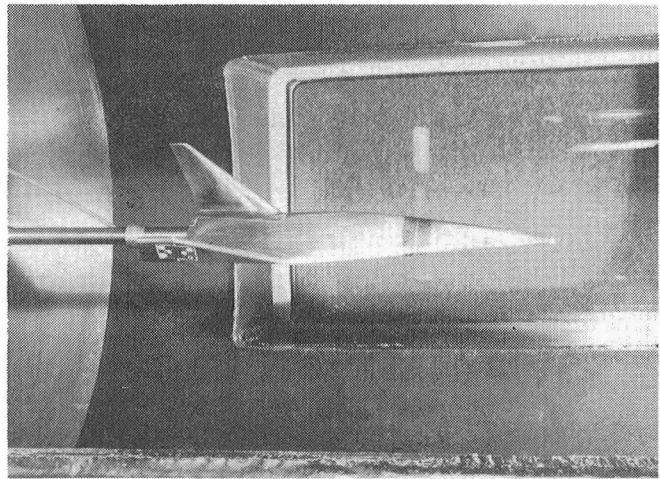
As part of the study of the MRRV, force and moment tests were conducted on a 3.5-percent scale model of the vehicle in the 20-Inch Mach 6 Tunnel and the Hypersonic Helium Tunnel. The tests were conducted at a nominal Mach number of 6 and Reynolds number of 3.6×10^6 per foot for an angle-of-attack range from -4° to 20° and a nominal Mach number of 20.3 and Reynolds number of 6.8×10^6 per foot for an angle-of-attack range from 0° to 25°. Lateral-directional data were obtained at sideslip angles of 0° to -4°.

The investigation determined rudder effectiveness, sideslip derivatives, and the effects of body flap and elevon deflection on pitch, as well as the effects of elevon deflections on roll. In addition, two noses of

different radii (0.138 and 0.302 in.) were tested to determine bluntness effects.

The baseline vehicle (0.138-in. nose radius) has longitudinal and lateral-directional stability at angles of attack from 12° (maximum lift-to-drag ratio) to 25°. The blunt-nose vehicle (0.302-in. nose radius) has longitudinal and lateral stability at angles of attack from 15° (maximum lift-to-drag ratio) to 25° and directional stability for angles of attack greater than 15°.

(Gregory J. Brauckmann, 2483)



MRRV configuration 3.5-percent scale model (0.138-inch nose radius) installed in Hypersonic Helium Tunnel.

Real-Gas Simulation on the Space Shuttle Orbiter

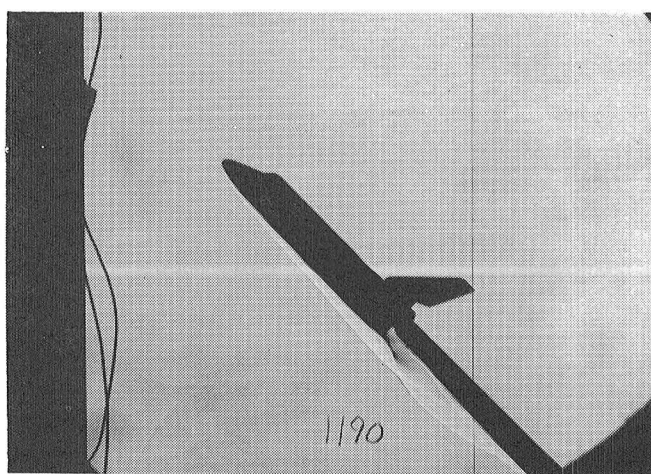
The extensive flight data obtained on the Space Shuttle orbiter allow the comparison of preflight predictions to flight values at high Mach numbers. The orbiter flight data show an increase in pitching-moment coefficient of 0.03 compared to preflight estimates. One explanation is that real-gas effects, which are associated with the ionization, dissociation, and excitation of the vibrational modes of the free-stream air as it passes through the bow shock cause this difference. Real-gas effects are characterized by increases in normal shock density ratios of about three times those found at lower Mach numbers

(15 compared to 5) and by lower ratios of specific heats (1.1 compared to 1.4). On a configuration such as the orbiter these factors cause an increase in pressures on the forebody and a decrease in pressures on the afterbody and thus produce a relative nose-up pitch increment.

In an effort to investigate these effects, a series of force and moment and oil flow visualization tests were conducted on a 0.004-scale model of the orbiter in the Hypersonic CF₄ Tunnel. This tunnel uses tetrafluoromethane (CF₄) as the test gas because its density ratio across a normal shock is approximately 12, which approaches the values obtained in flight.

The tests were conducted at a Mach number of 6, a Reynolds number per foot of 0.6×10^6 , and a ratio of specific heats of 1.12. Force and moment data were obtained at angles of attack from 20° to 45° in 5° increments. Body flap deflections of 0°, 5°, 10°, 12.5° and 16.3° and elevon deflections of 0°, 2°, and 5° were tested. Oil flow visualization photographs were obtained on the windward side of the model with the same body flap deflections at 25° and 40° angle of attack. The results from these tests are being compared with results from similar tests conducted in the 20-Inch Mach 6 Tunnel at the same Mach and Reynolds numbers, but with a ratio of specific heats of 1.4. Preliminary analyses of the data showed that the pitching-moment coefficient for the CF₄ tunnel test had a nose-up increment of at least 0.01 compared to that found in air over the range of angle of attack tested. These results indicate that real-gas effects may be part of the explanation for the difference in pitching moment.

(Robert L. Calloway, 3609)



Schlieren photograph of model in Hypersonic CF₄ Tunnel.

Forward-Located Jet Interaction Nozzles Study

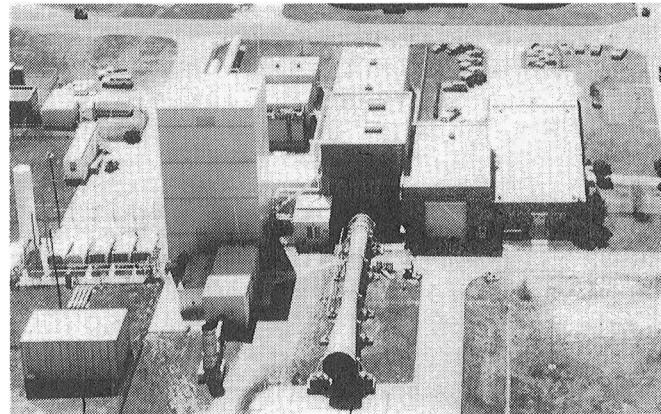
The use of secondary jets appears to be one alternative to conventional aerodynamic control surfaces for supersonic or hypersonic flight control systems. The forces generated by an underexpanded jet issuing normal to a surface in a supersonic/hypersonic stream are usually amplified relative to the thrust produced only by the jet. Several studies have been conducted on jet interaction phenomena, but most have been two-dimensional and have been conducted with jets located near the aft region of bodies. A cooperative experimental study was conducted with Martin Marietta Aerospace Corp. in the 20-Inch Mach 6 Tunnel which primarily concerned the three-dimensional effects of single and multiple circular jets on the forward part of a conical body. The total nozzle exit area was held constant.

A biconic model with an air handling system was used in the investigation. Interchangeable thrusters could be mounted at various locations, and the air supply system was regulated by a flowmeter for measurement of mass flow rate. Data were required with an internal strain gage balance and with surface pressure orifices.

Results showed that positive moment amplification was obtained with forward-located jets, with a peak amplification factor of 1.8 obtained at 15° angle of attack. Also, a triple nozzle configuration with unequal diameters produced approximately a 10-percent increase in the moment amplification factor relative to that produced by a single-nozzle configuration at the same injection flow rate.

(James L. Dillon, 4004)

Aerothermal Loads Complex



The Aerothermal Loads Complex consists of six facilities which are used to carry out research in aero-thermal loads and high-temperature structures and thermal protection systems. The 8-Foot High Temperature Tunnel is a Mach 7 blowdown type facility in which methane is burned in air under pressure and the resulting combustion products are used as the test medium with a maximum stagnation temperature near 3800°R in order to reach the required energy level for flight simulation. The nozzle is an axisymmetrical conical contoured design with an exit diameter of 8 ft. Model mounting is semispan or sting with insertion after the tunnel is started. A single-stage air ejector is used as a downstream pump to permit low-pressure (high-altitude) simulation. The Reynolds number ranges from 0.3 to 2.2×10^6 per foot with a nominal Mach number of 7, and the run time ranges from 20 to 180 sec. The tunnel is used for studying detailed thermal-loads flow phenomena as well as for evaluating the performance of high-speed and entry vehicle structural components. A major effort is under way to provide alternate Mach number capability as well as O_2 enrichment for the test medium. This is being done primarily to allow models that have hypersonic airbreathing propulsion applications to be tested.

The 7-Inch High-Temperature Tunnel is a $1/12$ -scale version of the 8-ft HTT with basically the same capabilities as the larger tunnel. It is used primarily as an aid in the design of larger models for the 8-ft HTT and for aero-thermal loads tests on subscale models. The 7-in. HTT is currently being used to evaluate various new systems for the planned modifications of the 8-ft HTT.

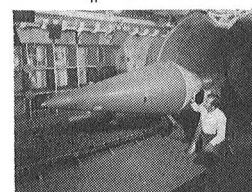
The 1- by 3-Foot High Enthalpy Aero-thermal Tunnel (1 by 3 HEAT) is a unique facility designed to provide realistic environments and test times for testing thermal protection systems proposed for use on high-speed vehicles such as the Space Shuttle. The

facility is a hypersonic blowdown wind tunnel that uses products of combustion as the test medium. Test panels mounted on the sidewalls can be as large as 2 ft wide and 3 ft long. The facility operates at dynamic pressures of 1 to 10 psi, Mach numbers from 4.7 to 3.5 (depending on the temperatures, which range from ambient to 5800°F), an altitude range simulating flight of 130,000 to 80,000 ft, and enthalpy levels from 1100 to 4400 BTU/lb depending on the oxygen levels used in the test medium.

The 20-MW, 5-MW, and 1-MW Aero-thermal Arc Tunnels are used to test models in an environment that simulates the flight reentry envelope for high-speed vehicles such as the Space Shuttle. The amount of energy available to the test medium in these facilities is 9 MW, 2 MW, and $1/2$ MW, respectively. The 5-MW is a three-phase AC arc heater and the 20-MW and 1-MW are DC arc heaters. Test conditions such as temperature, flow rate, and enthalpy vary greatly since a variety of nozzles and throats are available and model sizes can range from 3 in. in diameter to 1- by 2-ft panels.

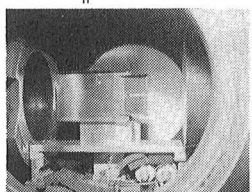
8-FOOT HIGH-TEMPERATURE TUNNEL

$$M = 7 \quad R_n = 0.3 - 2.2 \times 10^6$$



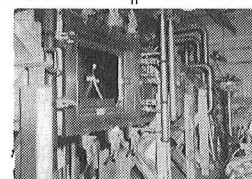
7-INCH HIGH-TEMPERATURE TUNNEL

$$M = 7 \quad R_n = 0.3 - 2.2 \times 10^6$$

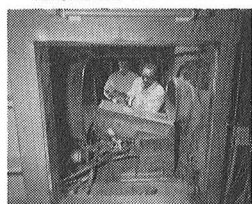


1 x 3 HIGH ENTHALPY AERO-HERMAL TUNNEL

$$M = 3.5 - 4.7 \quad R_n = 0.3 - 1.4 \times 10^6$$



AERO-HERMAL ARC TUNNEL

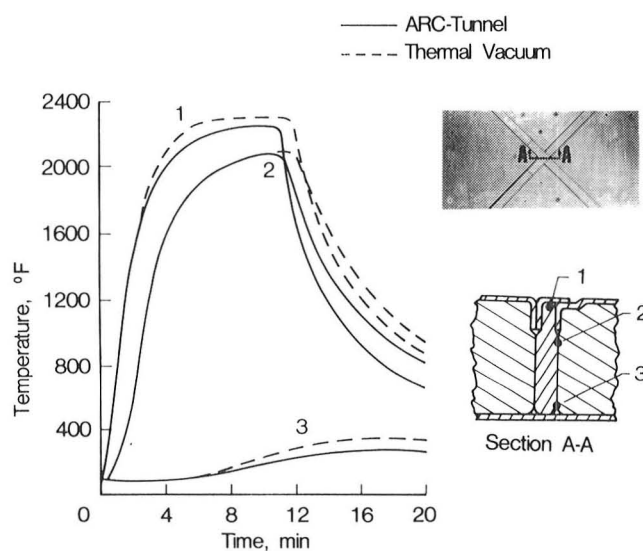


Aero thermal Tests of Advanced Carbon-Carbon TPS

The objective of this research is to develop high-temperature durable TPS (thermal protection systems). One of the most promising durable TPS concepts for application to the highly heated areas of future space transportation systems is advanced carbon-carbon (ACC), a derivative of the reinforced carbon-carbon (RCC) material which is being used successfully on the Shuttle nose cap and wing leading edges.

The RCC material was modified to improve strength and oxidation resistance and renamed ACC. The ACC TPS concept consists of large overlapping ACC panels (approximately 3 ft square) mounted on post supports with packaged fibrous insulation between the ACC panels and the main vehicle structure. The test article is composed of four panel segments, which represent the intersection of four ACC multipost concept panels. The overall size of the test article is 1 ft by 2 ft. The test article has been tested in both radiant heating and arc tunnel environments. A comparison of test data from radiant heating tests with data from arc tunnel tests suggests the existence of hot gas ingress through the overlapping joint down into the insulation joint. A redesign of the concept is in progress.

(Granville L. Webb, 2796)



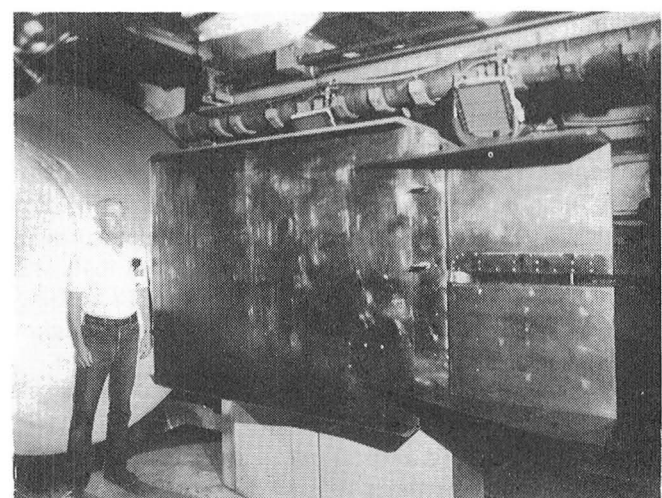
Effect of aero thermal exposure on gap temperature of ACC multipost.

Aero thermal Test of Shuttle Split-Elevon Model

The two elevons on each of the Shuttle wings are split and are separated with a chordwise gap of 6 in. where complex flow interactions are produced that are not amenable to proven analytical techniques. In the original Shuttle design, the specified aero thermal loads allowed the use of high-temperature reusable surface insulation (HRSI) tiles in the gap for thermal protection. However, test results from small-scale aminar tests at NASA Ames suggested that the HRSI tiles would not be adequate if the flow were turbulent, and replaceable ablation panels were used on the first five Shuttle flights. When it was clear that the heat load was much lower than expected, the original tile design was reinstated.

Flight results indicated that the present design is adequate, but that excessive heating occurs on the windward edge. Earlier large-scale test results in the Langley 8-ft HTT indicated that the gap heating was less than the original design level. To provide a detailed aero thermal load distribution with critical test parameters varied, a $1/3$ scale model of the Shuttle split elevon was mounted to the previously used model for tests in the 8-ft HTT for both laminar and turbulent flow conditions. The elevon portion of the existing model was modified to extend and streamline the elevons to a chord length of 24 in. and to vary the gap width from 1 to 3 in. The elevons were designed for a sharp or rounded windward leading edge to define possible edge effects on the aero thermal loads.

Tests were performed in the 8-ft HTT at a free-stream Mach number of 6.5, a unit Reynolds number



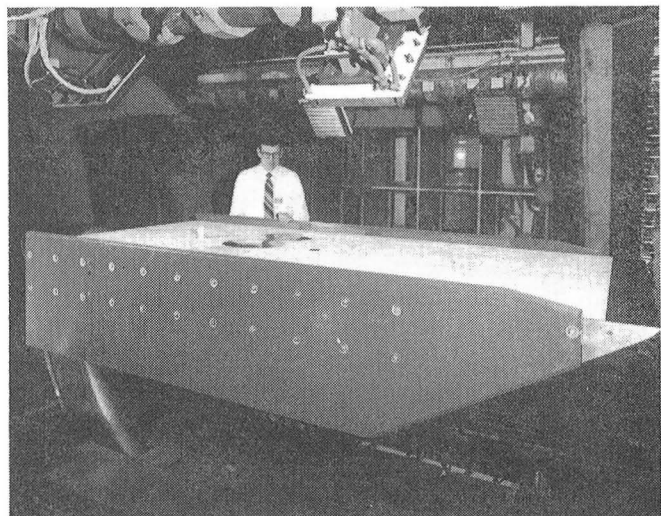
Shuttle split-elevon gap heating model in 8-ft HTT.

range from 0.4 to 1.5×10^6 , and a total temperature of 3500°R . The model wing angle was varied from 0° to 10° and the elevon angles were varied from 0° to 20° . The basic data from all 31 test runs have been reduced and preliminary data plots have been generated. Generally, the present results agree with the low heating level in the chordwise gap indicated in the earlier tests. The peak heating in the gap is driven by the elevon windward surface pressure and is not directly related to whether the wing boundary layer is laminar or turbulent. Also, the results were relatively insensitive to variations in edge radius.

(L. Roane Hunt, 3423)

dimensional Navier-Stokes results for laminar boundary layer flow obtained earlier.

(L. Roane Hunt, 3423)



Spherical dome protuberance model installed in 8-ft HTT.

Aerothermal Tests of Spherical Dome Protuberance Models

Metallic TPS (thermal protection system) panels on high-speed vehicles are subject to thermal distortions when they experience large through-the-thickness temperature gradients. The panels, anchored at the corners, bow up and form a spherical dome protuberance into the flow field. Although the protuberance height of the panels is expected to be less than the local boundary layer thickness, the complex interaction of the high-speed flow field and the bowed surface will affect the local and global aero thermal loads to the vehicle. An experimental aero thermal study was conducted to complement current analytical studies of this problem.

An array of spherical dome protuberance models were tested in the 8-ft HTT panel holder, which provides two-dimensional laminar or turbulent boundary layer flow. The dome dimensions were varied for diameters of 7 to 28 in. and heights of 0.05 to 0.8 in. The design included three types of domes (metallic pressure instrumented domes, metallic thin-wall heat transfer domes, and ceramic domes) to obtain surface temperatures approaching equilibrium from infrared photography. Aero thermal tests were performed at a free-stream Mach number of 6.5, a unit Reynolds number of 0.4×10^6 per foot, and a total temperature of 3500°R .

Preliminary data analyses of the 37 test runs have been completed. Results included surface pressure and heating rate distributions that compared various test parameter effects, pressure and heating rate contour plots, and boundary layer profiles. These results agree qualitatively with the three-

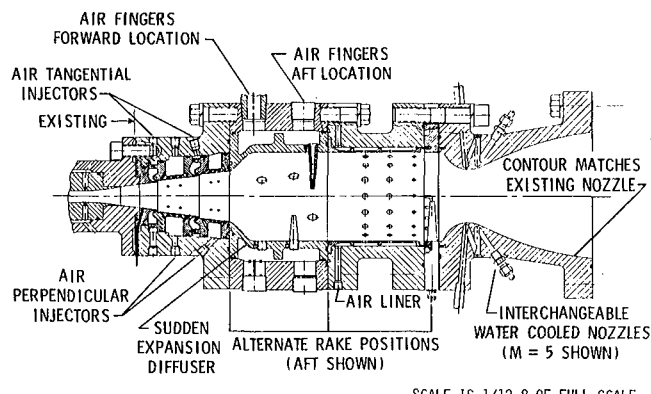
Development of Alternate Mach Number Capability for 8-ft HTT

The test capability of the 8-ft HTT is being enhanced to enable the testing of airbreathing hypersonic engines. These engines almost always begin operating at Mach 3.5 to 4.0 at altitudes of 40,000 to 50,000 ft, but the altitude capability of the current 8-ft HTT simulates flight from 80,000 to 130,000 ft. Use of the large-diameter test section requires that the mass flow be significantly increased and the total temperature decreased to 1600°R at Mach 4 and 2400°R at Mach 5. A mixer performs this function by mixing cold flow with hot flow from the combustor. The hot flow from the combustor is expanded to about Mach 3 and tangential and normal injection are used to cool the walls, start the mixing process, and diffuse the flow. The flow is decelerated to subsonic speeds by a normal shock wave, mixed with a massive injection of air normal to the flow to produce a sudden increase in area, and passed through a cooled chamber that stills it. The flow is then fed to a second nozzle, which expands it to Mach 4 or 5.

A scale model has been built and tested in the 7-in. HTT. To determine the effectiveness of the

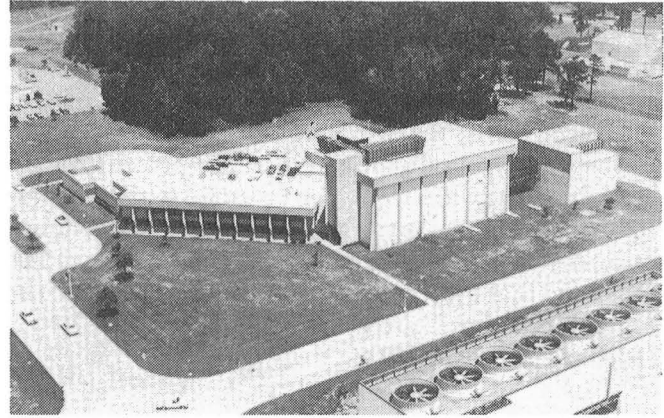
mixer, a subsonic temperature probe array was installed between the end of the mixer and the nozzle. In addition, total temperature in the test section was measured across the flow with three different types of probes. To evaluate the effect of the process on the container, the walls were instrumented with temperature and pressure taps. The uniformity of the temperature distributions and results of the oil flow studies indicated that the mixer works extremely well and the hot and cold gases are thoroughly mixed.

(Richard L. Puster, 3115)



Prototype of mixer with alternate Mach number nozzle.

Aircraft Noise Reduction Laboratory



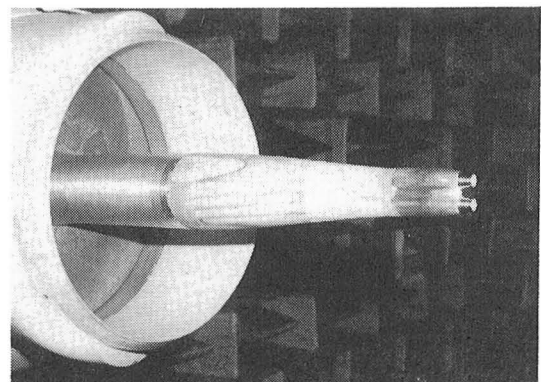
The Langley Aircraft Noise Reduction Laboratory (ANRL) consists of the quiet flow facility, the reverberation chamber, the transmission loss apparatus, the Anechoic Noise Facility, the Jet Noise Laboratory, and the human response to noise laboratories. The quiet flow facility has a test chamber treated with sound-absorbing wedges and is equipped with a low-turbulence, low-noise test flow to allow aeroacoustic studies of aircraft components and models. The test flow, which is provided by either horizontal high-pressure or vertical low-pressure air systems, varies in Mach number up to 0.5. In contrast, the Anechoic Noise Facility is equipped with a very high pressure air supply used solely for simulating nozzle exhaust flow.

The transmission loss apparatus has a source room and a receiving room which are joined by a connecting wall. A test specimen, such as an aircraft fuselage panel, is mounted in the connecting wall for sound transmission loss studies. The reverberation chamber diffuses the source noise and is used for measuring the total acoustic power spectrum of the test source. The Jet Noise Laboratory has two coannular supersonic jets for studying turbulence evolution in the two interacting shear flows which are typical of high-speed aircraft engines. The human response laboratories consist of the exterior effects room and the small anechoic listening room.

possible cause of this phenomenon is acoustic loading due to the supersonic jet exhaust. This study examines the acoustic near field generated by single- and dual-nozzle configurations to determine if closely spaced dual nozzles generate significantly higher acoustic loading than that encountered with a single nozzle.

A configuration consisting of two convergent nozzles with spacing and interfairing scaled from existing aircraft was tested in the Langley Aircraft Noise Reduction Laboratory quiet flow facility. A microphone attached to the nozzle interfairing measured the upstream traveling sound waves emitted by the jets. It was found that for a wide range of nozzle pressure ratios, an aeroacoustic coupling of the two jets enhanced the strength of the screech feedback cycle and resulted in amplitude increases of more than 20 dB over that of a single jet. These acoustic tones exceeded 150 dB with the dual jets, which indicated that high dynamic pressures (exceeding 0.1 psi) can indeed exist upstream of the exit plane of the nozzles.

(Thomas D. Norum, 2645)



Exhaust nozzle configuration tested in quiet flow facility.

Acoustic Loading From Dual Supersonic Jets

Structural failure of components of the exhaust nozzles on current aircraft has led to an increase in boattail drag and a subsequent loss of performance. One

Verification of Propeller Aircraft Interior Noise Model

A computer program entitled PAIN (Propeller Aircraft Interior Noise) has been developed for predicting the sound levels inside propeller-driven aircraft. PAIN can calculate the space average sound pressure levels in the cabin space at the blade passage frequency and its harmonics. The PAIN model is very comprehensive; it takes into account three important parameters which influence the sound field inside the cabin. First, the analysis requires a precise description of the propeller noise (pressure field) on the fuselage skin, such as that provided by the NASA ANOPP (Aircraft Noise Prediction Program). Second, the structural modal properties (mode shapes and resonance frequencies) are determined for a fuselage structure that includes a ring-stringer-stiffened cabin shell, stiffened floor, and sidewall trim. Finally, the PAIN model calculates the acoustic modal properties of the cabin space, including the specific cabin shape and absorption properties of the trim.

The analytical technique (formulated by Bolt Beranek and Newman, Inc., under NASA contract) is based on the concept of acoustic power flow. The analysis was initially validated in the quiet flow facility of the Aircraft Noise Reduction Laboratory by measurements on a simplified propeller/fuselage model and later on models with more realistic structural and interior trim details. Further validation was obtained from ground runup and flight test data for a Fairchild Aircraft Corp. Merlin 4C aircraft. Typical comparisons of predictions and flight test data at the blade passage harmonics (BPH) are shown. The flight measurements are for an executive version of the twin-engine commuter aircraft, which has a 66-in.-diameter cylindrical fuselage and is powered

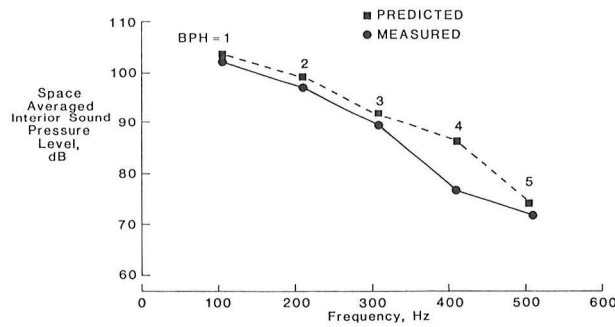
by 1000-shaft-horsepower turbine engines driving 106-in.-diameter propellers with a fuselage tip clearance of $6\frac{3}{4}$ in. The flight operation conditions for the data shown included an altitude of 5000 ft and an airspeed of 238 knots with 74-percent maximum engine torques. The good agreement between the predicted and measured data confirmed the general validity of the PAIN prediction model.

(William H. Mayes, 3561)

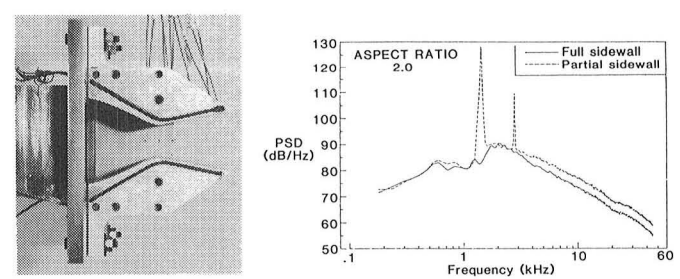
Acoustic Properties of Nonaxisymmetric Supersonic Nozzle

Future propulsion system concepts for high-performance aerospace vehicles may have to consider potential sonic fatigue criteria to achieve overall mission goals. To illustrate, consideration was recently given to the associated noise field of a two-dimensional C-D (convergent-divergent) supersonic exhaust nozzle with partial sidewalls. Performance studies showed that partial sidewalls enhance vectoring capability, lower cooling requirements, and reduce nozzle gross weight with negligible performance losses. Acoustic studies performed in the Anechoic Noise Facility, however, indicated that relative to the same two-dimensional C-D nozzle with full sidewalls, there is a drastic increase in acoustic energy emitted. This increase is composed of high-amplitude tones, as shown in the power spectral density (PSD) plot. The tone level is as much as 50 dB (300 fold) higher than the broadband component.

The high energy tones obtained in this study, when scaled to a full-size engine and fuselage location, would require additional structural weight to safeguard against sonic fatigue damage. This increase in structural weight could dramatically compromise



Prediction of interior noise levels of Fairchild Merlin 4C aircraft.



Effect of partial sidewalls on acoustic emissions from low-aspect-ratio two-dimensional C-D nozzles.

overall mission goals for the vehicle. Further tests are currently being conducted to determine the aerodynamic origin of the increased acoustic energy in order to develop efficient methods for suppression.

(John M. Seiner, 3094)

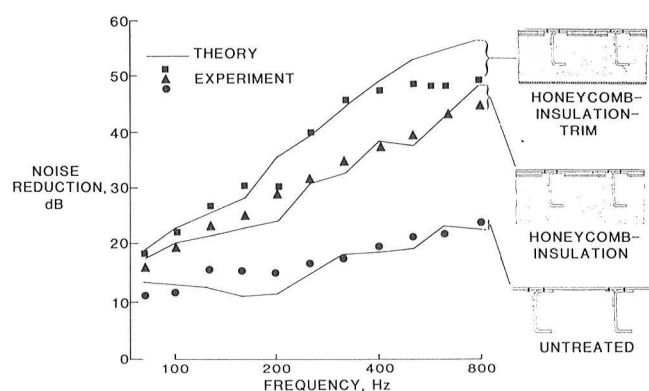
Noise Transmission of Aircraft Sidewall and Noise Control Materials

Control of aircraft cabin noise is important for passenger acceptance and crew performance. Treatment materials used on the inner walls of the aircraft fuselage for noise control must minimize noise transmission and provide acoustic absorption while having minimum weight. Optimization of treatment material requires evaluation of many candidate configurations, both experimentally as well as theoretically; therefore, testing is carried out in a laboratory apparatus to minimize cost.

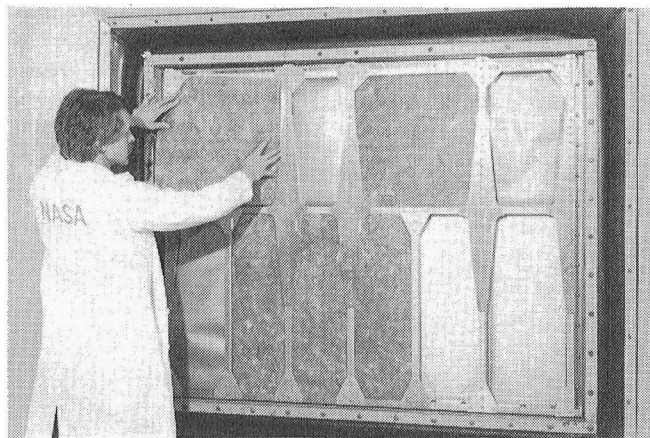
A specially designed panel which represents a sidewall segment of the Gulfstream Aerospace 1000 Commander light turboprop aircraft was constructed and installed in the Aircraft Noise Reduction Laboratory transmission loss apparatus. The in-flight forcing function is a convecting surface pressure caused by propeller and turbulent boundary layer noise. However, for laboratory conditions a random reverberant noise field is used. The additional noise reduction due to acoustic treatments such as porous fiberglass materials and trim panels is determined, as well as the noise transmission loss of the panel structure.

For the laboratory studies, noise reduction is defined as the difference between the measured sound pressure levels of microphones in the source and receiving rooms. Theoretical and experimental noise reductions were generally in good agreement for an untreated condition and for two add-on treatments. These treatments were developed theoretically by professor Rimas Vaicaitis of Columbia University as candidates for noise control in the Commander aircraft. Substantial reduction of noise transmission is obtained when the mass, stiffness and damping properties of the new treatment are chosen for improved matching with the noise and basic structural characteristics of the Commander. The surface density of the new treatment is 2 psf, or about 80 percent of the density of some current aircraft treatments.

(John S. Mixson, 3561)



Measured and predicted noise transmission of sidewall with several noise control materials.



Full-scale segment of aircraft fuselage sidewall in Langley transmission loss apparatus.

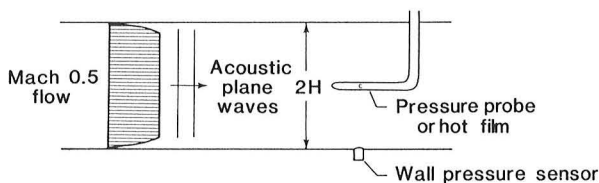
Comparison of Hot-Film Probe and Pressure Probe Responses

Acoustic excitation of laminar boundary layer instability waves may cause transition to turbulent flow. Accurate measurements of fluctuating pressures and velocities in boundary layers are needed in research on viscous drag reduction through laminar flow. Hot-film probes offer one approach to measurements within boundary layers because they are typically about one-hundredth the size of a pressure sensor.

An experiment was conducted to measure the responses of a hot-film probe and a pressure probe to acoustic excitation in flow. Each probe response was compared to the response of a wall pressure sensor to relate fluctuating quantities in the flow to those beneath the boundary layer. Since the acoustic velocity, density, and temperature can all contribute to the hot-film response, it was convenient to compare all transducers on the basis of fluctuating Reynolds number. At each test frequency, acoustic excitation levels ranged over at least 10 dB.

An equivalent fluctuating Reynolds number at the duct centerline location was inferred from the wall pressure sensor response and the stream probe response via the convected wave equation. On a decibel scale, the pressure probe response was within 1 dB of perfect agreement with the wall pressure sensor response. This behavior is consistent with increasing Mach number and is believed to be due to flow-induced impedance changes of the probe sensing ports.

For the hot-film probe, the deviation from the wall pressure sensor response amounted to approximately 3 dB. Considering the number of interacting variables involved in this experiment, these results are encouraging. These data suggest that hot films can be used to estimate acoustic pressure disturbances in a boundary layer in the proximity of a surface where a pressure probe would disturb the flow field. (T.L. Parrott, 4312)



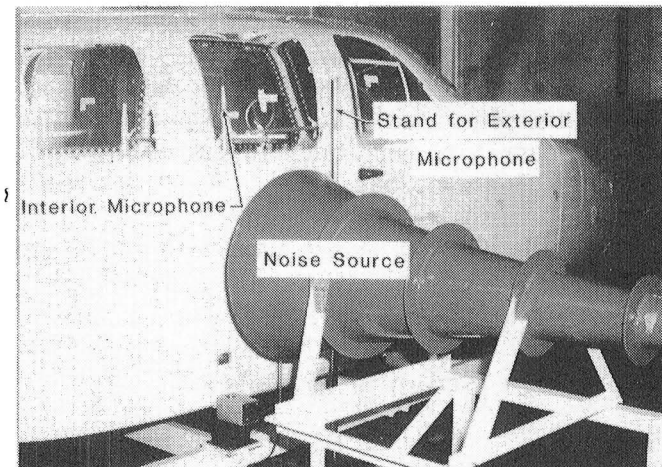
Experimental setup.

Laboratory Study of Sidewall Acoustic Treatment

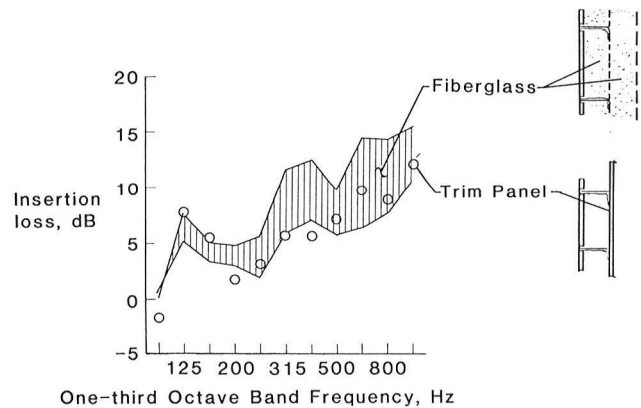
In recent years much attention has been given to reducing the interior noise of propeller-driven aircraft. Most of the recent experimental work has been performed on flat panels in the laboratory. The measurement of the transmission loss of flat panels, how-

ever, does not take into account the interior acoustic space or the vibrational modes of the aircraft as a whole. Some data from in-flight testing are also available. However, such testing can be expensive and time consuming, and the repeatability of the exterior sound field is questionable. For these reasons, a study was performed on an actual aircraft fuselage in the laboratory.

A small airplane fuselage surrounded by fiber-glass baffles was placed in a large chamber. Broad-band noise was emitted from an exponential horn attached to a pneumatic air driver. Interior sound pressure levels were measured and recorded at the approximate head positions of the six passengers. Data were acquired for four fuselage treatments: the baseline treatment (bare walls covered with damping



Light aircraft fuselage interior noise tests.



Insertion loss of fiberglass and trim-panel treatments.

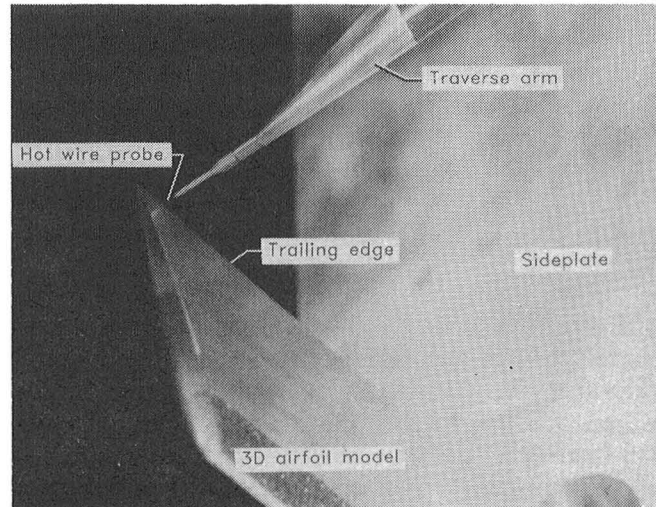
material); the trim-panel treatment (baseline treatment plus the manufacturer's production line trim); the 1.5-in. fiberglass treatment (1.5-in. fiberglass on the baseline treatment); and the 3-in. fiberglass treatment (3-in. fiberglass on the baseline treatment).

The effects of the treatments were evaluated from the standpoint of insertion loss, which is the change in interior sound pressure level due to a specific treatment relative to a second treatment, in this case the baseline. A comparison of the space-averaged one-third-octave-band insertion losses (of the trim-panel and fiberglass treatments) from 100 to 1000 Hz is shown. The insertion loss for the trim-panel treatment, which weighed 35 percent more than the 3-in. fiberglass treatment, was less than that for the 3-in. fiberglass treatment (upper bound of shaded area) except at 125 and 160 Hz. In the 125- and 160-Hz bands, the insertion loss of the two treatments was nearly the same. In addition, the insertion loss for the trim-panel treatment was nearly the same as that for the 1.5-in. fiberglass treatment (lower bound of shaded area) from 200 to 500 Hz. Thus the fiberglass treatments seemed to attenuate the sound as well as the trim-panel treatment, but with less weight.

(Karen E. Heitman, 3561)

edge and the maximum velocities existing there. This tip flow field depends on the aerodynamic loading. It was therefore not surprising to find that the interpretation of the data for different model sizes had to account for both wind tunnel and wing finite aspect ratio effects on the loading distributions. A quantitative normalization of the tip noise spectral data was produced. The findings will be utilized in total helicopter noise prediction programs.

(Thomas F. Brooks, 2645)



Hot-wire measurement setup for blade tip noise test.

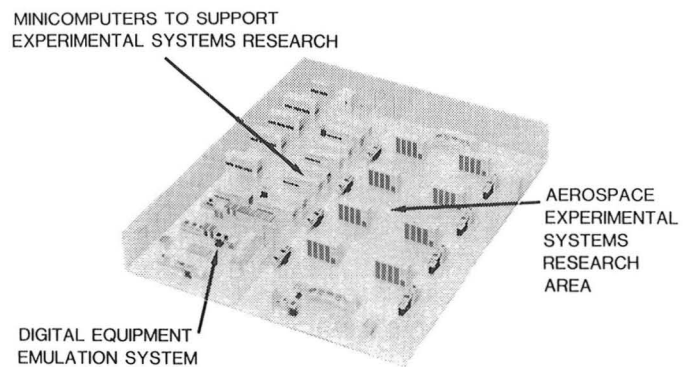
Tip Vortex Broadband Noise

The tip region of rotor blades can contribute significantly to high-frequency broadband noise. The responsible mechanism is the three-dimensional turbulent vortex flow that exists near the tip of the lifting blades. The present experiment is the first to isolate tip vortex noise in a quantitative manner.

The approach was to test stationary blade models. A number of three-dimensional models of rectangular planform with rounded tips were mounted on a sideplate in the vertical open jet of the ANRL Anechoic Noise Facility. Corresponding two-dimensional model tests that employed two side-plates were made for the same model chords, angles of attack, and tunnel velocities. The tip noise was isolated by comparison of sets of two- and three-dimensional model acoustic test data. Hot-wire measurements at the trailing edge of the models provided the detailed statistics of the noise-producing turbulence in the boundary layer and tip vortex region.

It was found that the tip noise scaled with both the size of the vortex roll-up region at the trailing

Avionics Integration Research Laboratory - AIRLAB



The United States leads the world in the development, design, and production of commercial and military aerospace vehicles. To maintain this leadership role throughout the 1990s and beyond will require the incorporation of the latest advances in digital systems theory and electronics technology into fully integrated aerospace electronic systems. Such efforts will entail the discovery, design, and assessment of systems that can dramatically improve performance, lower production and maintenance costs, and at the same time provide a high, measurable level of safety for passengers and flight crews.

AIRLAB has been established at Langley Research Center to address these issues and to serve as a focal point for U.S. government, industry, and university research personnel to identify and develop methods for systematically validating and evaluating highly reliable, fully integrated digital control and guidance systems for aerospace vehicles. The increasing complexity of electronic systems entails multiple processors and dynamic configurations. These developments allow greater operational flexibility in both normal and faulty conditions, thus impacting and compounding the validation process. Whereas a typical reliability requirement for current electronics systems is a probability of failure of less than 10^{-6} at 60 minutes, the requirement for flight-critical electronic controls is for a probability of failure of less than 10^{-9} at 10 hours. Obviously, a new validation process is essential if this significant increase in reliability (four orders of magnitude) is to be achieved and believed.

Validation research in AIRLAB encompasses analytical methods, simulations, and emulations. Analytical studies are conducted to improve the utility and accuracy of advanced reliability models and to evaluate new modeling concepts. Simulation and emulation methods are used to determine latent fault contributions to electronic system reliability and hence aircraft safety. Experimental testing of physi-

cal systems is conducted to uncover the latent interface problems for new technologies and to verify analytical methods.

AIRLAB is a 7600-ft² environmentally controlled structure located in the high-bay area of Building 1220. There are three rooms within the laboratory. The largest room is the experimental systems research area, which is configured into eight research stations and a central control and/or software development station. Each research station is supported by a VAX 11/750 minicomputer system that can be used, for example to control experiments (fault insertions, performance monitoring, etc.) and retrieve, reduce, and display engineering data. A VAX 11/780 minicomputer system supports the central control and/or software development station. The second largest room contains the VAX minicomputers, disk drives, and tape drives that support the research work stations. The third room contains the Digital Diagnostic Emulator, which is a special minicomputer (Nanodata QM-1A) interconnected to a VAX 11/750. The QM-1A is a nanocodable host computer with a unique emulation algorithm that allows gate logic level emulation of a target computer at a very fast rate. The diagnostic emulator provides the capability to experimentally address design issues of new fault-tolerant computer concepts and reliability issues in the fault behavior of fault-tolerant computers. Also included in AIRLAB are two advanced fault-tolerant computers, SIFT (software-implemented fault tolerance) and FTMP (fault-tolerant multiprocessor), which are designed to explore fault-tolerant techniques for future flight-critical aerospace applications. These computers, which have been under development by Langley Research Center for years, serve as research test beds for validation studies in AIRLAB.

AIRLAB provides research resources needed by the aerospace electronics research community to

address design and validation issues of flight-critical fault-tolerant flight control systems. In this role, AIRLAB functions as a "community center" in which AIRLAB researchers with diverse backgrounds can conduct research with common goals.

Fault-Tolerant Software Experiment

An objective in conducting AIRLAB fault-tolerant systems research is to determine an optimum philosophy for designing highly reliable fault-tolerant computer systems. A subgoal is to investigate the impact of fault-tolerant software on system design and reliability. This goal will be achieved via a comparative analysis of fault-tolerant software techniques incorporated on diverse fault-tolerant architectures.

An experiment has been conducted in AIRLAB to investigate the impact of fault-tolerant software on the design of SIFT (software-implemented fault-tolerant computer). The feasibility of implementing the n -version programming and recovery block techniques on the operating system has been successfully demonstrated. The implementations, however, are complicated by the strict scheduling and operating system requirements. In addition, system overhead is increased up to seven times the original amount of execution time due to redundancy. The absence of built-in fault-tolerant structures requires that routines be coded in software (i.e., recovery cache and voter). These investigations confirm the notion that fault-tolerant software applications will impact system design and strongly suggest that retrofitting

fault-tolerant software on existing designs will be inefficient and require system modification.

The effectiveness of the techniques in providing software fault tolerance has been experimentally evaluated. In most cases, the techniques masked software errors; however, the acceptance test routines and the specification of redundant routines occasionally produced system failures. AIRLAB experimentation will continue with the investigation of the n -version programming technique implemented at the application level of SIFT.

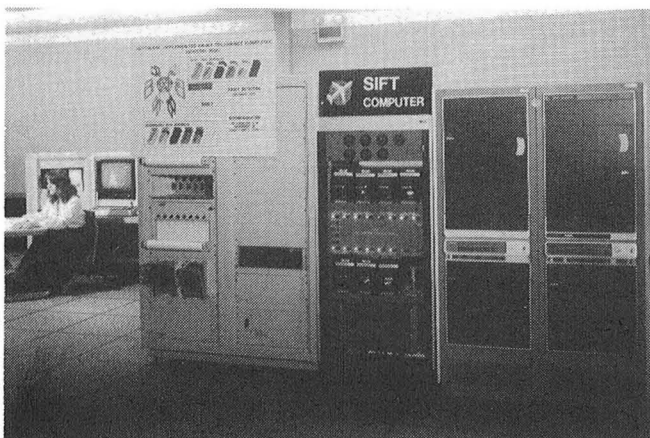
(Janet E. Brunelle, 3681)

Fault-Free Performance Validation of Fault-Tolerant Computers

Fault-tolerant computers achieve high reliability through the use of fault-handling capabilities to maintain normal functioning when faults occur. However, a performance baseline must be established before these capabilities can be verified to be consistent with the intended design and validated for use in specific applications. This baseline describes performance under normal and stressful conditions when the system is fault-free. Therefore, in validating fault-tolerant systems, fault-free performance validation is fundamental.

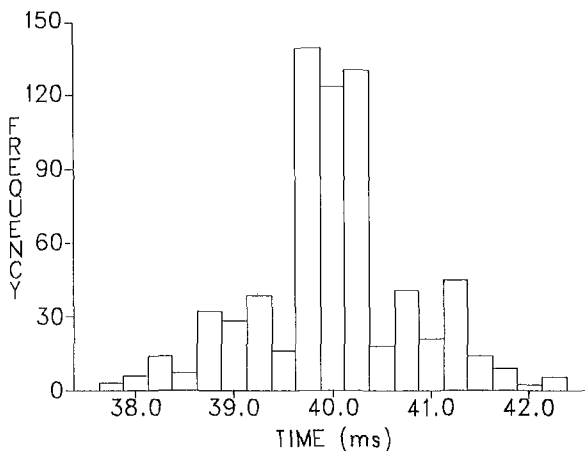
Carnegie-Mellon University researchers are applying fault-free performance evaluation techniques to fault-tolerant systems. Results thus far include the delineation of a framework for fault-free performance validation, the development of tools to expedite experimentation, and the execution of experiments on FTMP (fault-tolerant multiprocessor) in AIRLAB to measure performance parameters. Task frame lengths, clock access times, and instruction execution times were found to be consistent with design specifications and have become part of the performance baseline. Anomalies were found in the ability of FTMP to execute tasks in parallel (as shown in the histogram of time between the start of two parallel tasks) and in FTMP's frame-stretching mechanism. Because these anomalies could defeat the fault-handling capabilities and degrade reliability, they prompted further study of FTMP's design.

Experimentation on FTMP in AIRLAB is serving two functions. First, it is generating information useful in developing fault-free validation techniques. Second, it is producing data, previously unavailable,

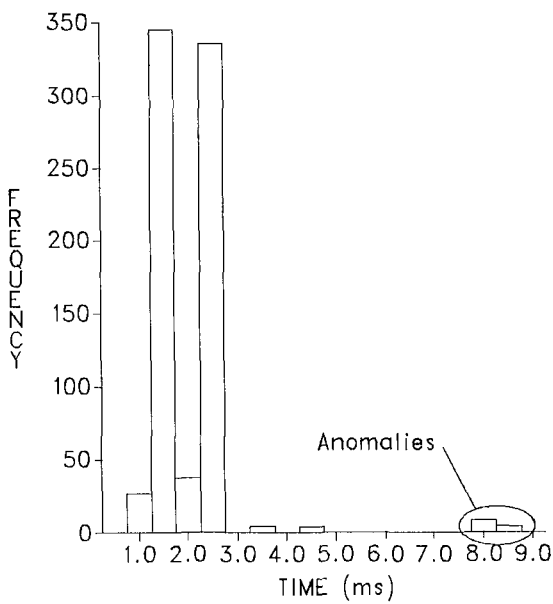


SIFT—target of fault-tolerant software application.

on the behavior of fault-tolerant computers designed specifically for aerospace vehicle applications.
(George B. Finelli, 3681)



Performance baseline—distribution of task frame lengths.



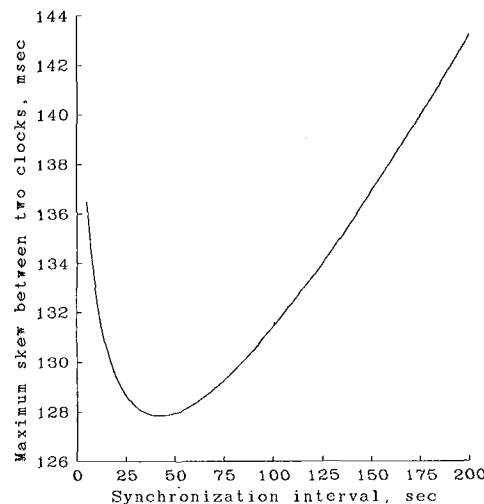
Anomalous behavior—time between start of two parallel tasks.

Validation Methodology for Fault-Tolerant Clock Synchronization

Most highly reliable computer systems achieve fault tolerance by voting between synchronized redundant processors. Validation of the synchronization subsystem is particularly difficult because of dependence between clock failures. To investigate methods of validation, the software-implemented fault tolerance (SIFT) clock synchronization algorithm was implemented on four VAX-11/750 computers in AIRLAB. A validation method combining formal design verification with experimental testing was then applied. The validation method relies on the formal proof process to uncover design and coding errors, and utilizes experimentation to validate the assumptions of the design proof.

The design proof defined the worst-case performance of the synchronization system in terms of several system parameters. A reliability analysis was performed to determine the confidence to which each parameter had to be estimated, and the parameters were measured by direct and indirect means. The worst-case performance of the synchronization system was then calculated. This estimated worst-case performance was compared with the actual system design value to validate the system. The system designer may also use the design proof to choose the values of some parameters, such as how often to synchronize clocks, to maximize the performance/overhead trade-off.

(Sally C. Johnson, 3681)



Performance/overhead trade-off.

DC-9 Full-Workload Simulator

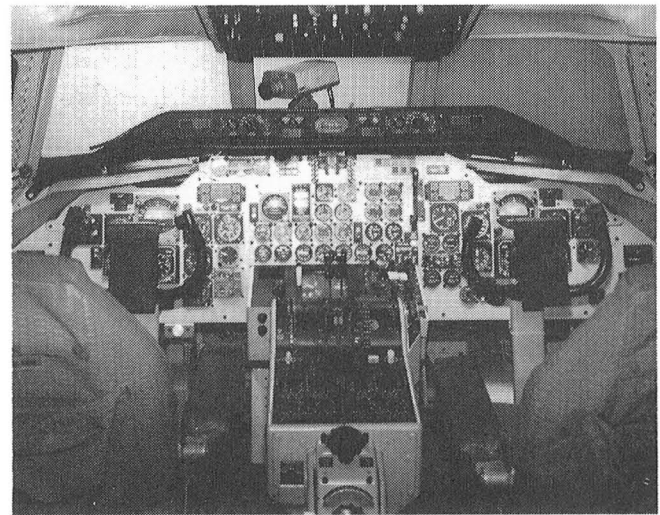


The DC-9 Full-Workload Simulator consists of a fixed-base McDonnell-Douglas DC-9-30 cockpit, a test console, and electronics cabinets. This cockpit was formerly a DC-8 cockpit, but was recently upgraded to provide the capability for dedicated DC-9 full-workload simulations. Stations are available in the cockpit for a Captain and a First Officer. Flight control responses for elevator, aileron, and rudder are simulated by forces from hydraulic servo systems. Manual throttle control for two engines is provided on the center console. The forward electronics panel of the center console is outfitted with a 9-in. color cathode ray tube (CRT) which can be used to display computer-generated graphic presentations, such as Cockpit Display of Traffic Information (CDTI) or Area Navigation (RNAV). A transparent touchpanel superimposed over the face of the CRT provides a discrete input to the computer when any point on the surface is touched. Work is progressing toward improvement of this simulator through retrofit of a modified aircraft center console with autothrottle capability and through the installation of a collimated visual display system to provide an out-the-window color display for both the Captain and the First Officer.

Full-workload studies can be performed in this simulator, since the capacity exists to simulate all aircraft instruments, annunciators, switches, and alarms. Three very high frequency (VHF) communication receivers are simulated for VOR/ILS (VHF Omnidirectional Range/Instrument Landing System). One ADF (Airborne Direction Finder) radio receiver and three marker beacon receivers are simulated in this cockpit. A DC-9/CDTI cockpit procedures study was completed with this facility during the past year, and preparations are under way to implement a microwave landing system (MLS) study within the next year. An oculometer has been

installed for studies to evaluate information transfer rate between instruments and pilots.

Prior to initiating dedicated research in this simulator, it was necessary to evaluate the full-workload aspects of the simulator, validate the fidelity of the aircraft and subsystem models, and obtain baseline data on airline procedures. Normal approach and departure operations in the Denver area were flown by five pilots from two different airlines. Baseline data on crew procedure, simulator performance, and subsystem modeling were obtained and have been incorporated in the overall simulation. Procedures for simulating Air Traffic Control (ATC) party-line communications were also developed and evaluated.



Interior view of DC-9 simulator.

CDTI Cockpit Procedures Study

The cockpit display of traffic information (CDTI) concept provides the crew of an airplane with a pictorial view of surrounding aircraft traffic. Increases in airport capacity, reduced risk of midair collisions, and a reduction in air traffic controller workload are possible benefits from the widespread use of CDTI. In order to realize these benefits, pilots must be able to incorporate CDTI tasks in the cockpit without adverse impact on the normal cockpit procedures.

A study was conducted in the DC-9 Full-Workload Simulator to evaluate the impact of CDTI on cockpit workload and procedures under realistic jet transport operating conditions. A full-systems simulation of present-day jet transport operations in the Denver terminal area was developed for this study. Traffic was presented to the crew on a 9-in. color cathode ray tube (CRT) mounted in the standard weather radar location. Airline pilot test subjects flew the DC-9 simulator through typical approach and departure operations in identical traffic situations both with and without CDTI.

Results of the study indicated that the addition of CDTI to the cockpit was well received by the pilots and did not result in an unacceptable increase in workload or a major disruption to normal procedures. Throughout the tests, the airline crews revealed no tendencies toward unilateral action or questioning of controllers concerning traffic. The test subjects were able to perform self-spacing tasks during the approach scenarios, and they achieved specified arrival times at the runway with greater accuracy than when vectored by ATC along the same approach.

Crew coordination was found to be essential for successful completion of a self-spacing task. Pilot comments stressed the importance of standardized procedures on the duties of the flying and nonflying pilots during such an approach.

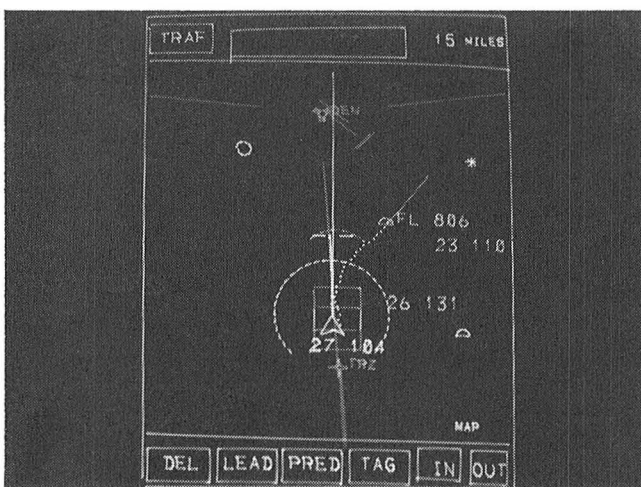
(David H. Williams, 3621)

Effects of Digital Altimetry on Pilot Workload

With the proliferation of cathode ray tubes and associated microprocessor hardware, the capability now exists to place almost any type of information on a pilot's display. A general effort is under way to determine the effects of the various types of information and information placements on pilot visual scanning behavior and workload. One information problem area has been that of altimetry. In spite of numerous attempts to find the best altimeter, incidents still occur as a result of missing an altitude assignment.

Seventy-two VOR-DME (VHF omnidirectional range/Distance Measurement Equipment) landing approaches were flown in the Langley fixed-base DC-9 Full-Workload Simulator to evaluate the effects of a digital altimeter on pilot scanning behavior and workload. Six pilots used a conventional counter-drum-pointer altimeter (CDPA) and a digital altimeter (DA), which consisted of five seven-segment LED digits 0.28 in. high. Pilot scanning data were collected with Langley's oculometer system. The oculometric data were reduced to dwell percentages, average dwell times, transition matrices, and dwell time histograms, and were analyzed statistically.

The results showed only slight differences in pilot scanning behavior with the DA versus the CDPA. Although the average dwell time on the DA was slightly shorter, there were more transitions to altitude information with the DA. The average dwell time on the attitude indicator was 0.2 sec shorter after looking at the CDPA than if the previous look had been at the DA. After looking at the DA, the pilots had to think longer about the digital altitude information than they did when using the CDPA. Pilot comments were generally negative toward the DA because of the lack of needle motion cues, the difficulty of forming a mental picture of altitude when using the DA, and the necessity for the pilot to perform mental arithmetic to estimate the distance to the



Traffic display used in DC-9 simulator.

assigned altitude. This research suggests that digital display of altitude requires more cognitive processes on the part of the pilot than conventional altimeter displays.

(Randall L. Harris, 3917)

Transport Systems Research Vehicle (TSRV) and TSRV Simulator



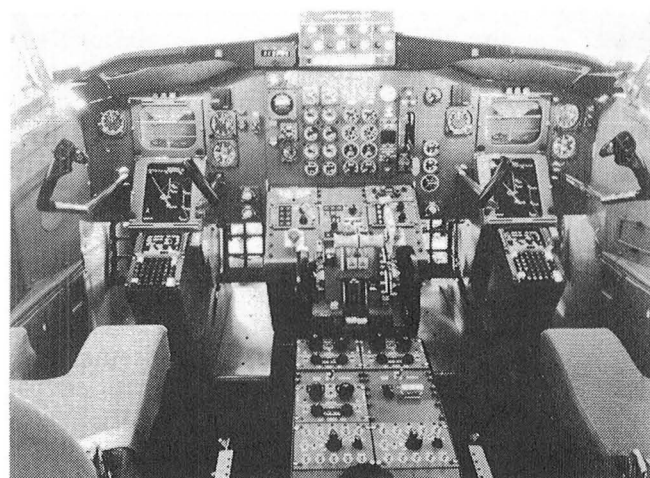
The TSRV and the TSRV simulator are primary research tools used by the Advanced Transport Operating Systems (ATOPS) Program. The goal of the ATOPS Program is the improvement of operational efficiency and safety in the evolving National Airspace System (NAS). Specific program objectives are to develop aircraft systems concepts and companion procedures that will permit the use of more airborne capabilities within the evolving NAS to achieve more efficient operations, and to improve aircraft capability to cope with external factors such as adverse weather and airspace restrictions.

The TSRV is a specially equipped Boeing 737 airplane used to conduct research flight tests. The airplane is equipped with a special research flight deck located about 20 ft aft of the standard flight deck. Two research pilots fly the airplane from the aft cockpit during test periods. In order to extend the viability of the TSRV as a research tool for the next decade, an experimental system upgrade has been undertaken. The first phase, completed in 1984, provides increased computational power and speed, higher order programming language, a single global bus (Boeing's DATAAC) in lieu of a multiple-bus architecture, display of real-time engineering data on strip charts and TV terminals, and provisions for reducing engineering units data on 540 channels in 1 day in lieu of 10 days. The second phase of the upgrade, targeted for completion in early 1986, will encompass provisions for an "all glass" flight deck in the aircraft with eight large hybrid color displays.

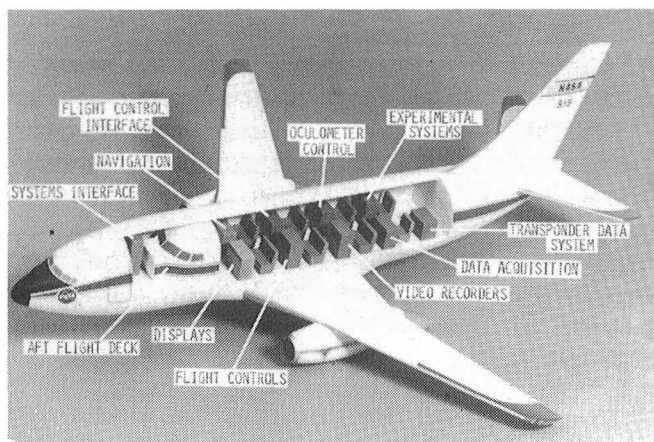
The TSRV simulator provides the means for ground-based simulation in support of the ATOPS research program. The simulator is also being modified to duplicate the upgraded aft flight deck located in the TSRV. It allows proposed concepts in such areas as guidance and control algorithms, new display techniques, operational procedures, and man/machine interfaces to be thoroughly evaluated.

Promising simulation research results later become the subjects of actual flight test research.

The ATOPS Program has completed the design of a new research cockpit for the TSRV. This new configuration is characterized by eight full-color hybrid (raster/stroke) display units (size D, 9-in. diagonal). Six of the units will allow research and development on advanced EADI (electronic attitude director indicator), EHSI (electronic horizontal situation indicator), and caution and warning displays, and the other two units will allow NASA and participating researchers to explore a variety of other uses, including ATC (air traffic control) messages, traffic displays, provisional paths, check lists, and emergency procedures. Such additional information and as yet undefined concepts are key elements in the more efficient operation of aircraft within the evolving ATC environment.



Present configuration of TSRV research cockpit with four monochrome displays.



Cutaway view of TSRV showing location of experimental equipment.

Advanced Airborne Energy Management

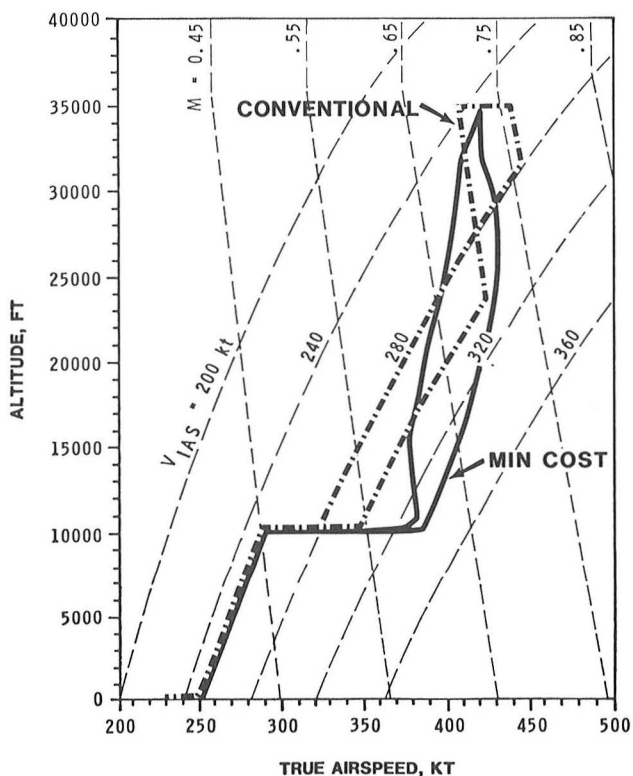
A feasibility study of the utility of a trajectory generation algorithm to compute on-board near-optimal fixed-range four-dimensional profiles is ongoing in the TSRV simulator. The optimization algorithm uses a calculus of variations technique on an energy state model to minimize a cost function throughout the trajectory. The cost function is a linear function of the cost of fuel and the cost of time. The program can generate near-optimal trajectories for both fixed and free time-of-arrival problems.

The study is being conducted in an effort to determine the flight crew interface requirements for real-time operational use of the algorithm in a time-based metered ATC environment. Various display formats will be tested to determine the benefits of specific guidance information for flying and recomputing the near-optimal trajectories. Also to be determined is the sensitivity of the optimal trajectory to mismodeling of the airplane's aerodynamic and thrust characteristics and to variations in the atmospheric parameters.

In 1984, the basic guidance requirements for manually flying the near-optimal trajectories were studied. The profiles generated by the optimization algorithm characteristically vary in both airspeed and flight path angle throughout climb and descent. This differs from the conventional "handbook" constant Mach/IAS (indicated airspeed) type climb and descent profiles. This variability in the climb and descent

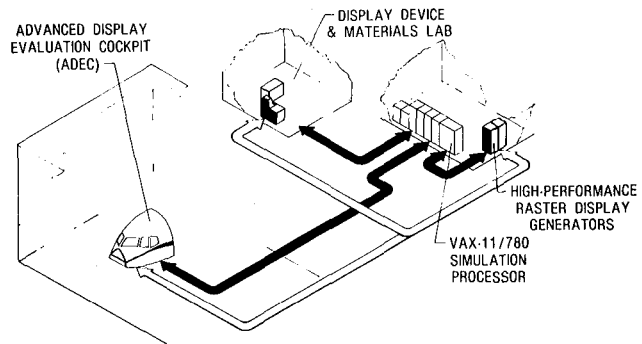
speeds raised some question as to whether conventional guidances would be adequate to fly the optimized trajectories. The studies compared the performance resulting from manual flight of the optimized trajectories with various types of conventional guidance. Subjective evaluations of the guidance options were also collected from the subject pilots used in the study. Results will be available in early 1985.

(Dan D. Vicroy, 3621)



Speed and altitude for conventional and minimum-cost profiles.

Crew Station Systems Research Laboratory (CSSRL)



The trend in modern civil cockpits has been to replace electromechanical instruments with electronic control and display devices. The NASA Crew Station Electronics Technology research program is at the forefront of this trend with research and development activities in the areas of advanced display media, display generation techniques, integrated control panels and keyboards, and cockpit systems integration. The experimental devices being developed have unique drive, interface, and systems integration requirements (as opposed to noncockpit electronics) as well as unique testing facility requirements. The Crew Station Systems Research Laboratory (CSSRL) is being implemented in order to provide for candidate device research in a near-real operational electronic and lighting environment in a timely and effective manner. This laboratory provides a unique civil capability to conduct display materials, device, and photometric characteristics research; establish combined display and graphics generation systems performance; determine synergistic features of integrated systems; and establish a data base on cockpit display systems that utilize emissive and reflective devices which are markedly different from their electromechanical counterparts and may be "washed out" by high ambient light or have poor viewability in darkness.

Major elements of the CSSRL are the Advanced Display Evaluation Cockpit (ADEC), which is a reconfigurable research cab, a simulation host processor, high-performance raster display generators to drive cockpit displays, and a Display Device and Materials Lab. During FY 85-86 a variable lighting system is being added for the ADEC to provide the capability of lighting intensities from darkness up to 10,000 footcandles with diffuse through direct-sunlight conditions.

Advanced Media Interface for Control of Modern Transport Aircraft Navigational Systems

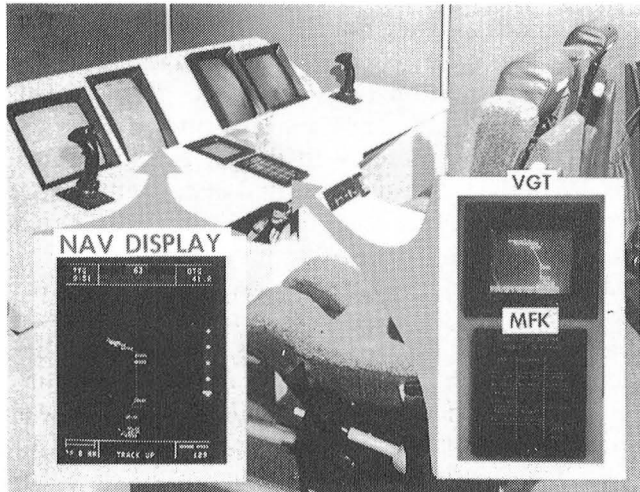
As modern transport aircraft become more sophisticated, pilot workload to manage the newly available information becomes much heavier. The need for a more efficient means of pilot data entry evolves from the increase in digital avionics functions. With the traditional method of data entry, this increase in functions requires additional dedicated controls and displays to be integrated into the remaining limited cockpit area. As part of the effort to improve information management systems, an advanced concept for managing the navigational tasks of a modern transport aircraft, which emphasizes the simplification of the pilot interface, was studied in the Advanced Display Evaluation Cockpit (ADEC) simulator. The system incorporates automation and intelligence into the pilot interface and utilizes three advanced-media multimode devices.

The devices which form the advanced navigational interface are a color navigation display (NAV), a multifunction keyboard (MFK), and a video graphics terminal (VGT). The NAV display is driven by an Adage 3000 programmable display generator with flight display software developed by Research Triangle Institute and NASA. It is essentially an integrated map display which shows the pilot's situation relative to the flight plan. The MFK consists of a scratch pad area and 15 light-emitting diode (LED) tactile feedback switches. The scratch pad and switches can be programmed through a host computer (VAX-11/780) to display various information. This device can be used in place of dedicated switches in the cockpit to declutter the console. The VGT contains a matrix-

addressed thin-film electroluminescent (TFEL) flat-panel display. The VGT can display either video or vector graphics. It also contains touch overlay, which can be used for input to the flight-control computers.

Preliminary evaluation in the simulator revealed that the concept of the navigational system greatly simplified the navigational tasks of the pilot. Pilot reaction to the use of touch overlay in the control of the NAV display scaling and in modifying the flight plan on the VGT was highly favorable. Implementation of the concept with a different digital-to-digital link will provide increased update speed for MFK operations and will thereby improve the performance of the simulator implementation of the concept. Formal evaluation of the improved system will then be conducted.

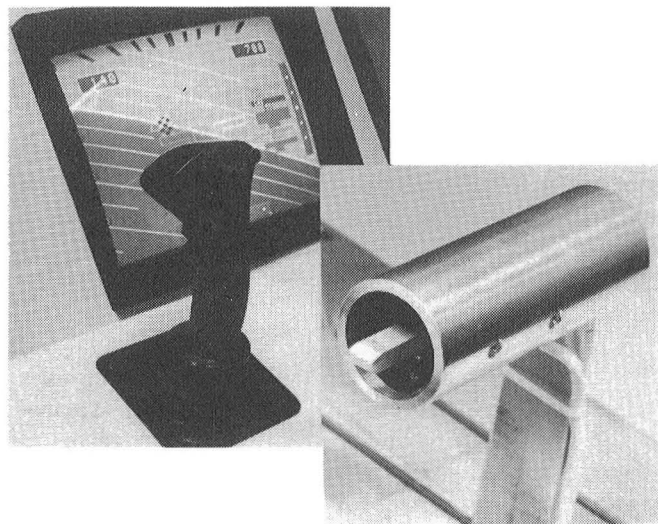
(Russell V. Parrish, 2259)



Advanced-media navigational interface made up of color navigation (NAV) display, multifunction keyboard (MFK) and video graphics terminal (VGT) flat-panel interactive touch display.

of dedicated controls that are crowding the available cockpit space, multifunction control strategies are being employed. One concept involves the activation of various flight systems/subsystems by the pilot without the necessity of releasing the flight controls (Multifunction Control Throttle and Stick, or MCTAS). This is accomplished by the use of switches and buttons built into the throttles and stick handles and whose functions are computer controlled. The idea behind the concept for transport aircraft is not necessarily to enable the pilot to keep his hands on the throttle and stick, but rather to reduce, without increasing task difficulty, the number of dedicated controls.

The initial application of this MCTAS concept was evaluated in the Advanced Display Evaluation Cockpit (ADEC) simulator. It was developed around a pilot/autopilot interface and contrasted a conventional, dedicated control/display unit (Automatic Guidance and Control Unit, or AGCU) for an advanced autopilot of a transport airplane with an MCTAS implementation of the same. The MCTAS implementation allows the pilot to select the various combinations and levels of automatic flight control assistance by activation of a cursor-selectable menu choice. Other aircraft systems operations, such as communication and navigation functions, could be controlled with the same throttle and stick switches and different menu displays.



Multifunction Control Throttle and Stick (MCTAS) implementation of pilot's interface to autopilot functions, including throttle and stick switches coupled with cursor-selectable menu on primary flight display.

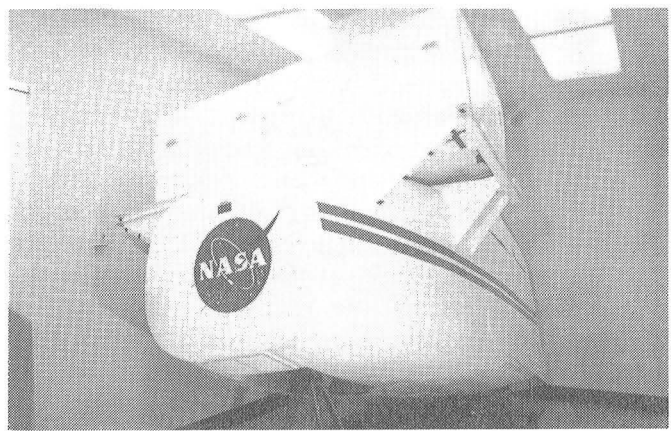
Multifunction Control Throttle and Stick As Autopilot Interface

The growth in complexity of modern transport aircraft cockpits is paralleled by the increase of specialized equipment necessary to control the vehicle. This leads to an increase in the number of dedicated controls/switches needed to provide the human interface to such devices. In an effort to reduce the number

The autopilot implementation of the MCTAS concept was evaluated in the simulator and initial pilot reaction was favorable, with particular emphasis placed on the ease of sharing attention between the primary flight display and menu operations. Several suggestions arising from this evaluation for incorporating more artificial intelligence into the interface are currently being implemented. More formal simulator evaluations of the autopilot interface are planned, and additional applications of the MCTAS concept to other cockpit functions are under way.

(Russell V. Parrish, 2259)

General Aviation Simulator

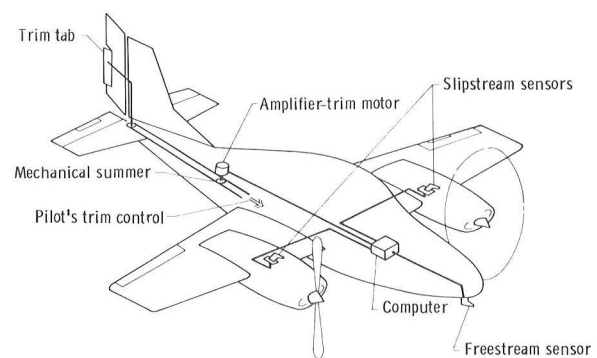


The General Aviation Simulator (GAS) consists of a general aviation aircraft cockpit mounted on a three-degree-of-freedom motion platform. The cockpit is a reproduction of a twin-engine propeller-driven general aviation aircraft with a full complement of instruments, controls, and switches, including radio navigation equipment. Programmable control force feel is provided by a "through-the-panel" two-axis controller that can be removed and replaced with a two-axis side-stick controller which can be mounted in the pilot's left-hand, center, or right-hand position. A variable-force-feel system is also provided for the rudder pedals. The pilot's instrument panel can be configured with various combinations of cathode ray tube (CRT) displays and conventional instruments to represent aircraft such as the Cessna 172, Cherokee 180, and Cessna 402B. A collimated-image visual system provides a 60° field-of-view out-the-window color display. The visual system can accept inputs from a model board system, computer-generated graphics, and a target aircraft/horizon scene. The simulator is flown in real time with a CDC Cyber 175 computer to simulate aircraft dynamics. Research applications of the GAS include the evaluation of systems for approach/landing displays, single-pilot IFR studies, stall/spin inhibiting techniques, evaluation of gust alleviation systems, investigation of flight control problems during engine failure, ride quality evaluation, and development of an autopilot system for light aircraft.

reducing the control forces on a light twin after an engine failure. The automatic trim system consists of dynamic pressure sensors behind each propeller and a computer and electric motors driving the elevator, aileron, and rudder trim tabs. The system schedules open-loop trim tab deflections as a function of the differential slipstream dynamic pressure and the free-stream dynamic pressure.

The study concentrated on an analysis of the sensitivity of the airplane handling qualities to the scheduling errors, system response rates, and required trim tab power. Three NASA research pilots participated in the study and evaluated the handling qualities for a sudden engine failure and for extended maneuvering and landing with one engine operating. The nominal system provided a 2- or 3-unit improvement in pilot rating for handling qualities following loss of an engine. The system was found to be of most benefit for a sudden engine failure but was also beneficial for making an engine-out landing. The handling qualities were fairly insensitive to scheduling errors, but fast response rates and power trim tabs were required.

(Eric C. Stewart, 2184)

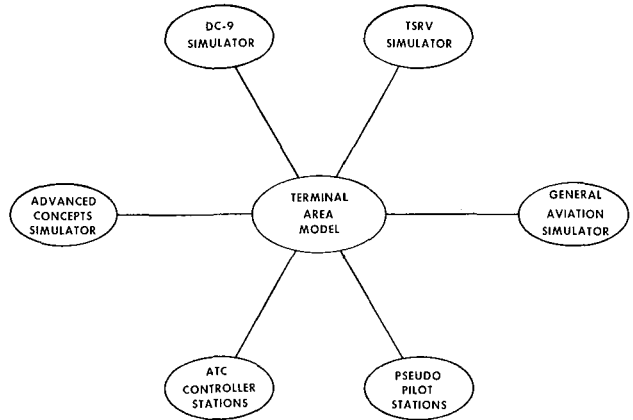


Automatic engine-out trim concept.

Light Twin Automatic Engine-Out Trim System

A study was conducted on the General Aviation Simulator to investigate an automatic trim system for

Mission Oriented Terminal Area Simulation (MOTAS)



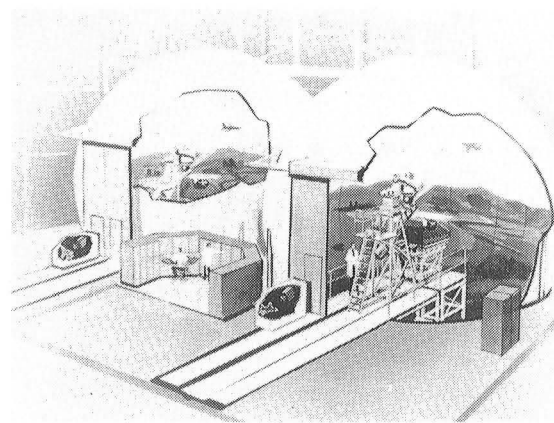
The Mission Oriented Terminal Area Simulation (MOTAS) is an advanced simulation capability that provides an environment in which flight management and flight operations research studies can be conducted with a high degree of realism. This facility provides a flexible and comprehensive simulation of the airborne, ground-based, and communications aspects of the airport terminal area environment. The major elements of the MOTAS facility are an airport terminal area environment model, several aircraft models and simulator cockpits, four pseudo pilot stations, four air traffic controller stations, and a realistic air-ground communications network. The airport terminal area environment model represents today's Denver Stapleton International Airport and surrounding area and includes either a computer-generated automated metering and spacing system of control or a present-day vectoring system of control with air traffic controllers. In addition, the model simulates various radar systems, navigation aids, wind conditions, and so forth.

The MOTAS facility combines the use of several cockpit simulators and pseudo pilot stations for flying aircraft in the airport terminal area. The MOTAS facility is presently fully operational with the Transport Systems Research Vehicle (TSRV) Simulator and the General Aviation Simulator. The DC-9 Full-Workload Simulator has been interfaced to the facility in a simplified mode and will be converted to full operational capability when called for by research requirements. The Advanced Concepts Simulator will be interfaced to the facility once it becomes operational as a stand-alone simulator. These cockpit simulators will allow full crews to fly realistic missions in the airport terminal area. The remaining aircraft flying in the airport terminal area are flown through the use of the pseudo pilot stations. The operators of these stations can control five to eight aircraft at a time by inputting commands to change

airspeed, altitude, direction, and so forth. The final major components of the facility are the air traffic controller stations, which are presently configured to display and control the two arrival sectors, the final approach sector, and the tower and/or departure sectors.

Because of its flexibility in reconfiguring according to research requirements, the MOTAS facility can support a variety of flight vehicle and/or air traffic control system research studies that would not be possible in the real world due to safety, economy, and repeatability considerations.

Differential Maneuvering Simulator



The Langley Differential Maneuvering Simulator (DMS) provides a means of simulating two piloted aircraft operating in a differential mode with a realistic cockpit environment and a wide-angle external visual scene for each of the two pilots. The system consists of two identical fixed-base cockpits and projection systems, each based in a 12.2-m-diameter (40 ft) projection sphere. Each projection system consists of a sky-Earth projector to provide a horizon reference and a system for target image generation and projection. The internal sky-Earth scene provides reference in all three rotational degrees of freedom in a manner that allows unrestricted aircraft motions. The sky-Earth scene has no translational motion. The internal visual scene also provides continuous rotational and bounded (300 to 45,000 ft) translational reference to a second (target) vehicle in six degrees of freedom. The target image presented to each pilot represents the aircraft being flown by the other pilot in this dual simulator. Each cockpit provides essential instruments and displays along with a wide-angle head-up display. Kinesthetic cues in the form of a g-suit pressurization system, helmet loader system, g-seat system, cockpit buffet, and programmable control forces are provided to each pilot consistent with the aircraft's motions. Research applications include studies of high-angle-of-attack flight control laws, evaluation of evasive maneuvers for various aircraft and rotorcraft, and evaluations of the effect of parameter changes on the performance of several baseline aircraft.

incorporating significant levels of inherent pitch instability (RSS) for high-speed cruise efficiency while meeting stringent maneuverability and agility requirements at lower airspeeds. Classically, these are conflicting requirements because at the lower speeds, RSS results in an unstable airframe with degraded high-angle-of-attack aerodynamic control effectiveness. Thus, there is a need to develop design approaches and guidelines that will allow these requirements to be met in future fighter aircraft. The primary objectives of the program were: (1) to develop a data base for control requirements (control power and actuator rate capability) versus airframe instability level; (2) to develop and evaluate a flight control law concept that provides maximum maneuverability while reflecting the control limitations of the airplane; and (3) to investigate the levels of maneuverability and agility that are desired in view of current and future air-to-air weapons capability.

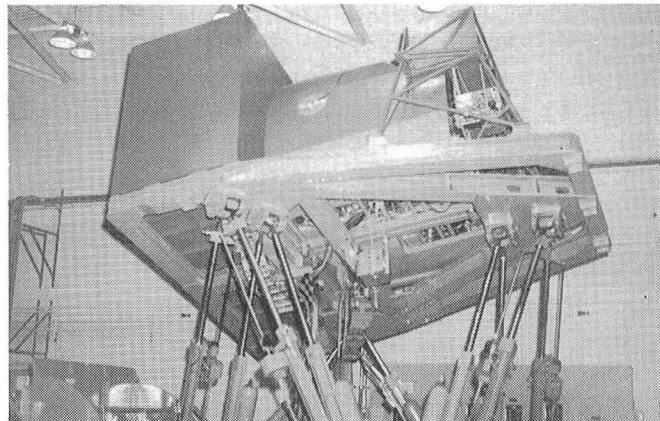
The study was successfully completed, with follow-on studies planned to further explore and refine the control law concepts developed in the subject investigation.

(Luat T. Nguyen, 2184)

Control of Highly Maneuverable Unstable Aircraft

A manned simulation investigation was conducted to study control of advanced fighter aircraft

Visual/Motion Simulator



The Visual/Motion Simulator (VMS) is a general-purpose simulator consisting of a two-man cockpit mounted on a six-degree-of-freedom synergistic motion base. A collimated visual display provides a 60° out-the-window color display for both left and right seats. The visual display can accept inputs from several sources of image generation. A programmable hydraulic-control loading system is provided for column, wheel, and rudder in the left seat. A second programmable hydraulic-control loading system for the right seat provides roll and pitch controls for either a fighter-type control stick or a helicopter cyclic controller. Right-side rudder control is an extension of the left-side rudder control system. A friction-type collective control is provided for both the left and the right seats.

A realistic center control stand installed in 1983 provides transport type control features as well as autothrottle capability for both the forward and reverse thrust modes. Motion cues are provided in the

simulator by the relative extension or retraction of the six hydraulic actuators of the motion base. Washout techniques are used to return the motion base to the neutral point once the onset motion cues have been commanded. In addition, a g-seat is provided which can be interchanged between the left and right seats to augment the motion cues from the base.

Research applications have included studies for transport, fighter, and helicopter aircraft. These studies addressed problems associated with wake vortices, high-speed turnoffs, microwave landing systems, energy management, multibody transports, and maneuvering stability flight characteristics. Numerous simulation technology studies have also been conducted to evaluate the generation and usefulness of motion cues.



Interior view of VMS.

Allowable Time Delays in Large Aircraft Response

The present military specifications allow a maximum time delay in the flight control system of an airplane (regardless of airplane size or intended mission) for Level 1 (satisfactory) handling qualities of not more than 0.1 sec. However, many of today's large aircraft, which have good flying qualities, have transport lags much greater than 0.1 sec. It is therefore believed that the present criteria for maximum allowable time delay are too stringent when applied to large aircraft whose large inertias result in maneuvering requirements and piloting tasks which are markedly different from those of fighter class aircraft, and that this needless imposition of structural and actuation capabilities on these large airplanes can make their design expensive and operationally inefficient.

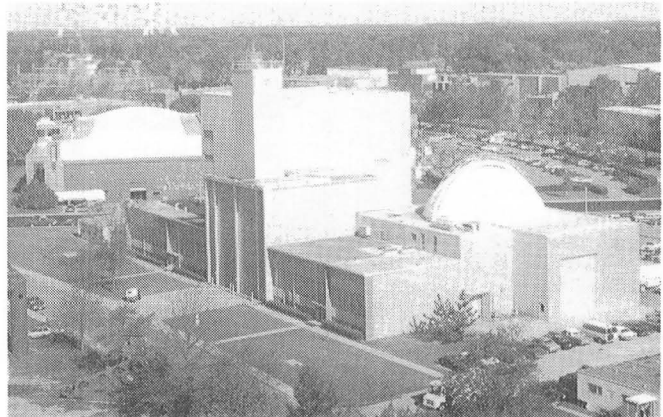
A piloted simulator investigation has been conducted with the Visual Motion Simulator and a math model of a derivative Lockheed L-1011 transport. The objective of this study was to build on the existing large-aircraft data base in the area of control system delays and to utilize the results as the basis for suggested allowable response time delays for the various levels of handling qualities. The present criteria for allowable phase shift between cockpit input and control surface deflection also appear to be too stringent when applied to large aircraft, and therefore these were also addressed in this study.

The simulation results indicated that requirements for a 0.1-sec maximum delay in aircraft response are much too conservative for large aircraft where an offset landing maneuver is the critical design task. Pilots were more tolerant of lagged time delays (responses slowed down) than they were of discrete time delays (nothing happens until delay has elapsed). Delays in the lateral axis appeared to be more critical than those in the longitudinal axis because pilots are more sensitive to the lateral (roll) axis during landing tasks. These tests suggest limits of 0.3 sec in the lateral axis and 0.5 sec in the longitudinal and directional axes on Level 1 handling qualities for discrete time delay, instead of the universal 0.1-sec limit of the present military specification.

In the area of phase shift between cockpit input and control surface deflection, the present specification states that the response of the control surfaces in flight shall not lag the cockpit control force inputs by more than 15° for a Level 1 handling qualities airplane in the Category C flight phase (approach and landing). The results of these simulator tests suggest much less severe phase shift limitations, again differentiating between axes, of 75° in roll and 95° in pitch and yaw axes for the approach and landing task.

(William D. Grantham, 4681)

Structural Dynamics Research Laboratory



The Structural Dynamics Research Laboratory is designed for conducting research on the dynamic behavior of spacecraft and aircraft structures, equipment, and materials. It offers a variety of environmental simulation capabilities, including acceleration, vacuum, and thermal radiation.

A main feature of the laboratory is a 55-ft-diameter thermal-vacuum chamber with a removable 5-ton crane, flat floor, 64-ft dome peak, and large centrifuge or rotating platform. Access is by an air-lock door and an 18-ft-high, 20-ft-wide test specimen door. There are 10 randomly spaced 10-in.-diameter view ports, and closed circuit television visually monitors tests. A vacuum level of 10^{-4} torr can be achieved in 160 minutes with diffusion pumps. A centrifuge attached to the floor of the chamber is rated at 100 g, with a 50,000-lbf capacity and a maximum allowable specimen weight of 2000 lb. Six-foot test specimen mounting faces are available at 16.5-ft or 20.5-ft radius. A temperature range of 100°F is obtained from 250 ft² of portable radiant heaters and liquid-nitrogen-cooled plates.

The other predominant feature of the laboratory is a 38-ft-high backstop of I-beam construction. Test areas available around this facility are 15 by 35 by 38 ft high and 12 by 12 by 95 ft high. Available excitation equipment includes several types of small shakers. The largest is a hydraulic shaker with a capacity of 1200 lbf, a 3-in. stroke, and a range of 0 to 170 Hz.

Closed-circuit television cameras monitor all test areas. Both the vacuum chamber and the backstop test areas are hard-wire connected to a central data acquisition and processing room. This room contains signal conditioning equipment and analog and digital data recording capability for up to 128 channels of data. A Hewlett-Packard 5451C Fourier Analyzer System is available along with a VAX 11-780/EAI 2000 hybrid computer system for simulation

and on-line test control. A variety of auxiliary data logging and signal processing equipment is also available.

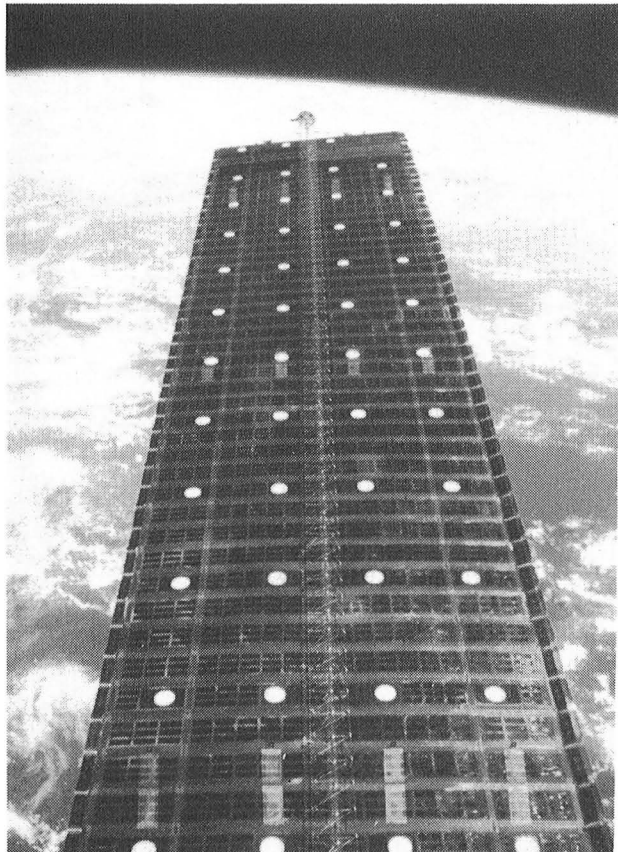
Photogrammetric Measurement Tests for Solar Array Experiment

The objective of this research is to develop a photogrammetric measurement method for determining on-orbit dynamic responses of large space structures. The initial application is a solar array tested in the MSFC/OAST orbital Solar Array Flight Experiment. The measurement approach is to use video images of the solar array recorded during vibration tests. A ground-based system was designed to analyze this data by tracking the position change of specific targets from frame to frame. Data from multiple TV cameras are merged in a triangulation program to determine a displacement time history of the large structure being studied. This motion history is then analyzed with appropriate system identification techniques to determine the modal and frequency characteristics in response to input excitations.

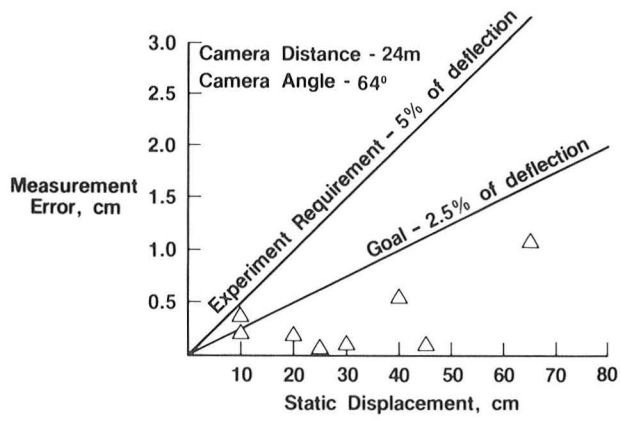
To evaluate this approach, a ground test was conducted on a full-scale mock-up of the solar array extended to the 70-percent deployed position. A series of tests determined the capability of the system to achieve the development resolution goal of 2.5 percent or less of the displacement. This goal is a factor of 2 better than the experiment requirement of 5 percent of the displacement. The system surpassed the goal in six of seven test cases. The figure shows the

results of the seven tests compared to lines representing the experiment requirement and the development goal.

(M. Larry Brumfield, 3196)



Solar array experiment.



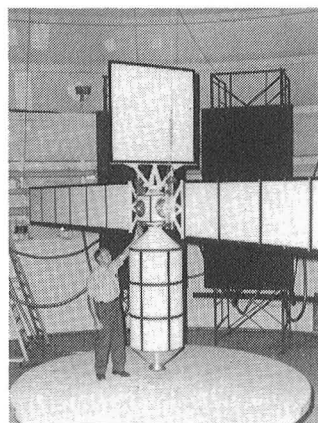
Experiment requirements and test results.

Generic Space Station Model Dynamic Tests

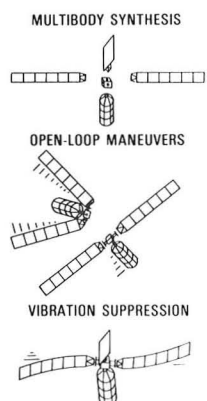
This research is intended to identify technology areas in which better analytical and/or experimental methods are needed to adequately predict the dynamic characteristics of multibody space platforms such as the Space Station. A multibody generic space station model is used to experimentally evaluate current dynamic analysis capabilities. The model is also used to evaluate ground tests of space station components and subassemblies. The Generic Space Station Dynamics Model has been fabricated and is undergoing ground vibration tests in the three areas of dynamic tests shown. Component modal vibration tests are being used to extract natural frequencies, mode shapes, and damping information from each of the five components. These data are then used with analytical model synthesis procedures to predict the modal properties of the assembled model.

In addition to modal tests, transient tests will be performed to validate analysis assumptions. The degree of damping coupling between modes and the level of modal participation for maneuvers such as solar array slewing and shuttle berthing will be determined. Active suppression of solar array vibrations is being studied with torque actuators at the root of each solar array. These active suppression tests will identify the hardware requirements and robustness of various control laws. After completion of the three types of dynamic tests, the model architecture will be revised to more closely resemble the space station reference configuration. This revised model will be used to study the role of scaled dynamic models in the space station program.

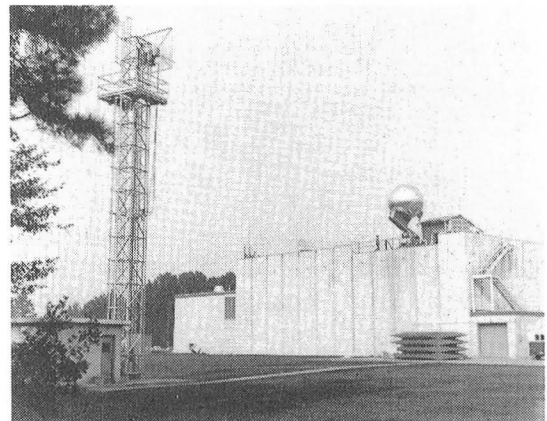
(W. Keith Belvin, 2446)



Multibody generic space station model.



Vehicle Antenna Test Facility



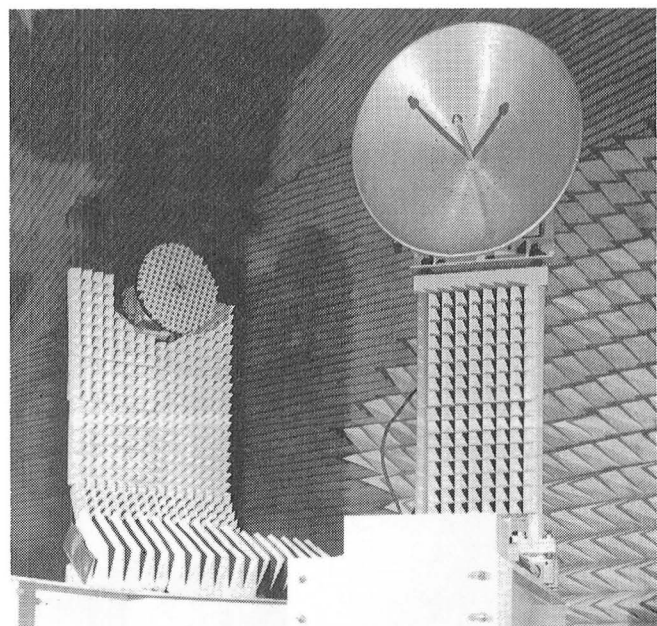
The Vehicle Antenna Test Facility (VATF) is a research facility used to obtain data for new antenna designs and antenna systems and to provide antenna performance and electromagnetic scattering data in support of various research programs. The VATF consists of two indoor radio frequency anechoic test chambers and an outdoor antenna range system. The anechoic chambers provide simulated free-space conditions for measurements from 100 MHz to greater than 40 GHz. The anechoic chambers, which are shaped like pyramidal horns to reduce specular reflections of the walls, are over 100 ft long and have test area cross sections approximately 30 by 30 ft.

A spherical near-field (SNF) measurement capability was added to the low-frequency chamber. A precision antenna positioning system, antenna source tower, and optical alignment system designed for SNF measurements were installed in the low-frequency chamber and the capability now exists for automatically performing precision SNF measurements up to at least 18 GHz. Antennas with diameters up to 12 ft can be measured if their electrical size is no greater than 100 wavelengths (i.e., diameter/wavelength ≤ 100). This limitation is imposed by the SNF system software, which transforms the near-field data to obtain the desired far-field data. Measured data stored on disc can be processed to provide antenna directivity, polar or rectangular plots of the radiation patterns, and three-dimensional contour plots of the antenna radiation characteristics.

The high-frequency anechoic chamber was used to establish a Compact Range Facility. The compact range is an electromagnetic measurement system used to simulate a plane wave illuminating an antenna or scattering body. The plane wave is necessary to represent the actual use of the antenna or scattering from a target in a real-world situation. The compact range utilizes an offset-fed parabolic reflector to create the simulated plane wave test conditions. The

standard commercially available compact range is limited to the measurement of antennas or models with maximum dimensions of 4 ft over the frequency range of 4 to 100 GHz.

The outdoor antenna range system is available for use when the antenna or test model size or frequency precludes the use of the anechoic chambers. The outdoor range consists of two remote transmitting towers that are spaced 150 and 350 ft from the test positioner mounted on the VATF roof. The VATF has several electronic laboratories with the extensive measurement capability needed to support the design of unique antennas prior to their evaluation in the antenna chambers or on the outdoor antenna range system.



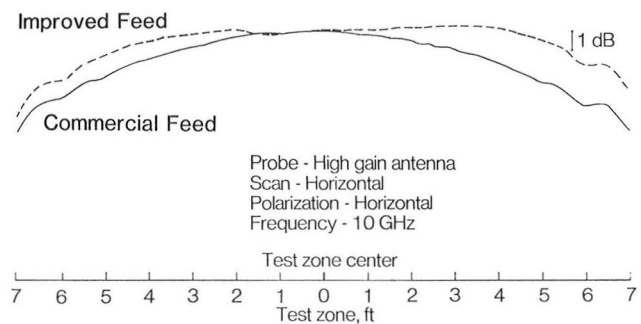
Spherical near-field equipment.

Compact Range Technology

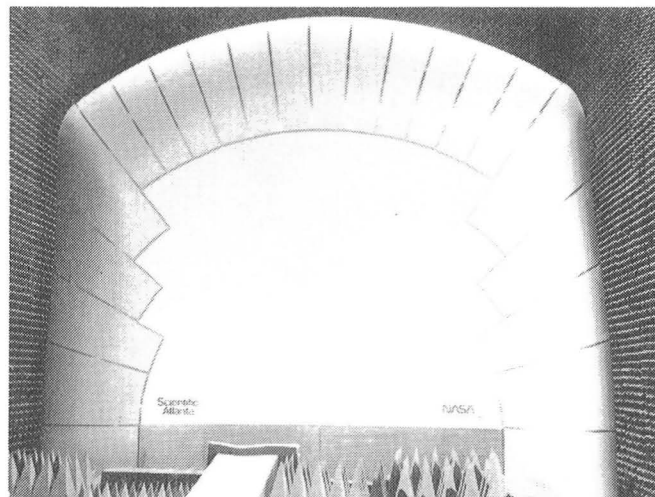
The compact range is an electromagnetic measurement system used to simulate a plane wave illuminating an antenna or scattering body. The plane wave is necessary to represent the actual use of the antenna or scattering from a target in a real-world situation. Traditionally, a compact range has been designed as an offset-fed parabolic reflector with a knife-edge or serrated-edge termination. The edge termination of the parabolic surface has limited the extent of the plane wave region or, more significantly, the antenna or scattering body size that can be measured in the compact range. As a result, the compact range has had limited use as well as limited accuracy. The compact range concept has not been applied to larger systems because of the large discrepancy between target and reflector size.

NASA Langley has been involved in the development of compact range technology in the VATF high-frequency chamber. Modifications to the standard commercially available compact range reflector were made and improved feed designs were developed. Measurements made at 10 GHz of the planar wavefront in the compact range test area after these modifications and feed improvements were made indicate the test zone size has increased to at least 8 ft, to double the test capability of the commercially available compact range. Measurements made at lower frequencies indicate the modified reflector should perform well down to at least 1 GHz, which is an improvement over the 4-GHz minimum-frequency limitation of the commercial reflector.

(Melvin C. Gilreath, 3631)

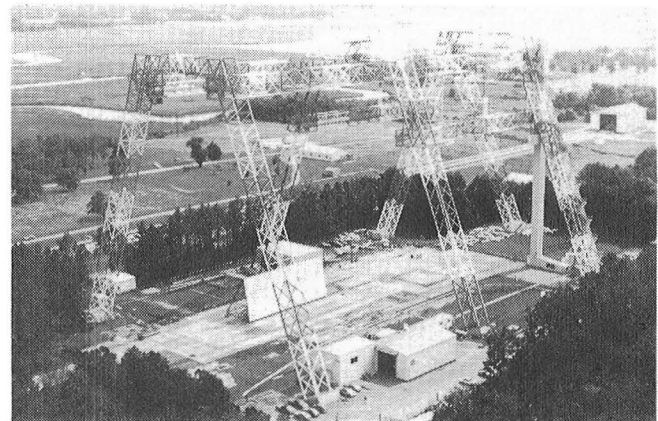


Amplitude data for modified compact range reflector.



Modified compact range reflector.

Impact Dynamics Research Facility



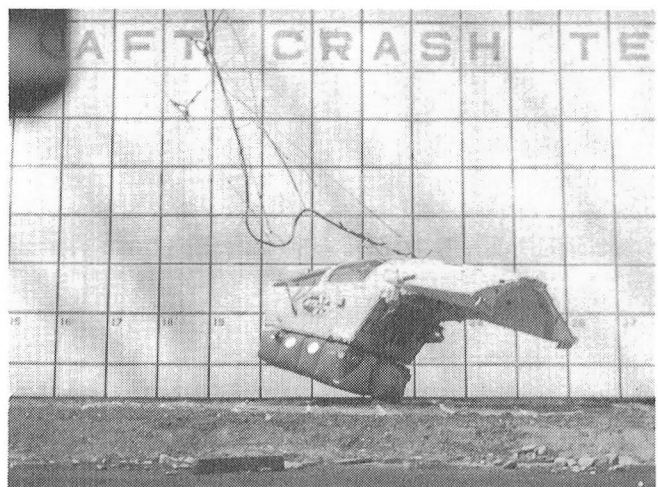
This facility, which was originally used by the astronauts during the Apollo Program for simulation of lunar landings, has been modified to simulate crashes of full-scale aircraft under controlled conditions. The aircraft are swung by cables, pendulum-style, into the concrete impact runway from an A-frame structure approximately 400 ft long and 230 ft high. The impact runway can be modified to simulate other ground crash environments, such as packed dirt with trees. In the past the impact runway has been modified with soil to meet a specific test requirement.

The aircraft is suspended by swing cables from two pivot points 217 ft off the ground. It is then pulled back along an arc to a predetermined height by a pullback cable from a movable bridge on top of the A-frame, released from the pullback cable, and allowed to swing, pendulum-style, into the ground. An instant before impact, the swing cables are separated from the aircraft by pyrotechnics. The length of the swing cables regulates the aircraft impact angle from 0° (level) to approximately 60°. Impact velocity can be varied up to approximately 65 mph (governed by the pullback height) and to 90 mph with rocket assist. Variations of aircraft pitch, roll, and yaw can be obtained by changes in the aircraft suspension harness attached to the swing cables. Onboard instrumentation data are obtained through an umbilical cable attached to the top of the A-frame. Data are transmitted by hard wire to the control room at the base of the A-frame. Photographic data are obtained by ground cameras and cameras mounted on top of the A-frame. Maximum allowable weight of the aircraft is 30,000 lb.

Full-Scale Impact Testing of F-111 Crew Escape Capsule

Twelve swing tests and five drop tests were conducted on an F-111 crew escape capsule at the Impact Dynamics Research Facility. The capsule test article was equipped with air bag external energy absorbers, specially designed energy absorbing seats for pilot and copilot, and anthropomorphic dummies in the seats. Test conditions for the swing tests were ground impact at 34 ft/sec horizontal velocity and 32 ft/sec vertical velocity with various yaw and roll angles. Test conditions for the drop tests were ground impact at 32 ft/sec vertical velocity. The test capsule was instrumented to measure seat loads and deformations and loads transmitted to dummy occupants during impact.

Results from the tests show that substantial reductions in crash deceleration pulse delivered to occupants can be attained with the energy-absorbing



Impact test of crew escape capsule.

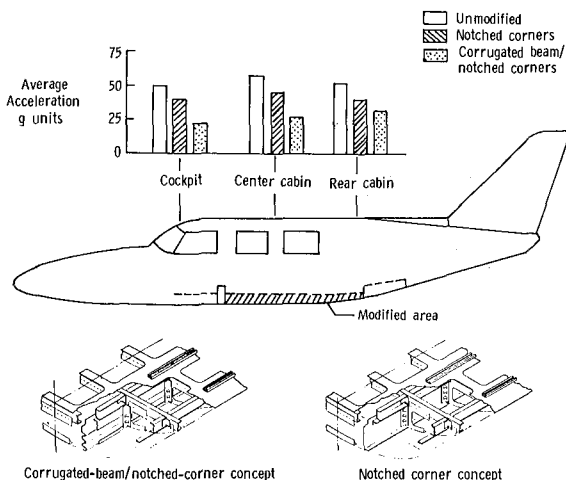
features tested. Both air bags and energy-absorbing seats are required to contain crash pulses within human tolerance under these impact conditions. Data are being used to improve the designs of the air bag and energy-absorbing seat systems.

(Claude Castle, 3795)

Full-Scale Crash Test Evaluation of Two General Aviation Airframe Subfloor Load-Limiting Concepts

Three low-wing twin-engine six-passenger general aviation aircraft test specimens were crash tested in the Langley Impact Dynamics Research Facility at 80 mph (sink speed = 30 ft/sec) and at a flight path angle of 15° from the horizontal. The aircraft impacted with the cabin floor parallel to the ground.

One unmodified aircraft was the baseline specimen for the test series. On the other two aircraft, the fuselage subfloor structure from the main wing carry-through spar to aft of the rear cabin door was replaced with crashworthy subfloor structure. Of the existing structure, the upper floor panel was left in place. The keel beams, bulkheads, stringers, and lower contour skin were removed, and either the corrugated-beam or the notched-corner concept was installed. Seat tracks were installed on the upper floor panel to provide seat attachment capability.



Average peak normal crash pulse magnitudes for three test specimens.

The average peak normal crash pulse magnitudes measured on the cabin floor for the three test specimens are shown for three different fuselage stations. An analysis of the data indicates that in order of decreasing severity, the tests ranked as follows: the unmodified structure, the notched corners structure, and the corrugated-beams/notched-corners structure. The magnitude of the normal accelerations for the unmodified aircraft was between 50 and 55 g over the length of the cabin because of the flat impact attitude. In comparison, the magnitude of accelerations for the corrugated-beams/notched-corners structure, which allowed the most extensive subfloor crushing, was reduced to approximately 25 g, a 50-percent reduction in acceleration magnitude compared with that of the unmodified aircraft.

(Huey D. Carden, 3795)

Boeing 707 Fuselage Section Drop Test

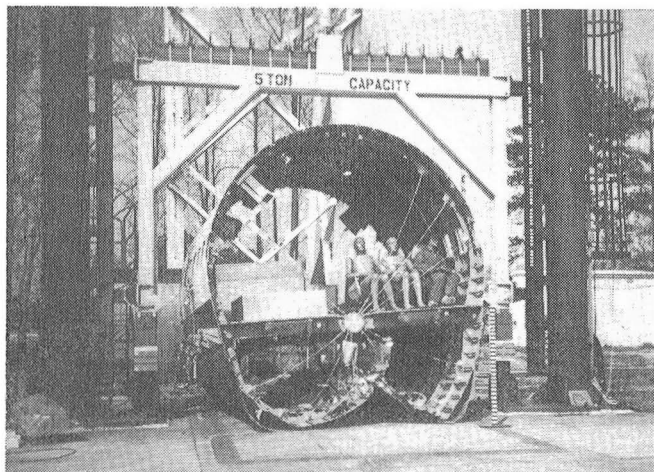
The Full-Scale Transport Controlled Impact Demonstration (CID) was conducted December 1, 1984, at Dryden Flight Research Facility, Edwards Air Force Base, CA. The 352-channel data acquisition system and the 10-camera photographic system built at Langley functioned successfully during the crash impact and subsequent fire. More than 95 percent of the data channels were active during the initial impact, recording the structural loads, seat performance, dummy response, lap belt and shoulder harness loads, and other experimental parameters. All 10 onboard high-speed cameras functioned and recorded significant and unique visual information.

The principal NASA experiment onboard the Boeing 720 aircraft was the measurement of the structural response during the crash impact and slideout. Consequently, NASA Langley Research Center undertook responsibility for developing the complete data-gathering system. Langley designed, built, and tested a 352-channel digital Data Acquisition System (DAS) and a 10-camera Photographic System (PS) within the constraints of a tight schedule. These systems were delivered to Dryden Flight Research Facility on schedule early in December 1983.

An extensive development and testing activity for the DAS and PS was performed at Langley. This activity culminated on March 20, 1984, when a third 707 fuselage section was drop-tested at the vertical drop tower of the Impact Dynamics Facility. This test

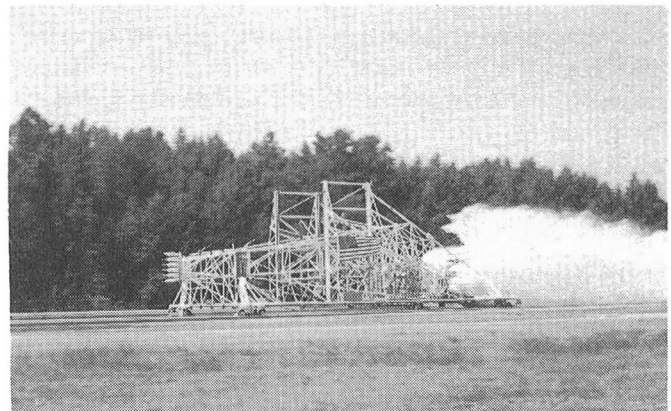
was conducted to demonstrate the performance of the integrated DAS and PS during a realistic vertical crash pulse. Both systems performed as planned during the 20-ft/sec impact of the 707 fuselage section, which qualified the system for use in the full-scale crash test.

(Robert J. Hayduk, 3795)



Boeing 707 fuselage section at Impact Dynamics Facility.

Aircraft Landing Dynamics Facility



The NASA Langley Research Center has recently updated the Landing Loads Track to the Aircraft Landing Dynamics Facility (ALDF) to improve the capability of low-cost testing of wheels, tires, and advanced landing systems. The main features of the updated facility are the propulsion system, the arresting gear system, the high-speed carriage, and the track extension.

The ALDF uses a high-pressure water jet system to propel the test carriage along the 2800-ft track. The propulsion system consists of an L-shaped vessel which holds 26,000 gallons of water pressurized to 3150 psi by an air supply system. A timed, quick-opening shutter valve is mounted on the end of the "L" vessel and releases a high-energy water jet which catapults the carriage to the desired speed. The propulsion system produces a thrust of 1.8 million lb at maximum pressure, which is capable of accelerating the 108,550-lb test carriage to 220 knots within 400 ft. This thrust creates a peak acceleration of approximately 17 g's. The carriage coasts through an 1800-ft test section and decelerates to a velocity of 175 knots or less when it intercepts the five arresting cables that stretch across the track. The arresting system brings the test carriage to a stop in 600 ft or less. Essentially any landing gear can be mounted on the test carriage, including those exhibiting new concepts, and any runway surface and weather condition can be duplicated on the track. Research on slush drag, hydroplaning, tire braking, steering performance, and runway grooving has been conducted in the past.

Future research programs include the Space Shuttle Orbiter main and nose gear tire spin-up wear characteristics and cornering force measurements at high speeds as well as frictional properties of radial and H-type aircraft tires for comparison with conventional bias-ply tires. A surface traction program to study the effect of different runway surface textures and various runway grooving patterns on the stop-

ping and steering characteristics of aircraft tires will be conducted. Finally, tests associated with the National Tire Modeling Program will also be conducted.

Vortex Research Facility



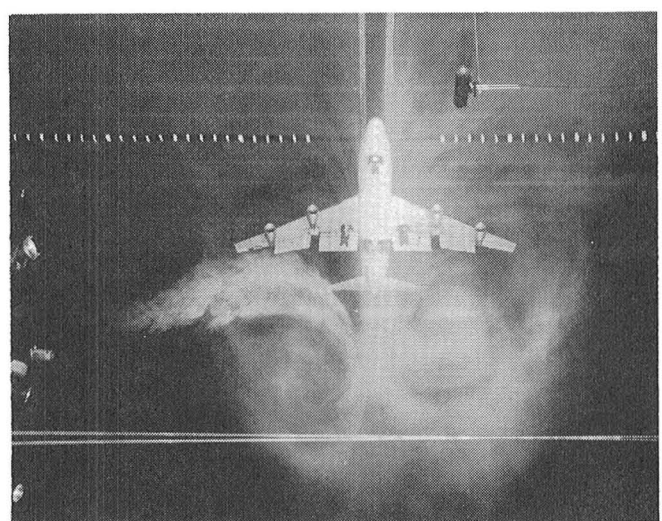
The Vortex Research Facility is a unique experimental facility in which the research model is towed the length of the facility instead of air being moved past the research model, as is done in conventional wind tunnels. With this capability, wake flow fields may be studied over downstream distances of over 2 scale miles. The facility is a converted towing basin about 1800 ft in length with a test section length of 500 ft and a cross section 17 ft wide and 14 ft high. An instrumented automobile-type research vehicle is used to accelerate the research test model to a constant test speed of approximately 100 ft/sec. The aerodynamic characteristics of the research model are measured during the entire length of the facility and are transmitted via an optical telemetry data link to a data acquisition system. A laser velocimeter system is located in the test area to acquire detailed wake velocity measurements. The laser velocimeter system incorporates a high-speed scanning system which provides 16 discrete measurements across the test section at rates up to 30 scans per second. Flow visualization is also acquired to provide a qualitative image of the wake which is recorded on high-speed movie film and video tape.

The Vortex Research Facility has been involved in several research programs during the last 15 years, including the Aerial Applications program and the Wake Vortex Hazard/Alleviation program. The facility is currently being utilized only in the Wake Vortex program. The research objective for the facility is to provide a basic understanding of the physics of vortex flows. To achieve this objective, the facility has been upgraded and experimental data are being acquired to develop methods which reduce vortex wake intensity and to verify computational methods that predict vortex flow behavior.

Density Stratification Effects on Vortex Flows

The state of the atmosphere plays a dominant role in determining the lifetime of an aircraft wake. Turbulence, wind shear, and cross winds are known to influence vortex decay. In addition, the variation of temperature with altitude (the lapse rate) can have a strong effect, both as a direct influence on wake lifetime and as a parameter characterizing the stability or turbulence characteristics of the atmosphere.

The facility is currently being used to investigate the effects of density stratification in the test section, which simulates the dynamics of wake development in the real atmosphere. Density stratification in the test section was produced by a vertical temperature gradient and resulted in significant effects on the decay of the wake vortex system. The results showed



Vortex-generating model mounted in Vortex Research Facility.

that for cases with mild stratification effects, the dynamics of the wake vortex system were dominant over the buoyancy forces generated by the density stratification. Larger amounts of stratification produced larger effects on the wake vortex system and caused significant changes in wake lifetime. Results obtained in the Vortex Research Facility have been compared with results from flight test data and water tunnel data and show similar conclusions.

(Dale R. Satran, 2543)

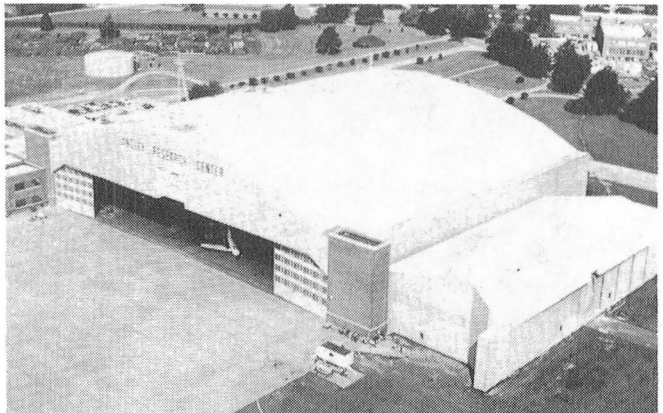
Flight Research Facility

The truss-supported roof of the huge hangar of the Flight Research Facility provides a clear floor space with nearly 300 ft in each direction (over 87,000 ft²).

Door dimensions will allow entry of a Boeing 747. Features such as floor air and electrical power services, radiant floor heating to eliminate corrosion-causing moisture, a modern deluge fire suppression system, energy-saving lighting, modern maintenance spaces, and entry doors and taxways on either side of the building make this structure equal or superior to any hangar in the country. Extensive and modern maintenance equipment makes it possible to repair aircraft ranging in sophistication from modern metal and composite airliners, fighters, and helicopters to fabric-covered light airplanes. Surrounding the hangar are ramp areas with a load-bearing capacity sufficient to handle the largest wide-body jet now flying. The high-power turnup area can also handle a wide variety of aircraft.

The present array of research and research support aircraft includes an airliner, military fighters, trainers, experimental one-of-a-kind designs, helicopters, and single- and multi-engine light airplanes. This variety enables research to be carried out over a wide range of flight conditions, from hover to Mach 2 and from the surface to 60,000 ft. Research pilot currency in this wide spectrum of aircraft is important in conducting credible in-flight experiments as well as in flight simulator assessments. A variety of research can be conducted in such areas as terminal traffic flow, Microwave Landing System (MLS) approach optimization, airfoil properties, single-pilot IFR, engine noise, turbulence research, natural laminar flow, winglet studies, stall/spin, and severe storm hazards.

One of the support helicopters is used to drop unpowered remotely controlled models of high-performance airplanes to study high-angle-of-attack



control characteristics. The drop model test site is located at Plum Tree Island, near Langley Research Center.



NASA 501, modified American Aviation AA-1 Yankee.



NASA 503, Cessna C-402.



NASA 504, modified Beech C-23 Sundowner.



NASA 515, Boeing 737-100.



NASA 507, Cessna C-172.



NASA 519, modified Piper PA-28RT-200 Arrow.



NASA 512, OV-10B Mohawk.



NASA 816, F-106 B.

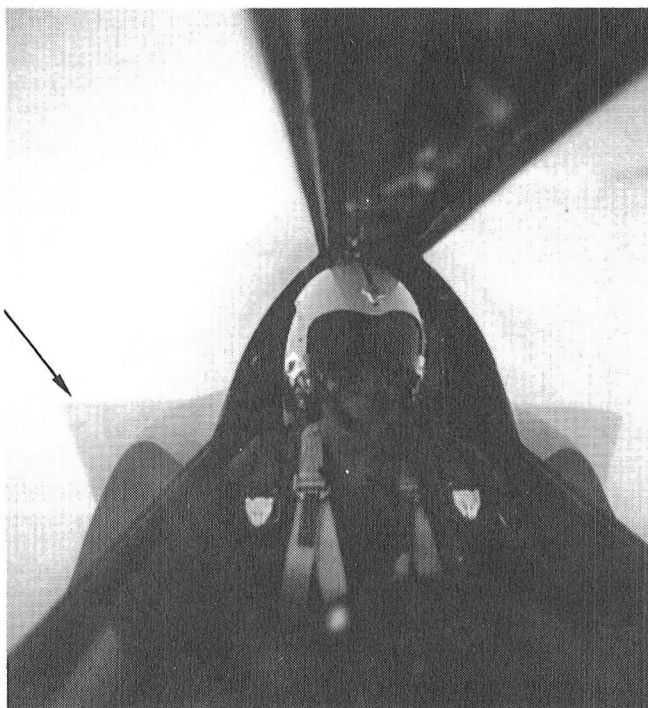
Storm Hazards Program — 1984 Results

The NASA Storm Hazards Program continued operations in 1984 with the F-106B airplane receiving 247 additional direct lightning strikes. This brought the total to 637 hits in the 5 years of thunderstorm flying. Twelve channels of 5- and 10-nanosecond time resolution recording of electromagnetic transients are provided, along with several video and film camera systems.

Results obtained in 1984 confirm the earlier experience of higher strike rates at colder temperatures aloft; in fact, one flight through the anvil portion of a thundercloud resulted in 72 direct strikes to the airplane. However, 24 direct strikes were experienced at altitudes below 20,000 ft during 1984. Preliminary data indicate that as many as two strikes may have been cloud-to-ground flashes; the maximum current in any strike experienced to date has been 54,000 amps. The photograph (from the aft-facing Hasselblad camera) shows a lightning discharge channel from the right wing tip. The onboard camera systems have shown that, contrary to established design guidelines, any exterior surface of this airplane may be susceptible to direct lightning

attachment. Based on the high-altitude strike experience with this airplane, it is concluded that a suitably hardened all-metal airplane can readily survive high-altitude lightning strikes with no significant effects on the aircraft or its systems. The generalization of these results to composite aircraft with low-voltage digital systems via mathematical models is now beginning.

(Bruce D. Fisher, 3274)



Lightning discharge channel from right wing tip of F-106B during thunderstorm penetration.

1. Report No. NASA TM-87585	2. Government Accession No.	3. Recipient's Catalog No.	
4. Title and Subtitle LANGLEY AERONAUTICS AND SPACE TEST HIGHLIGHTS — 1984		5. Report Date September 1985	6. Performing Organization Code
7. Author(s)		8. Performing Organization Report No.	
9. Performing Organization Name and Address NASA Langley Research Center Hampton, VA 23665		10. Work Unit No.	
12. Sponsoring Agency Name and Address National Aeronautics and Space Administration Washington, DC 20546		11. Contract or Grant No.	
13. Type of Report and Period Covered Technical Memorandum			
14. Sponsoring Agency Code			
15. Supplementary Notes			
16. Abstract The role of the Langley Research Center is to perform basic and applied research necessary for the advancement of aeronautics and space flight, to generate new and advanced concepts for the accomplishment of related national goals, and to provide research advice, technological support, and assistance to other NASA installations, other government agencies, and industry. This report highlights some of the significant tests which were performed during calendar year 1984 in Langley test facilities, a number of which are unique in the world. The report illustrates both the broad range of the research and technology activities at the Langley Research Center and the contributions of this work toward maintaining United States leadership in aeronautics and space research. Other highlights of Langley research and technology for 1984 are described in "Research and Technology—1984 Annual Report of the Langley Research Center." Further information about both reports is available from the Office of the Chief Scientist, Mail Stop 103, Langley Research Center, Hampton, Virginia 23665 (804-865-3316).			
17. Key Words (Suggested by Author(s)) Research and technology Tests Facilities Wind tunnels Models		18. Distribution Statement Unclassified - Unlimited	
Subject Category 99			
19. Security Classif. (of this report) Unclassified	20. Security Classif. (of this page) Unclassified	21. No. of Pages 88	22. Price A05

